Analysis of Wireline Interval Pressure Transient Tests From Single and Layered Reservoir Systems

by

Tang Chuin Cherng

Dissertation submitted in partial fulfillment of
the requirements for the
Bachelor of Engineering (Hons)
(Petroleum Engineering)

MAY 2013

Universiti Teknologi PETRONAS
Bandar Seri Iskandar
31750 Tronoh
Perak Darul Ridzuan

CERTIFICATION OF APPROVAL

Analysis of Wireline Interval Pressure Transient Tests From Single and Layered Reservoir Systems

by

Tang Chuin Cherng

A project dissertation submitted to the
Petroleum Engineering Programme
Universiti Teknologi PETRONAS
in partial fulfilment of the requirement for the
BACHELOR OF ENGINEERING (Hons)
(PETROLEUM ENGINEERING)

Approved by,

_____

(Prof. Dr. Mustafa Onur)

UNIVERSITI TEKNOLOGI PETRONAS

TRONOH, PERAK

May 2013

CERTIFICATION OF ORIGINALITY

This is to certify that I am responsible for the work submitted in this project, that the original work is my own except as specified in the references and acknowledgements, and that the original work contained herein have not been undertaken or done by unspecified sources or persons.

_____

TANG CHUIN CHERNG

ABSTRACT

This project examines the methodology of the packer-probe wireline formation tests (WFT) to interpret and analyse the pressure transient data acquired at the packer and probes along the wellbore for single layer and multi-layered systems. Such tests are often called WFT interval pressure transient tests or simply WFT IPTTs. IPTTs offer some advantages over the conventional (extended) well tests in terms of cost, time, and providing important properties such as horizontal and vertical permeability over a scale larger than cores but smaller than that of extended well tests. In this project, the same methodology applied to a packer-probe WFT in single layer system will be applied to various multi-layered systems to investigate the feasibility and validity of using the single-layer analysis methodology for the WFT IPTTs conducted in multi-layered systems. A number of papers were presented on interpretation of packer-probe transient test because it is important to know the horizontal and vertical permeability along a wellbore for the benefits of secondary recovery and enhanced oil recovery purposes. However, most papers available in the literature present analysis methods for interpreting pressure transient test data acquired by packer-probe WFTs in single-layer systems. Only a few of them considered interpretation of packer-probe interval pressure-transient tests in multi-layered systems. Thus, one of the main objectives in this project is in detail to access the methodology used for analyzing a single layer system and apply the same to multi-layered system. Various averaging formulas of horizontal and vertical permeabilities will be used to represent the multi-layered system. The validity of the representation is tested through pressure response matching. The methodology will be thoroughly discussed in this project. The interpretation is to conduct in step by step manners by covering the main steps of pressure transient interpretation and analysis; i.e., flow regime identification, parameters estimation, averaging permeability as well as pressure response matching.

ACKNOWLEDGEMENTS

First of all, I would like to extend my sincere appreciation to my supervisor, Prof. Dr. Mustafa Onur for his help and supervision in conducting this study. His professional advice, guidance, and motivation throughout the course tremendously helped me to a better understanding of pressure transient test analysis. He had spent a considerable time and efforts in developing my analysis skills in order to complete this project. I appreciate his trust in my capabilities, which builds my confidences in working on this project.

I would also like to thank my colleagues who have provided assistance and views. My sincere appreciation also extends to university and Final Year Project coordinators, Mr. Muhammad Aslam and Dr. M Nur Fitri for the course arrangement and coordination.

Last but not least, special thanks go to my family members for their patience, support and understanding over the entire period of my studies.

TABLE OF CONTENTS

LIST OF TABLES

LIST OF FIGURES

Chapter 1
INTRODUCTION

1.1 Background

Wireline formation testing is part of pressure transient testing methods. It is an evolution of DST, Drill Stem Test. DST usage is limited to the hole condition and the cost of repetitive runs of DST for formation evaluation. Thus, wireline formation tester is often used for formation evaluation work. This method is usually performed in a open hole using a cable-operated formation tester with sampling module ability which is anchored down-hole while the communication is established by several pressure and sampling probes. The first tool was introduced in the 1950's concentrated on fluid sampling. RFT, Repeat formation tester is then introduced to add capability of the tool to repeatedly measure formation pressure in a single run into the well (Ireland et al. 1992). Since 1962, common application of wireline formation tester are:

1. To obtain formation pressure and reservoir pressure gradient
2. To determine reservoir fluid contacts
3. To obtain fluid samples for formation fluid characterization
4. To estimate reservoir permeability and skin
5. For reservoir characterization

According to (Schlumberger, 2006), pressure transient tests are conducted at all stages in the life of a reservoir; exploration, development, production and injection. During exploration stage, tests are conducted to obtain fluid samples and static pressures of all permeable layers of interest. These pressures can be used to obtain formation fluid gradient to identify fluid contact in the reservoir. During development stage, the emphasis is on static reservoir pressures, which are used to confirm fluid contacts and fluid density gradients. On that basis, the different hydraulic compartments of the reservoir will be determined and tied into geological model.

During production stage, tests are for reservoir monitoring and productivity tests to access to need for stimulation.

In this project, the main focus is on the interval pressure-transient tests (IPTTs) which are conducted by packer-probe formation testers to provide dynamic permeability and anisotropic information with high resolution along the wellbore (Zimmerman et al. 1990, Pop et al. 1993, Kuchuk 1994, Onur et al. 2011).

1.2 Problem Statement

Wireline formation testing ability to isolate and test a certain layer and its ease of conducting repeated tests has quickly turn it to an attractive method for interval pressure-transient tests. Furthermore, permeability and anisotropy have significant affect on all reservoir displacement processes (Onur et al. 2011). Therefore, it is important to know the horizontal and vertical permeability for the benefits of secondary recovery and enhanced oil recovery purposes. A number of papers were presented on interpretation of packer-probe transient test. However, most papers are for interpreting single-layer system. A few papers have presented interpretation of interval pressure-transient test in multi layered system like the work of Kuchuk (1994) and Larsen (2006).

1.3 Objective

The objective of this project or study is to review the methodology used for analyzing and interpreting wireline pressure-transient test data acquired at the packer and observation probes along the wellbore for both for single layer and multi-layered systems. In addition, the same methodology applied to a packer-probe WFT in single layer system will be applied to various multi-layered systems to investigate the feasibility and validity of the single-layer analysis methodology to the WFT IPTTs conducted in multi-layered systems. A sensitivity study with respect to various flow parameters like layer horizontal and vertical permeability and layer thickness will be conducted to see the effects of these parameter at the dual-packer and observation probe pressure responses by using general multilayer analytical solutions. Besides the main interpretation methodology of the WFT IPTTs will be demonstrated by considering synthetic tests. This includes identification of flow regimes, parameter estimation, and validation of the results.

1.4 Scope of Study

Wireline formation testing can be conducted by using a multiprobe or a packer-probe module. In this project, the scope of the study will be limited to packer-probe WFT module. Thus, throughout the analysis will be mainly involving packer-probe module data and interpretation. The methodology used in this study is valid for all inclination angles of a well by using methodology introduced by Pop et al. (1993), Kuchuk (1994), and Onur et al. (2011). Besides the reservoir system to be investigated in this study consists of a single layer as well as multi-layered system. In this project, both drawdown and buildup and variable-rate pressure-transient data will be considered for the analysis. The single-layer and multilayer analytical and numerical solutions [available in Ecrin, Eclipse, and the solution in the codes developed by Onur (2013)] will be used for this investigation.

Chapter 2
LITERATURE REVIEW

2.1 Packer-Probe Configuration

Figure 2-1 shows a schematic of a packer-probe WFT IPTT configuration. In this test, a dual-packer is set to isolate a section or reservoir across two straddle packers to create pressure diffusion. During the interference test, the dual-packer draws fluid while the vertical (observation) probes measure the pressure responses. Thickness of a reservoir often is very thick, results in the packed off thickness is always less than the thickness of the reservoir thickness. This creates a condition resemble partial penetration condition where spherical flow will occur early during the transient periods. The pressure disturbance will propagates spherically until one impermeable barrier such as a bed boundary is reached. The spherical flow regime will be altered and becomes hemispherical until another impermeable zone is detected to change the flow regime to radial. This is explained graphically in **Figure 2-2**. Radial flow regime usually is observed at the later stage of the test when the pressure disturbance hit the limiting bed boundaries. With the observed spherical and radial flow data, the horizontal and vertical permeability of the near wellbore region can be computed individually (Schlumberger, 2006). The packers allow zones to be tested where the probes cannot seal like fractured and fissured formations. The larger area of reservoir isolated, allows a greater flow rate to be achieved, increasing the depth of investigation to about 100ft (Ireland et al. 1992).

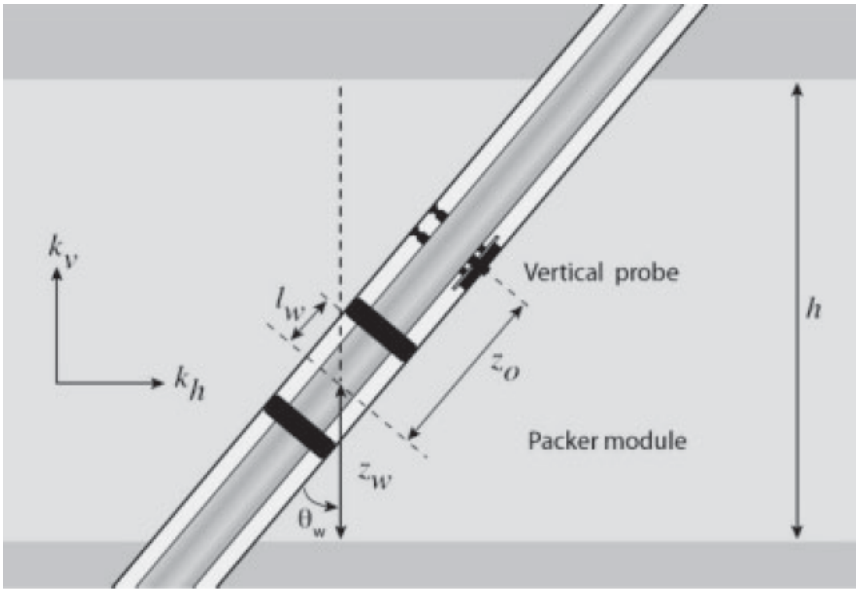

Figure 2-1: Schematic of a packer probe IPTT configuration in single layer system (Onur et al. 2011)

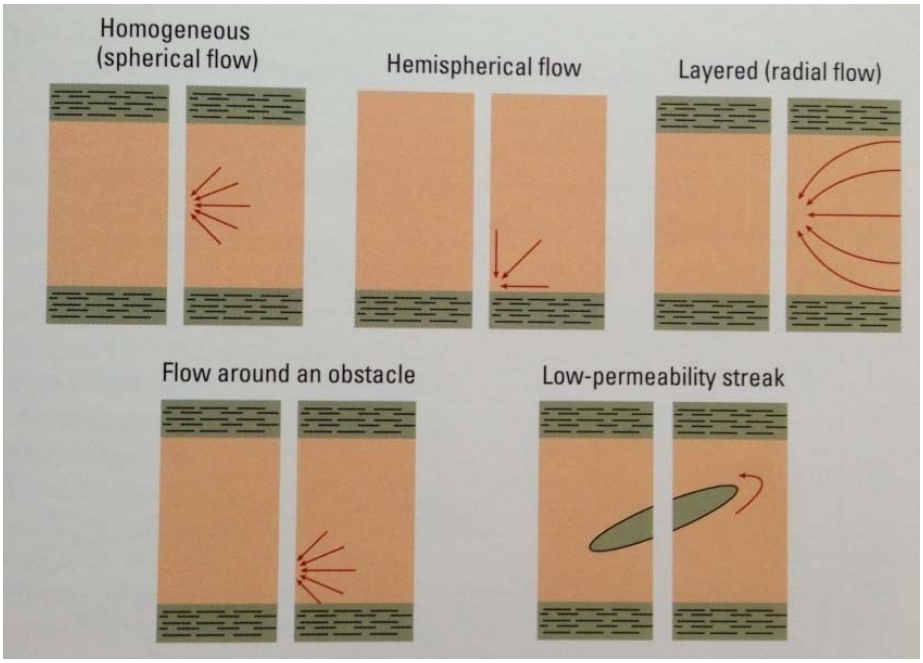

Figure 2-2: Samples of Flow Regimes (Schlumberger, 2006)

2.1.1 Flow Regime Identification

The first step of interpretation of packer-probe IPTT data always starts with flow regime identification. Correct flow regime identification is important for multiprobe formation tester because local heterogeneities tend to play a significant role in the observed pressure response. In this project, flow regime identification will be on the basis of pressure derivative analysis (Bourdet et al. 1989). He suggested that flow

regimes can have clear characteristic shapes if the pressure derivative rather than pressure is plotted versus time on log-log plot. Pressure derivative analysis offer the following advantages: (Ahmed & McKinney, 2005)

- Heterogeneities hardly visible on the conventional plot of well testing data are amplified on the derivative plot.
- Flow regimes have clear characteristic shapes on derivative plot.
- The derivative approach improves the definition of the analysis plots and therefore the quality of the interpretation.

In derivative approach, the time rate of change of pressure during a test period is considered for analysis and it is given by Bourdet et al. 1989, (Bourdet 2002) :

$$\Delta p' = \frac{dp}{d\ln\Delta t} = \Delta t \frac{dp}{d\Delta t} \qquad (2.1)$$

When the infinite acting radial flow regime is established, the derivative becomes constant. This regime does not produce a characteristic log-log shape on the pressure curve, but it can be identified when derivative of the pressure is considered. The radial flow is characterized by the following equation: (Bourdet, 2002)

$$\Delta p = 162.6 \frac{qB\mu}{kh}\left[\log\Delta t + \log\frac{k}{\phi\mu c_t r_w^2} - 3.23 + 0.87S\right] \qquad (2.2)$$

Differentiating this radial flow equation with the respect to time (Δt) by using the expression introduced by Bourdet et al. (1989) yields a constant term for the pressure derivative. Hence, in pressure derivative log-log plot, radial flow is identified as a constant horizontal line as shown in **Figure 2-3.**

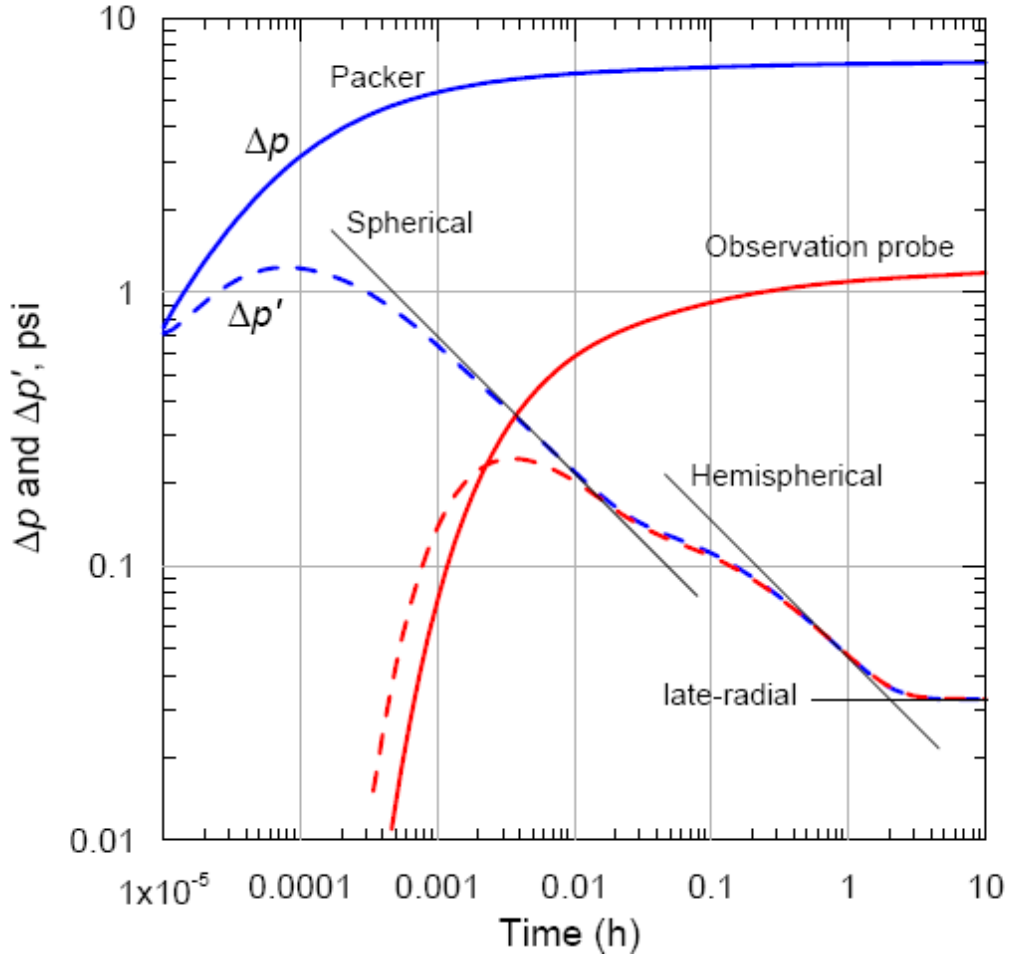

Figure 2-3: Example of Log-Log Derivative Plot of Packer Interval & Observation Probe Pressure Behaviour (Onur et al. 2004)

On the other hand, during the spherical flow regime, the shape of the log-log pressure curve is not characteristic. The derivative follows a straight line with a negative half-unit slope. The spherical flow due to limited entry is characterized by the Equation 2.3 for packer probe pressure change and Equation 2.4 for observation probe pressure change: (Onur et al. 2004)

$$\Delta p_p(t) = \frac{141.2q\mu}{k_h(2l_w)}\left[\frac{(2l_w)\sqrt{k_h/k_v}}{2r_{sw}} + s\right] - \frac{2453q\mu\sqrt{\phi c_t \mu}}{k_s^{3/2}}\frac{1}{\sqrt{t}} \quad (2.3)$$

$$\Delta p_o(t) = \frac{141.2q\mu}{2\sqrt{k_h k_v}(2l'_w)}\ln\left[\frac{z_o+l_w}{z_o+l_w}\right] - \frac{2453q\mu\sqrt{\phi c_t \mu}}{k_s^{3/2}}\frac{1}{\sqrt{t}} \quad (2.4)$$

Where r_{sw} is the effective spherical wellbore radius. If $l'_w >> r'_w$, r_{sw} given by

$$r_{sw} \approx \frac{2l'_w}{2\ln\left(\frac{4l'_w}{r'_w}\right)} \quad (2.5)$$

And l'_w is the half-length of the open interval in an equivalent isotropic formation defined by

$$l'_w = l_w\sqrt{(k_h/k_{v)}\cos^2\theta_w + \sin^2\theta_w} \quad (2.6)$$

And effective wellbore radius, r'_w is defined by

$$r'_w = (r_w/2)\left\{1 + \left[1/\sqrt{\cos^2\theta_w + (k_v/k_h)\sin^2\theta_w}\right]\right\} \quad (2.7)$$

When Equations 2.3 and 2.4 are expressed to the derivative expression introduced by Bourdet et al. (1989), the spherical flow exhibits a negative half-slope, on log-log plots of the packer and probe pressure-derivative data as shown in **Figure 2-3**.

2.1.2 Interpretation Methodology

The interpretation of the IPTT data is done by analyzing packer and each of the probe pressure data. Numerous authors had presented the analytical solutions to obtained permeability anisotropy in both single and multilayer systems reservoir.

Kuchuk et al. (2002) presented a mathematical model and analytical solution to interpret the pressure behavior of IPTT tests. The maximum likelihood (ML) method is presented for nonlinear parameter estimation to handle uncertainty in error variances in observed data. This paper proved the advantage of maximum likelihood method over weighted least squares method, maximum likelihood method eliminates the trial and error procedure required to determine appropriate weights to be used in the weight least square method. However, the solution will not be discussed here due to its complexities and difficulty.

Onur et al. (2004) presented a new approximate analytical equations for spherical flow, which is often exhibited by dual packer interval and observation probe. The analytical solutions provided by Onur et al. (2004) are valid for all inclination angles for a slanted well and provides a technique to estimate of determine the formation parameters from spherical flow exhibited by packer and probe pressure transient measurement in a single layer system. (Onur et al. 2004)

Onur et al. (2004) then further verify and refine the estimated formation parameter by using nonlinear regression. This nonlinear regression is as explained in Onur et al. (2000). This is especially important in variable rate cases during drawdown as well as for cases having distorted spherical flow regimes and transition data (Onur et al. 2004). This approximation technique is reported as highly accurate estimation. Besides, this paper also reported the benefits of inclusion of obervation probe pressures in determining a reliable individual values of horizontal and vertical permeabilities as well as inclination angle, provided that the storativity is known. This is due to the probe pressures are independent of tool storage and mechanical skin effects at packer interval and show significant sensitivity to well's inclination angle and permeabilities. Furthermore, Onur et al. (2004) also suggest that simultaneous matching packer and vertical probe pressures using nonlinear regression provides more confidence on the estimates of formation parameters because each set of data has different information content.

Onur et al. (2011) presented a new spherical-flow cubic analysis method to estimate horizontal and vertical permeability from pressure transient test data acquired at an observation probe of the dual packer probe for all inclination angles of the wellbore. However, this paper reported that for a slanted well case, the analysis procedure yields two possible solutions for the horizontal and vertical permeability. Therefore, one must use more information from core or pretest data to determine the correct solution for a slanted well. Besides, if the late radial flow data exist, one can also use these data to determine the appropriate solution. It is worth noticing that this new analysis method do not require the use of formation thickness and hence are very useful when formation thickness is not straight forward to determine because formation might consist of various flow units. For example a carbonate formation openhole log often is insufficient to differentiate adjacent layers with different permeability (Onur et al. 2011).

Very recently, Onur et al. (2013) presented a new infinite-acting radial-flow analysis procedure for estimating horizontal and vertical permeability solely from pressure transient data acquired at an observation probe during an interval pressure transient test (IPTT) conducted with a single-probe or dual-packer module. The procedure is based on an adaptation of a well-testing method presented by Prats (1970) for vertical wells with 2D permeability anisotropy. Onur et al. (2013) extended this method to all inclination angles of the wellbore in a single-layer, 3D anisotropic, homogeneous

porous medium. These equations provide new ways to determine both horizontal and vertical permeability from radial flow analysis procedure as the new analysis does not require that both spherical and radial flow prevail at the observation probe during the test. This new analysis has been tested with field and synthetic data and the result reported is promising. However, Prats' requirement of $\Delta Z_R > 25 r_w \sqrt{k_v/k_h}$ is reported to be important in the analysis, where when it is violated, error is seen in the k_v; k_h is always determine without error. ΔZ_R is the distance from the observation perforation to the producing perforation and in this packer-probe case $\Delta Z_R = z_o$. In the case of k_v exceeds k_h by a factor of two or more, the observation probe spacing may be designed to meet the Prats' requirement. Furthermore, Onur et al. (2013) also reported that for a dual-packer IPTT tests where analysis requirements on the length of the flowing interval are exceeded by a large margin, the synthetic and the field cases test show an error of less that 10% of estimated k_v value, which is acceptable.

Kasap et al. 1996 presented a formation rate analysis technique to interpret wireline formation tests combining drawdown and buildup analysis. The new pressure versus formation rate analysis is applied to three numerical and two field data sets and it performs as well as conventional spherical-flow, cylindrical or drawdown analysis. This new technique does not require determination of flow regimes or even separation of drawdown and buildup data (Kasap et al. 1996). Conventional analysis technique by using pseudo-steady-state drawdown, spherical buildup and cylindrical buildup to estimates formation permeabilities are also discussed in the paper. This paper also reported that conventional analysis techniques of using straight lines with small slopes are prone to errors. Besides, permeability obtained from conventional pressure transient analysis requires a very careful examination of pressure history and diagnostic plots to properly identifying flow regimes.

Chapter 3
METHODOLOGY

In this project, the analytical solutions presented by Onur et al.(2011) and Onur et al. (2013) will be adopted. These solutions involve spherical-flow cubic analysis and radial flow analysis methods to estimate horizontal and vertical permeability from pressure transient test data acquired at an observation probe of the dual packer probe for all inclination angles of the wellbore. These analytical solutions will be used to solve for horizontal permeability, vertical permeability and other formation parameters. Then, these methods based on these analysis procedures will be considered to investigate their validity and feasibility for tests conducted in multi-layered systems.

3.1 Pressure Transient Interpretation

Any pressure transient test interpretation starts with flow regime identification. For this purpose, a log-log plot of pressure change and its logarithmic pressure-derivative (Bourdet et al. 1989) data versus elapsed or superposition time functions is inspected for specific flow regimes (wellbore storage, spherical or radial flow, etc.) identification. Once these flow regimes are identified, special straight-line analysis methods based on the specific flow regimes identified on the log-log plot are performed for estimation of formation parameters such as horizontal, vertical permeability, etc. Then, these parameter estimates are used as initial guesses in more general analytical or numerical solutions to further refine these parameter estimates by history matching observed pressure transient data for the specific portions (usually buildup portions) of the test with the corresponding model data. The last stage of the data interpretation is to verify the results by inspecting the match of the pressure data recorded during the entire tests with the model data and also by comparing the parameter estimates obtained from pressure data analysis with those from other sources like log and core.

3.1.1 Flow Regimes Identification

Accurate flow regime identification is very important in analysing packer-probe pressure-transient data because local heterogeneities will significantly affect the pressure response. Furthermore, in all kind of well testing, wellbore storage effect must be identified to prevent analyzing the wellbore as the parameters of the reservoir. Presumably the data obtained are following a constant drawdown, a log-log plot of pressure derivative technique is used for flow regime identification. Example of the plot is as shown in **Figure 2-3** in the previous chapter. Flow regime is identified through the identification of the slope exhibit by the pressure derivative curve, where a -1/2 slope represent spherical flow and horizontal slope represent radial flow. The pressure derivative curve will be plot based on the centred difference approximation technique. The pressure derivative is given by (Bourdet D. 2002, Bourdet et al. 1989) :

$$\Delta P' = \frac{dP}{d\ln\Delta t} = \Delta t \frac{dP}{d\Delta t} \tag{3.1}$$

And by centred difference approximation:

$$\left(\Delta t \frac{dP}{d\Delta t}\right) i = \Delta ti \frac{P_{i+1} - P_{i-1}}{\Delta t_{i+1} - \Delta t_{i-1}} \tag{3.2}$$

However, Bourdet's data differentiation algorithm will be used in this project to build the pressure derivative curve. The algorithm uses three points, one point before and one after the point *i* of interest. It estimates left and the right slopes, and attributes their weighted mean to the point *i*. (Bourdet, 2002)

$$\frac{dp}{dx} = \frac{\left[\frac{\Delta p}{\Delta x}\right]_1 \Delta x_2 + \left[\frac{\Delta p}{\Delta x}\right]_2 \Delta x_1}{\Delta x_1 + \Delta x_2} \tag{3.3}$$

Software Ecrin uses the above algorithm to generate the pressure derivative curve and this formulation will be used to generate the derivative curve for all data sets considered for this project.

3.1.2 Parameters Estimation

After the flow regime has been identified, the spherical and radial-flow time interval will be used to estimates the formation parameters.

3.1.2.1 Spherical-Flow Cubic Analysis Procedure for Drawdown Tests

If the observation probe data exhibit spherical flow regime, Onur et al. (2011) spherical-flow cubic analysis procedure will be used to estimates formation permeabilities for an inclined well having any inclination angle including vertical and horizontal wells. The analytical solution for the pressure drop at the observation probe caused by a constant-rate production at the dual-packer interval is given by (Onur et al. 2011)

$$\Delta p_o(t) = p_{i,o} - p_{wf,o}(t)$$
$$= \frac{141.2q\mu}{4\sqrt{k_h k_v}(l'_w)} \ln\left[\frac{z_o+l_w}{z_o-l_w}\right] - \frac{2453q\mu\sqrt{\phi\mu C_t}}{k_s^{3/2}} \frac{1}{\sqrt{t}} \quad (3.4)$$

Therefore, a Cartesian plot of pressure, $\Delta p_o(t)$ vs. time function , $\frac{1}{\sqrt{t}}$ at the identified spherical flow time interval will be use to obtained the gradient to compute the spherical permeability k_s. The intercept , $a_{1/\sqrt{t=0}}$ will be used to solve the following equation :

$$\frac{\sqrt{k_h k_v}\, l'_w}{l_w} = \frac{141.2q\mu}{4l_w\, a_{1/\sqrt{t=0}}} \ln\left[\frac{z_o+l_w}{z_o-l_w}\right] \quad (3.5)$$

Computed $\sqrt{k_h k_v}\, l'_w/l_w$ and k_s are used to solve the cubic equation for horizontal permeability, k_h introduced by Onur et al. (2011) .

$$\cos^2\theta_w k_h^3 - \left(\frac{\sqrt{k_h k_v}\, l'_w}{l_w}\right)^2 k_h + k_s^3 \sin^2\theta_w = 0 \quad (3.6)$$

This cubic equation applies for all inclination angles from $0^0 to\ 90^0$. The solution for the cubic equation depends on the inclination angle θ_w. Onur et al. (2011) categorize this into 3 different cases namely:

Case 1 – Vertical well ($\theta_w = 0^0$)

Case 2 – Horizontal well ($\theta_w = 90^0$)

Case 3 – Slanted well ($0^0 < \theta_w < 90^0$)

The solution for these 3 cases is throughly explained by Onur et al. (2011). Thus, by having $k_h\ and\ k_s$, vertical permeability k_v can be compute by:

$$\frac{k_s^3}{k_h^2} = k_v \tag{3.7}$$

It should be noted that in this study, only the vertical well cases are considered.

3.1.2.2 Spherical-Flow Cubic Analysis Procedure for Buildup Tests

The analytical solution for the pressure drop at the observation probe caused by buildup test following a constant-rate production during spherical-flow regime is computed from superposition of two constant-rate drawdown solutions. The analytical solution is :

$$P_{ws,o}(\Delta t) = P_{i,o} - \frac{2453 q\mu\sqrt{\phi c_t \mu}}{k_s^{3/2}} t_{bs} \tag{3.8}$$

Where

$$t_{bs} = \frac{1}{\sqrt{\Delta t}} - \frac{1}{\sqrt{t_p + \Delta t}} \tag{3.9}$$

Therefore, a Cartesian plot of pressure vs. spherical time function , $\frac{1}{\sqrt{\Delta t}} - \frac{1}{\sqrt{t_p+\Delta t}}$ at the identified spherical flow time interval will be use to obtained the gradient to compute the spherical permeability k_s. The intercept is expect to be the $P_{i,o}$ and will be used to solve the following equation :

$$\frac{\sqrt{k_h k_v}\, l'_w}{l_w} = \frac{141.2 q\mu}{4 l_w P_{i,o} - P_{wf,os} - m_{sp}/\sqrt{t_p}} \ln\left[\frac{z_o + l_w}{z_o - l_w}\right] \tag{3.10}$$

Similarly, computed $\sqrt{k_h k_v}\, l'_w / l_w$ and k_s are used to solve the cubic equation for

horizontal permeability, k_h introduced by Onur et al. (2011) .

$$\cos^2\theta_w k_h^3 - \left(\frac{\sqrt{k_h k_v}\, l'_w}{l_w}\right)^2 k_h + k_s^3 \sin^2\theta_w = 0 \qquad (3.11)$$

Similar with drawdown data analysis, by having k_h *and* k_s , vertical permeability k_v can be computed.

3.1.2.3 Radial-Flow Analysis Procedure for Drawdown Tests

If the observation probe data exhibit radial flow regime, then Onur et al. (2013) radial flow analysis procedure will be used to estimate horizontal and vertical permeability for an inclined well having any inclination angle including vertical and horizontal wells. The analytical solution for the pressure drop at the observation probe caused by a constant-rate production at the dual-packer interval is given by (Onur et al. 2013)

$$P_{i,o} - P_{wf,o}(t) = m \log t + b \qquad (3.12)$$

Where,

$$m = 162.6 \frac{q\mu}{k_h h} \qquad (3.13)$$

and

$$b = 162.6 \frac{q\mu}{k_h h}\left[\frac{G^* + \frac{h}{\sqrt{\cos^2\theta_w + (k_v/k_h)\sin^2\theta_w}|z_0|}}{2.303} + \log\left(\frac{0.0002637 k_v}{\phi\mu c_t h^2}\right)\right] \qquad (3.14)$$

Therefore, a semi-log plot of $P_{i,o} - P_{wf,o}(t)$ against t will yield a slope, m at the radial-flow regime time interval and the intercept, b. Horizontal permeability, k_h can be solve by using the slope, m. Vertical permeability can be obtained by solving the following expression by graphical method which involves plotting $f(k_v)$ versus k_v or by Newton-Raphson iteration method :

$$f(k_v) = b - 162.6 \frac{q\mu}{k_h h}\left[\frac{G^* + \frac{h}{\sqrt{\cos^2\theta_w + (k_v/k_h)\sin^2\theta_w}|z_0|}}{2.303} + \log\left(\frac{0.0002637 k_v}{\phi\mu c_t h^2}\right)\right] =$$

$$0 \qquad (3.15)$$

Where

$$G^* = \frac{1}{\tilde{Z}+\tilde{Z}'} - 2\ln 2 - \gamma - \frac{1}{2}\sum_{i=1}^{4}\Psi\left(\frac{\tilde{a}_i+1}{2}\right) \quad (3.16)$$

and

$$\tilde{Z} = (z_w + \sqrt{\cos^2\theta_w + (k_v/k_h)\sin^2\theta_w}\, z_o)/\, h \text{ , and } \tilde{Z}' = z_w/h \quad (3.17)$$

and

$$\tilde{a}_1 = 1 + \tilde{Z} + \tilde{Z}';\ \tilde{a}_2 = 1 + \tilde{Z} - \tilde{Z}';\ \tilde{a}_3 = 1 - \tilde{Z} + \tilde{Z}';\ \tilde{a}_4 = 1 - \tilde{Z} - \tilde{Z}' \quad (3.18)$$

and

$$|z_o| > \frac{12.5 r_w\sqrt{k_v/k_h}}{\sqrt{\cos^2\theta_w+(k_v/k_h)\sin^2\theta_w}}\left(1 + \frac{1}{\sqrt{\cos^2\theta_w+(k_v/k_h)\sin^2\theta_w}}\right) \quad (3.19)$$

In this work, only vertical well cases, where $\theta_w = 0$ is being considered.

3.1.2.4 Radial-Flow Analysis Procedure for Buildup Tests

The analytical solution for the pressure drop at the observation probe caused by buildup test following a constant-rate production is computed by subtracting the drawdown solution evaluated at time $t = t_p$ from the build up response of superposition of two constant-rate drawdown solutions. Hence, the analytical solution is :

$$P_{ws,o}(\Delta t) - P_{wf,o}(t_p) = m\log\left[\frac{t_p\Delta t}{t_p+\Delta t}\right] + b \quad (3.20)$$

Similarly,

$$m = 162.6\frac{q\mu}{k_h h} \quad (3.21)$$

and

$$b = 162.6\frac{q\mu}{k_h h}\left[\frac{G^*+\frac{h}{\sqrt{\cos^2\theta_w+(k_v/k_h)\sin^2\theta_w}|z_o|}}{2.303} + \log\left(\frac{0.0002637 k_v}{\phi\mu c_t h^2}\right)\right] \quad (3.22)$$

Since only vertical well cases, where $\theta_w = 0$ is being considered in this work, Equation 3.22 can be express as :

$$b = 162.6\frac{q\mu}{k_h h}\left[\frac{G^*+h/|z_o|}{2.303} + \log\left(\frac{0.0002637 k_v}{\phi\mu c_t h^2}\right)\right] \quad (3.23)$$

Therefore, a semi-log plot of $P_{ws,o}(\Delta t) - P_{wf,o}(t_p)$ against $\frac{t_p \Delta t}{t_p + \Delta t}$ will yield a slope, m at the radial-flow regime time interval and the intercept, b. Horizontal permeability, k_h can be solve by using the slope, m. Similar as drawdown analysis procedures, vertical permeability can be obtained by solving the following expression by graphical method which involves plotting $f(k_v)$ versus k_v or by Newton-Raphson iteration method :

$$f(\mathrm{k_v}) = \mathrm{b} - 162.6\frac{\mathrm{q\mu}}{\mathrm{k_h h}}\left[\frac{\mathrm{G^* + \frac{h}{\sqrt{\cos^2\theta_w + (k_v/k_h)\sin^2\theta_w}|z_0|}}}{2.303} + \log\left(\frac{0.0002637\mathrm{k_v}}{\phi\mu\mathrm{c_t h^2}}\right)\right] =$$

$$0 \qquad (3.24)$$

This radial-flow analysis is based on the assumption of a zero-radius well (Onur et al. 2013). For the method to apply to a finite-radius wellbore,

$$|\Delta Z_R| > 25 r_w \sqrt{k_v/k_h} \qquad (3.25)$$

This methodology will be used for both packer probe and vertical observation probe pressure data (drawdown and buildup data) obtained from an inclined well having any inclination angle including vertical and horizontal wells. All the above slope calculation will be based on least-squares regression fitting method.

3.2 Multi-layered System Interpretation

In a multi-layered system, the same methodology as applied in single layer system will be applied here to describe multi-layered system formation parameters. In order to simulate the multi-layered system, the layers permeabilities are generated by using a log-normal distribution with specified mean and variance. Equation 3.26 and 3.27 shows the input mean and variances to generate log-normal distribution layers permeabilities.

$$\mu_{lnk} = ln\mu_k - \frac{1}{2} ln\left(1 + \frac{\sigma_k^2}{\mu_k^2}\right) \qquad (3.26)$$

$$\sigma_{lnk}^2 = \ln\left(1 + \frac{\sigma_k^2}{\mu_k^2}\right) \quad (3.27)$$

The level of heterogeneity of the generated layers permeabilities is characterized by using Dykstra-Parsons Coefficient (Dykstra & Parsons, 1950):

$$V = \frac{k_{50} - k_{84.1}}{k_{50}} \quad (3.28)$$

The generated permeabilities are average into one single k_h and k_v to describe the reservoir. Averaging permeability can be done by using arithmetic averaging :

$$k_{avg} = \frac{\sum_{i=1}^{n} k_i.h_i}{h} \quad (3.29)$$

Or averaging permeablity can also be done by using harmonic averaging :

$$k_{avg} = \frac{\sum_{i=1}^{n} h_i}{\sum_{i=1}^{n} \frac{h_i}{k_i}} \quad (3.30)$$

Or by using geometric averaging :

$$k_{avg} = exp\left[\frac{\sum_{i=1}^{n}(h_i \ln(k_i))}{\sum_{i=1}^{n} h_i}\right] \quad (3.31)$$

Further work such as matching pressure response of this single layer representation of multi-layered system will be done to evaluate the feasibility of this representation. Besides, a sensitivity study with respect to various flow parameters like layer horizontal and vertical permeability and thickness will be conducted to see the effects of these parameters at the dual-packer and observation probe pressure responses.

3.3 Key Milestones

The key milestone in this project mainly focuses in several sections in order to ensure the objective of the project can be achieved within the time period. The key milestones identified in this project are:

1. Sufficient literature review before starting the project
    - Sufficient information should be gathered from any journals, books and others regarding the research topic before starting to conduct any analysis works
2. Design of the methodology
    - The proper methodology should be designed based on the information gained from the literature review.
    - Data and tools required should be made available prior to the beginning of analysis work
    - The analytical solution for analysis pressure-transient data should be identified and adopted from other authors.
3. Data analysis and validation works
    - Data obtained from synthetic data or field data will be analyzed and used to estimating the result.
    - Estimated parameters will be validated with simulation works
4. Documentation of project
    - Results and discussion made from the analysis obtained will be reported
    - Further discussion made on the recommendation for the project future works

Table 3-1: Gantt Chart for FYP II

NO	DETAIL / WEEK	1	2	3	4	5	6	7		8	9	10	11	12	13	14
1	Generating and collecting synthetic and field data		■													
2	Analysing synthetic and field data (Single Layer)															
3	Estimating parameters and validating (Single Layer)															
4	Analysing synthetic and field data (Multi-Layered)															
5	Estimating parameters and validating (Multi-Layered)															
6	Single layer representation and conclude findings									■						
7	Pre-SEDEX & Preparation															
8	Submission of Draft Report															
9	Submission of Softbound Dissertation															
10	Submission of Technical Paper															
11	Oral Presentation															
12	Submission of Final Project Dissertation															■

- Suggested Milestone

Chapter 4
RESULT AND DISCUSSION

4.1 Single-Layer Reservoir System

To demonstrate the applicability of the adopted solutions, synthetic packer-probe IPTTs data will be used.

4.1.1 Synthetic IPTT Example 1

The input parameters used to simulate an IPTT via a dual-packer tool and a single vertical-observation probe is as shown in **Table 4-1**

Table 4-1: Input Parameters for Synthetic IPTT for Example 1

ϕ (Fraction)	0.15
h (ft)	80
c_t (psi^{-1})	1.0×10^{-5}
μ (cp)	1.5
r_w (ft)	0.354
S (Dimensionless)	1.0
C_w (B/psi)	1.0×10^{-6}
l_w (ft)	1.6
k_h (md)	40
k_v (md)	10
$P_{i,o}$ (psi)	1500.0
$P_{wf,os}$(psi)	1492.9
z_w(ft)	40
z_o(ft)	6.4
q (B/D)	10
θ_w(Degrees)	0

To observe both spherical flow and radial flow in this test, the formation thickness is

set at 80 ft, large enough to ensure spherical flow regime prevailed throughout the test and the test consisted of 2 hours flowing period followed by 2 hours buildup, sufficient for radial flow regime to prevail in the test. **Figure 4-1** shows the test pressure data for observation probe 1. **Figure 4-2** shows the diagnostic log-log plot of buildup pressure change and derivative at the packer interval and observation probe. The packer and probe buildup data exhibit a clear negative half-slope from Δt= 0.24 to Δt= 0.32 hours. **Figure 4-3** displays the observation.probe buildup pressure on a spherical-flow plot for buildup. And slope of $m_{sp} = -0.43$ and the intercept $a_{tbs=0} = 1496.81psi$ are determined. Spherical cubic-analysis as explained in methodology part is used to analyze the observation probe data. As expected, due to the well is a vertical well, only one positive root, with $k_h = 40.21md$ (Error by 0.53%) is obtained. The analysis has also obtained $k_v = 10.19md$ (Error by 1.9%). These values are very close to the input values given in **Table 4-1**. A drawdown spherical-flow analysis has also carried out (due to this is a synthetic data with constant drawdown of 10 B/D for 2 hours), $k_h = 39.74md$ (Error by 0.65%) and $k_v = 9.74\ md$ (Error by 2.6%) are obtained. The good agreement of the input values and computed values has proved the feasibility of the adopted solution for single layer reservoir system.

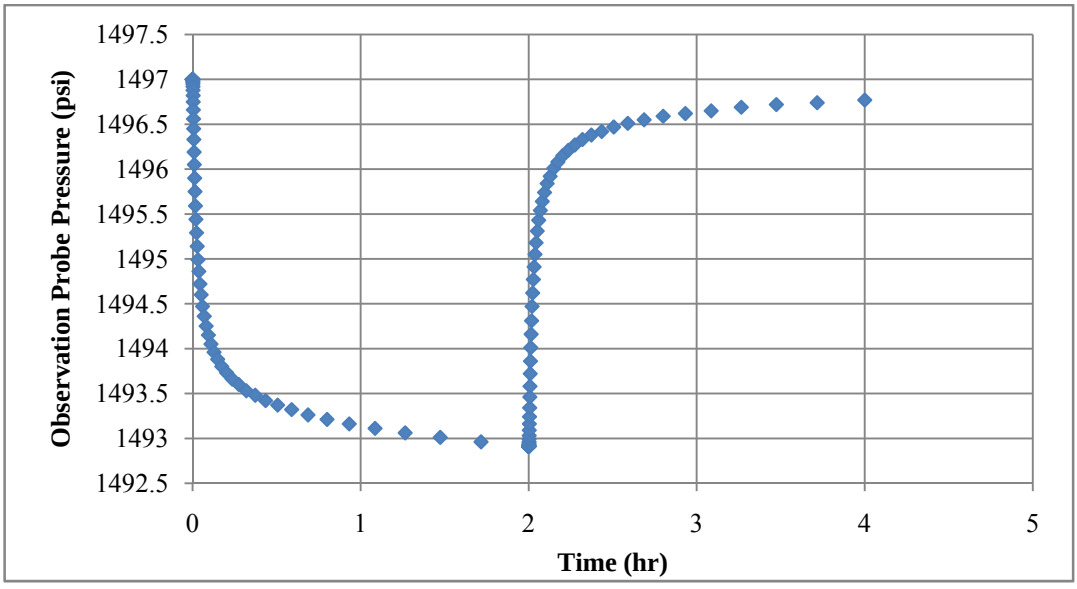

Figure 4-1 : Pressure Response for Observation Probe 1, Example 1

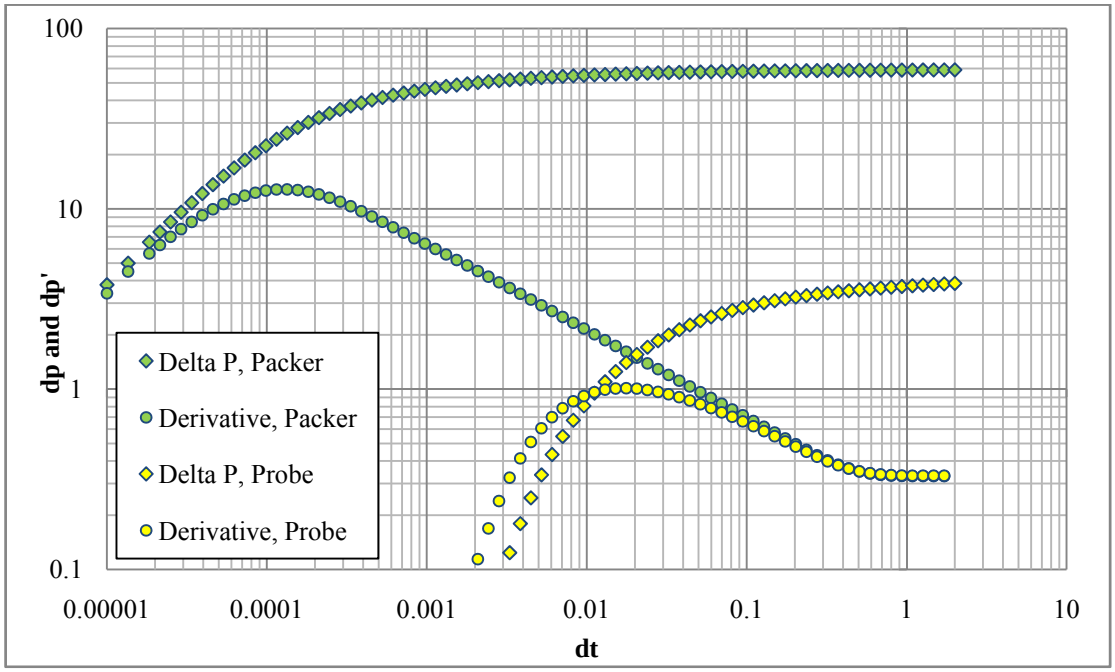

Figure 4-2: Pressure change and derivative at the packer interval and observation probe during buildup, Example 1

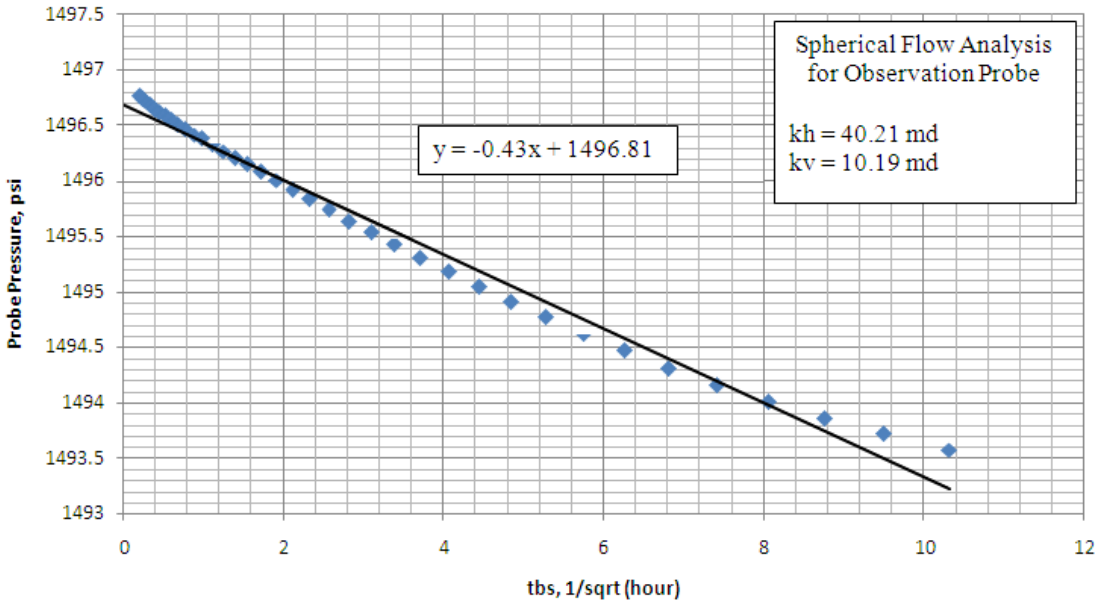

Figure 4-3 : Spherical-flow plot for buildup of observation probe, Example 1

Besides, radial-flow analysis as explained in methodology part is used to analyse the observation probe data as well. For this example, $\Delta Z_R = 6.4\ ft$ and $25 r_w \sqrt{k_v/k_h} = 4.43\ ft$, so the requirement of Equation 3.25 is met. From **Figure 4-2**, the system

reaches radial flow after 1.0 hours of buildup. **Figure 4-4** presents the radial-flow plot from which the slope m=-0.749 and intercept, b=3.859 is obtained. Using the steps explained in methodology section, values of k_h and k_v are computed where $k_h = 39.96md$ (Error by 0.1%) and $k_v = 13.0md$ (Error by 30.0%) is obtained through plotting $f(k_v)$ versus k_v as shown in **Figure 4-5**. These values are very close to the input values given in **Table 4-1**. A drawdown analysis has also carried out (due to this is a synthetic data with constant drawdown of 10 B/D for 2 hours), $k_h = 40.00md$ (Error by 0.0%) and $k_v = 13.0\,md$ (Error by 30.0%) are obtained. The good agreement of the input values and computed values has proved the feasibility of the adopted solution for single-layer reservoir system.

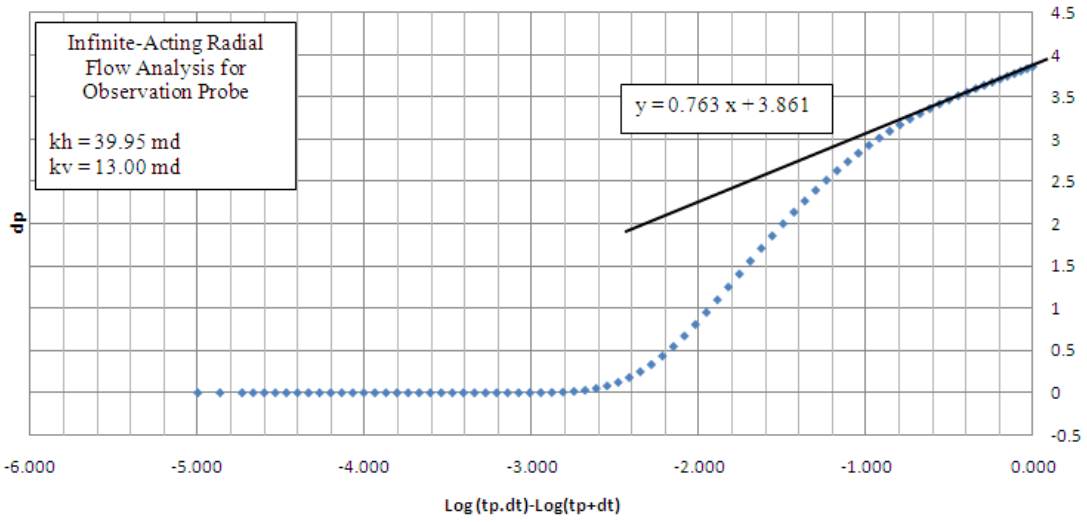

Figure 4-4 : Radial flow (Or Horner) plot for buildup of observation probe, Example 1

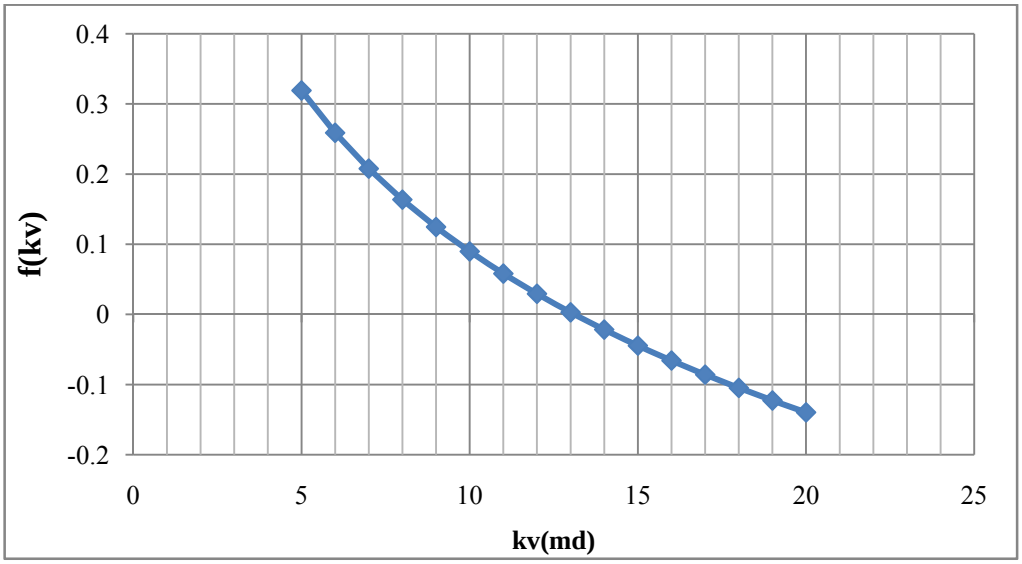

Figure 4-5 : $f(k_v)$ vs. k_v , Example 1

4.1.2 Synthetic IPTT Example 2

Example 2 will demonstrate the importance of meeting the requirement of Equation 3.25. Synthetic IPTT Example 2, the input parameters used to simulate the IPTT is as shown in **Table 4-2.**

Table 4-2: Input Parameters for Synthetic IPTT for Example 2

ϕ (Fraction)	0.15
h (ft)	80
c_t (psi^{-1})	1.0×10^{-5}
μ (cp)	1.5
r_w (ft)	0.354
S (Dimensionless)	1.0
C_w (B/psi)	1.0×10^{-6}
l_w (ft)	1.6
k_h (md)	40
k_v (md)	40
$P_{i,o}$ (psi)	1500.0
$P_{wf,os}$(psi)	1492.43
z_w(ft)	44
z_o(ft)	6.4
q (B/D)	10
θ_w(Degrees)	0

The formation thickness is set at 80 ft, large enough to ensure spherical flow regime prevailed throughout the test and the test consisted of 2 hours flowing period followed by 2 hours buildup, sufficient for radial flow regime to prevail in the test. **Figure 4-6** shows the test pressure data for observation probe 1. **Figure 4-7** shows the diagnostic log-log plot of buildup pressure change and derivative at the packer interval and observation probe. The packer and probe buildup data exhibit a clear negative half-slope at Δt= 0.04 hours. **Figure 4-8** displays the observation probe buildup pressure on a spherical-flow plot for buildup. And slope of $m_{sp} = -0.208$ and the intercept $a_{tbs=0} = 1496.48psi$ are determined. Spherical cubic-analysis as explained in methodology part is used to analyse the observation probe data. As expected, due to the well is a vertical well, only one positive root, with $k_h = 40.32md$ (Error by 0.8%) is obtained. The analysis has also obtained $k_v = 43.31md$ (Error by 8.3%). These values are very close to the input values given in **Table 4-2**. A drawdown spherical-flow analysis has also carried out (due to this is a synthetic data with constant drawdown of 10 B/D for 2 hours), $k_h = 40.18md$ (Error by 0.5%) and $k_v = 43.61\ md$ (Error by 9.0%) are obtained. The good agreement of the input values and computed values has proved the feasibility of the adopted solution for single layer reservoir system.

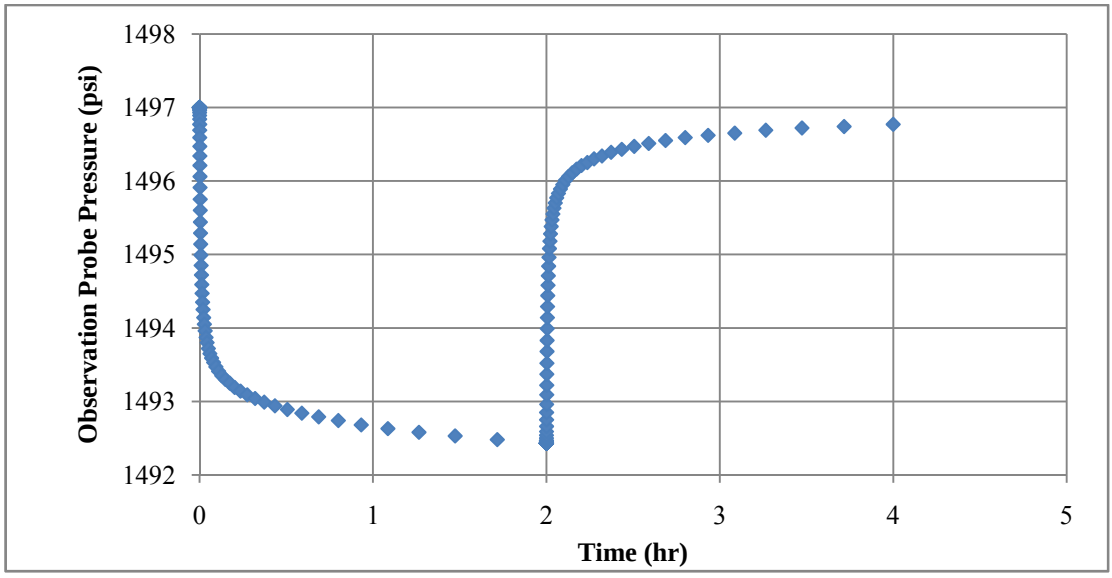

Figure 4-6: Pressure Response for Observation Probe 1, Example 2

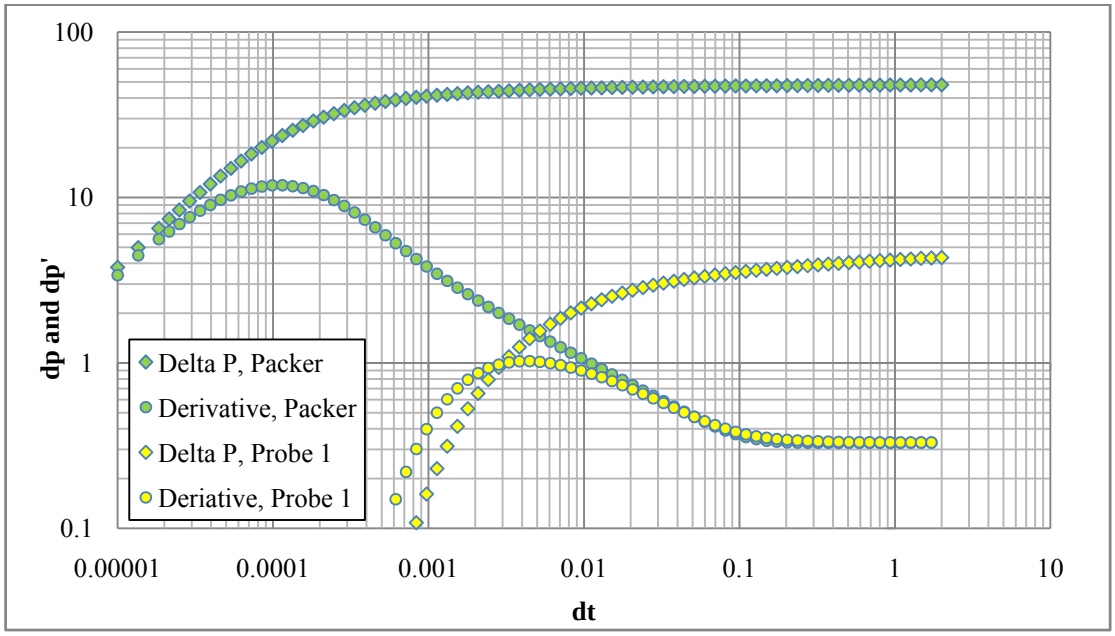

Figure 4-7: Pressure change and derivative at the packer interval and observation probe during buildup, Example 2

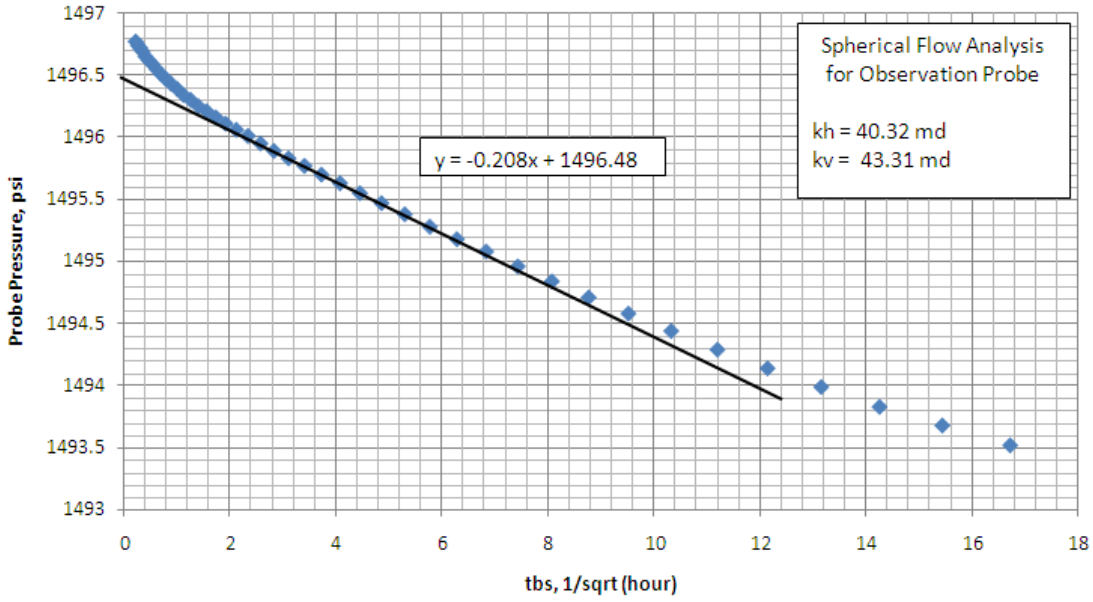

Figure 4-8 : Spherical-flow plot for buildup of observation probe, Example 2

Radial-flow analysis used to analyse the observation probe data as well. For this example, $\Delta Z_R = 6.4\ ft$ and $25 r_w \sqrt{k_v/k_h} = 8.85\ ft$, so the requirement of Equation 3.25 is not met. From **Figure 4-7**, the system reaches radial flow after 0.51 hours of buildup. **Figure 4-9** presents the radial-flow plot from which the slope *m*=-0.762 and

intercept, b=4.338 is obtained. Using the steps explained in methodology section, values of k_h and k_v are computed where $k_h = 40.0md$ and $k_v = 60.0md$ is obtained through plotting $f(k_v)$ versus k_v as shown in **Figure 4-10**. k_h obtained is very close to the input values given in **Table 4-2**, whereas k_v obtained is in error by 33.3%. A drawdown analysis has also carried out (due to this is a synthetic data with constant drawdown of 10 B/D for 2 hours), $k_h = 40.0md$ and $k_v = 60.0\ md$ (Error by 33.3%) are obtained. This error is caused by the failure to meet the requirement of Equation 3.25 where there is not enough of probe separation.

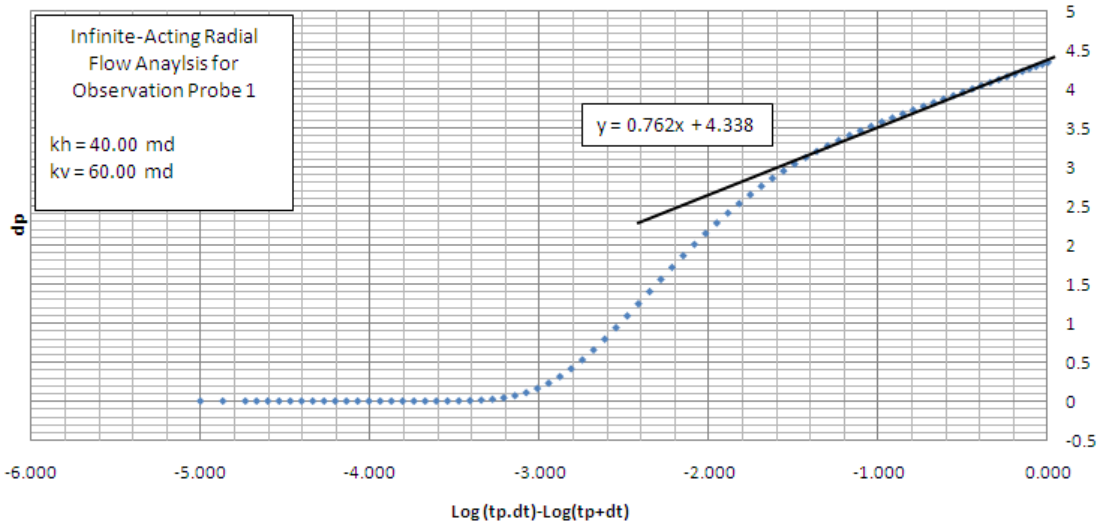

Figure 4-9 : Radial flow (Or Horner) plot for observation probe, Example 2

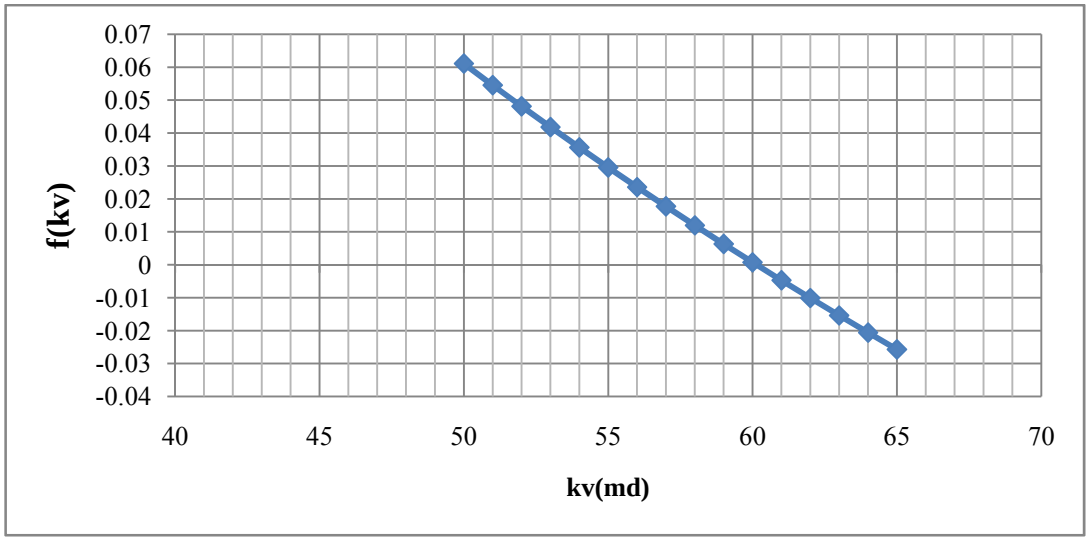

Figure 4-10 : $f(k_v)$ vs. k_v , Example 2

4.1.3 Synthetic IPTT Example 3

Example 3 was generated using the same input as Example 2, except the probe separation, z_o was change to $z_o = 14.4\,ft$ in order to meet the requirement of Equation 3.25.

For this example, $\Delta Z_R = 14.4\,ft$ and $25r_w\sqrt{k_v/k_h} = 8.85\,ft$, so the requirement of Equation 3.25 is met. **Figure 4-11** shows the test pressure data for observation probe. From **Figure 4-12**, the system reaches radial flow after 1.0 hours of buildup. **Figure 4-13** presents the radial-flow plot for buildup from which the slope *m*=-0.762 and intercept, *b*=1.996 is obtained. Using the steps explained in methodology section, values of $k_h\,and\,k_v$ are computed where $k_h = 40.0md$ (0.0% error) and $k_v = 40.9md$ (Error by 2.3%) is obtained through plotting $f(k_v)$ versus k_v as shown in **Figure 4-14**. A drawdown analysis has also carried out (due to this is a synthetic data with constant drawdown of 10 B/D for 2 hours), $k_h = 40.0md$ (0.0% error) and $k_v = 40.9\,md$ (Error by 2.3%) are obtained. This example suggests that meeting the requirement of Equation 3.25 reduce the magnitude error of k_v estimation.

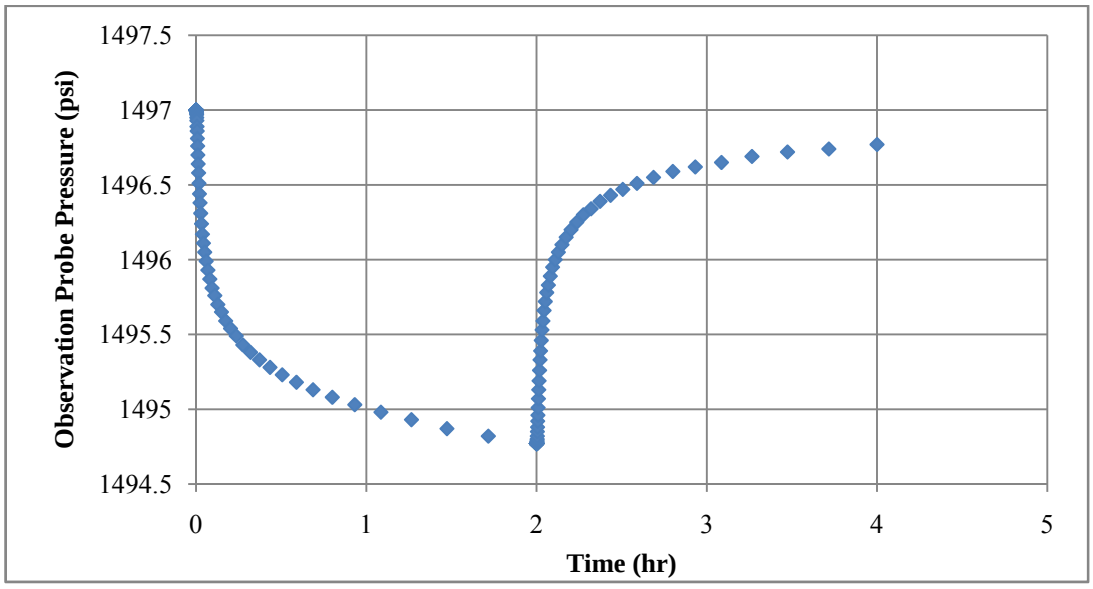

Figure 4-11: Pressure Response for Observation Probe 1, Example 3

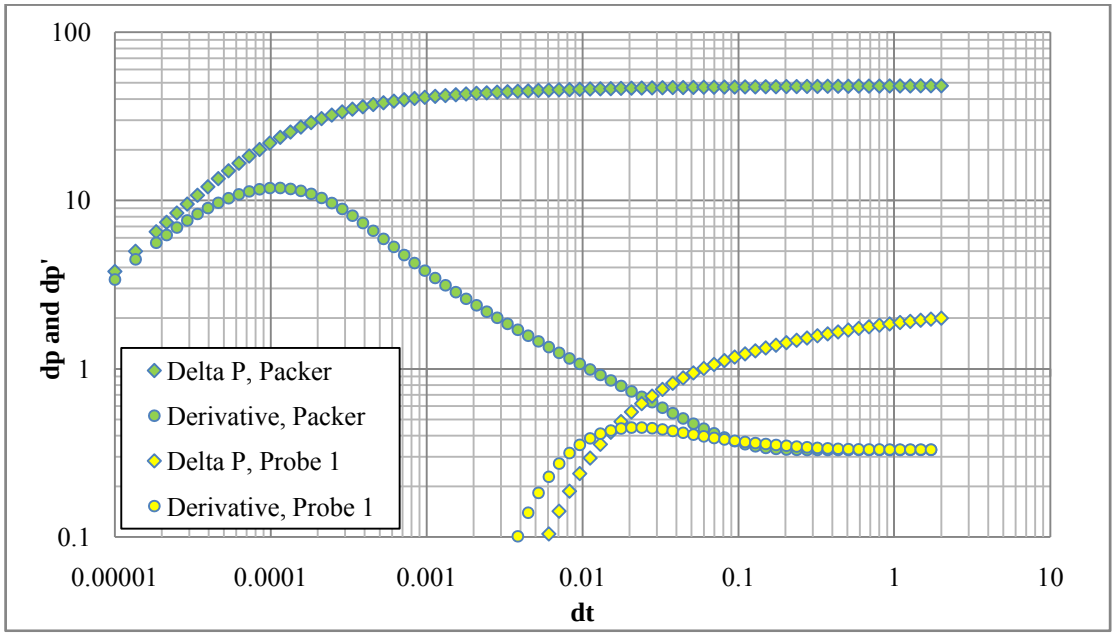

Figure 4-12: Pressure change and derivative at the packer interval and observation probe during buildup, Example 3

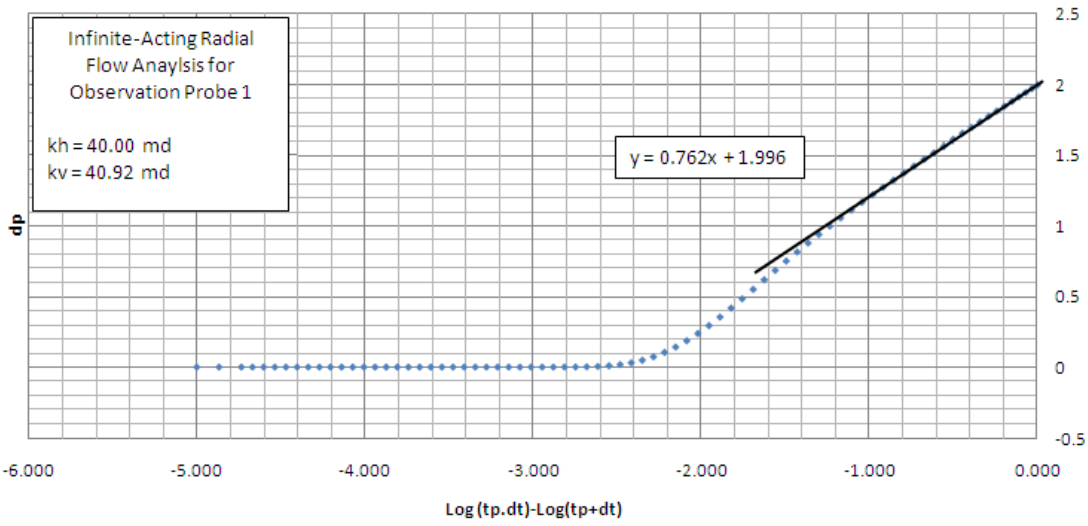

Figure 4-13: Radial flow (Or Horner) plot for observation probe, Example 3

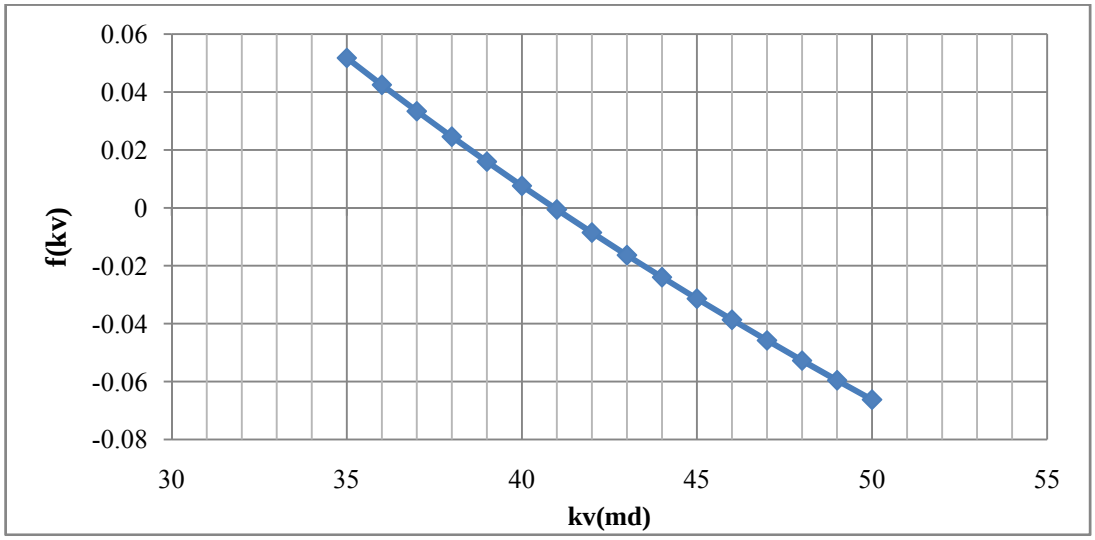

Figure 4-14: $f(k_v)$ vs. k_v , Example 3

4.2 Multi-Layered Reservoir System

To evaluate the application of Onur et al (2011) and Onur et al. (2013) methods for analysis of pressure data acquired at a multi-layered reservoir system, a number of synthetic cases have been analysed; we present four cases here. All the synthetic data are generated by using solution in codes developed by Onur (2013) for dual-packer tool. To access the applicability of the above mentioned methods in multi-layered reservoir system, all cases evaluated are reservoir system with different heterogeneity level. In here, we measured the heterogeneity level by using Dykstra-Parsons coefficient (VDP), which is an indicative of variance in permeability (Dykstra & Parsons, 1950). A reservoir is considered to be completely heterogeneous with a coefficient of 1 and coefficient of 0 refers to a completely homogeneous reservoir.

4.2.1 Case 1, Heterogeneity of Dykstra-Parsons Coefficient = 0.05

Synthetic IPTT Case 1, the input parameters used to simulate the IPTT is using the same input as Example 1 except the following parameters in **Table 4-3** and **Table 4-4**:

Table 4-3: Input Parameters for Synthetic IPTT for Case 1

No. of layers	11
Source layer	6
h (ft)	88
z_w(ft)	44
$z_{o,Probe\ 1}$(ft)	6.4
$z_{o,Probe\ 2}$(ft)	14.4

Table 4-4 : Permeability Input for Synthetic IPTT for Case 1

Layers	**h (ft)**	**k_h (md)**	**k_v (md)**
1	8.00	97.85	9.27
2	8.00	99.53	9.43
3	8.00	93.14	9.77
4	8.00	101.33	10.18
5	8.00	97.69	9.69
6	8.00	100.87	9.28
7	8.00	94.49	10.54
8	8.00	100.86	10.53
9	8.00	98.15	10.02
10	8.00	104.58	10.39
11	8.00	111.72	11.02
Arithmetic Average		100.02	10.01
Harmonic Average		99.80	9.98
Geometric Average		99.91	10.00

The test consisted of a 6-hours flowing period followed by a 6-hours buildup. The heterogeneity level for this case is measured at 0.05 by Dykstra-Parsons coefficient. **Figure 4-15** shows the test pressure data for observation probe 1. **Figure 4-16** shows the diagnostic log-log plot of buildup pressure change and derivative at the packer interval and observation probes. The packer and probe 1 buildup data exhibit a clear negative half-slope at Δt= 0.33 hours to Δt= 0.45 hours. **Figure 4-17** displays the observation probe 1 buildup pressure on a spherical-flow plot. And slope of $m_{sp} = -0.164$ and the intercept $a_{tbs=0} = 1496.85psi$ are determined. Spherical cubic-analysis resulted with $k_h = 102.58md$ (Error by 2.56%) and $k_v = 10.76md$ (Error by 7.49%). These values are very close to the averages of the input values given in **Table 4-4**. A drawdown spherical-flow analysis has also carried out (due to this is a synthetic data with constant drawdown of 10 B/D for 6 hours), $k_h = 100.63md$

(Error by 0.61%) and $k_v = 9.60\,md$ (Error by 4.10%) are obtained. The good agreement of the input values and computed values has proved the feasibility of the adopted solution for multi-layered reservoir system with heterogeneity of 0.05 by Dykstra-Parsons coefficient.

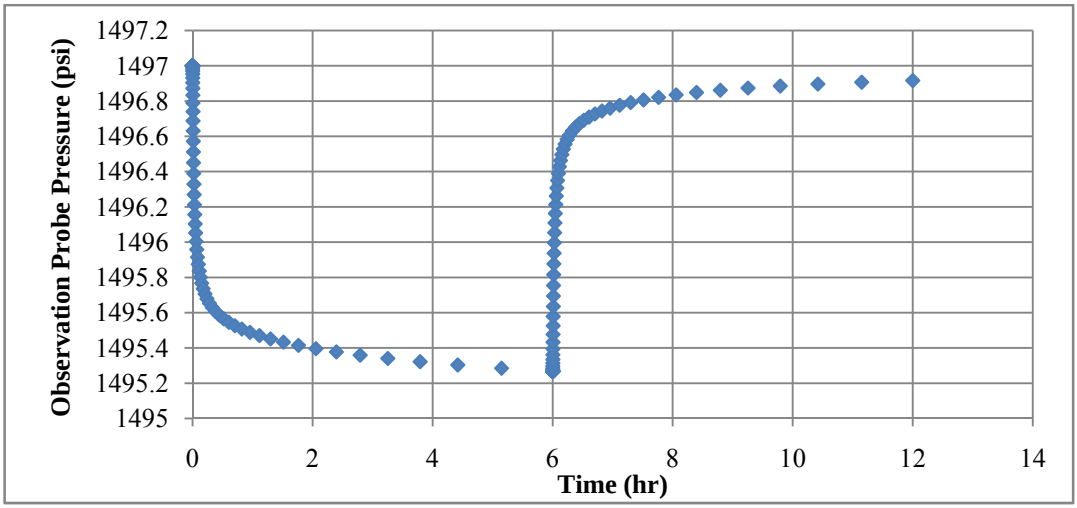

Figure 4-15: Pressure Response for Observation Probe 1, Case 1

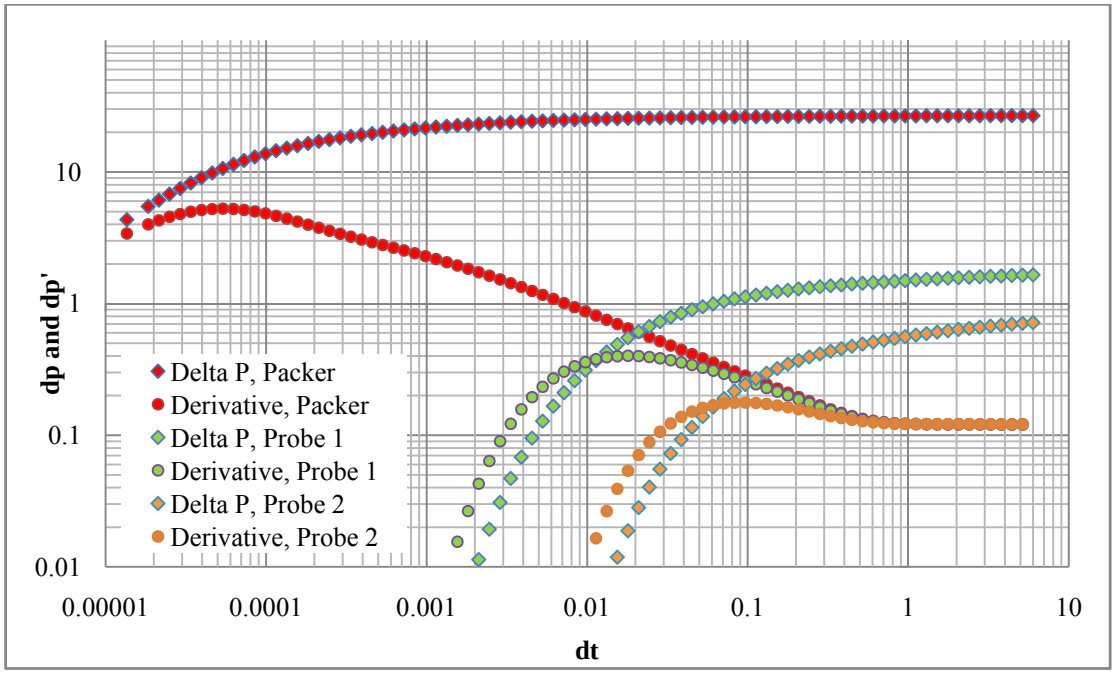

Figure 4-16 : Pressure change and derivative at the packer interval and observation probes during buildup, Case 1

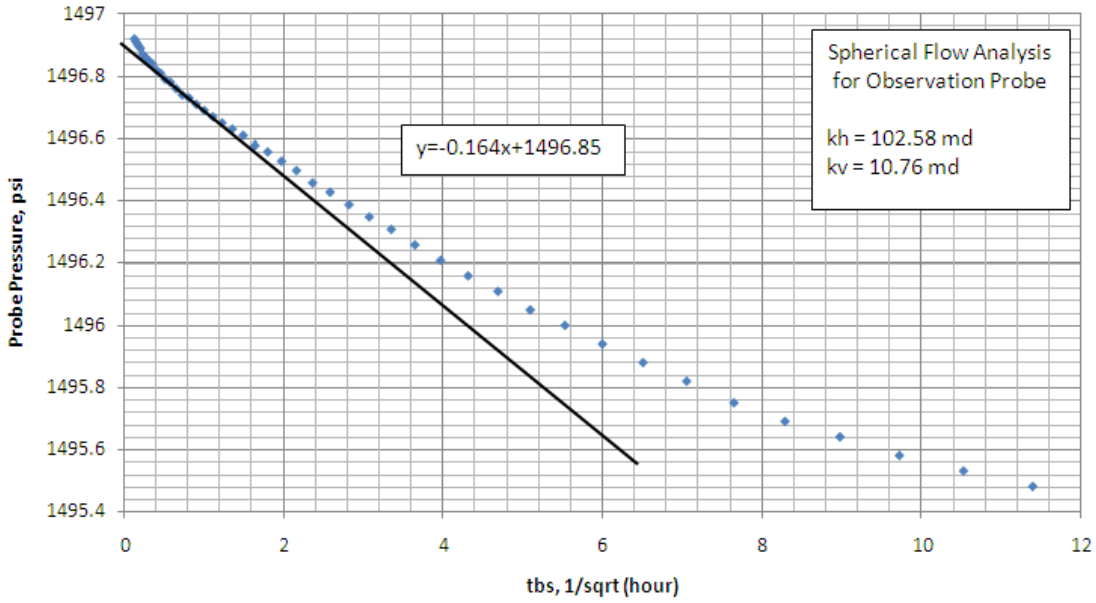

Figure 4-17 : Spherical-flow plot for buildup of observation probe , Case 1 (Probe 1)

Radial-flow analysis is used to analyse the observation probes data as well and from **Figure 4-16**, the system reaches radial flow after 1.0 hours of buildup. For this example, $\Delta Z_R = 6.4\,ft$ for probe 1, 14.4 *ft* for probe 2 and $25r_w\sqrt{k_v/k_h} = 2.80\,ft$, so the requirement of Equation 3.25 is met. **Figure 4-18** presents the radial-flow plot from which the slope *m*=-0.278 and intercept, *b*=1.517 is obtained. Using the steps explained in methodology section, values of $k_h\,and\,k_v$ are computed from obervation probe 1 data where $k_h = 99.70md$ (Error by 0.32%) and $k_v = 11.0md$ (Error by 9.89%) is obtained through plotting $f(k_v)$ versus k_v as shown in **Figure 4-19**. These values are very close to the averages of the input values given in **Table 4-4**. A radial-flow analysis for buildup pressure is also performed on observation probe 2 with $k_h = 99.38md$ (Error by 0.64%) and $k_v = 9.50md$ (Error by 5.09%). A drawdown radial-flow analysis has also carried out (due to this is a synthetic data with constant drawdown of 10 B/D for 6 hours), $k_h = 99.70md$ (Error by 0.32%) and $k_v = 11.0\,md$ (Error by 9.89%) are obtained from observation probe 1 data and $k_h = 99.70md$ (Error by 0.32%) and $k_v = 9.80\,md$ (Error by 2.10%) from observation probe 2 data. In summary, the good agreement of the input values and computed values has proved the feasibility of the adopted radial-flow solution for multi-layered reservoir system with heterogeneity of 0.05 by Dykstra-Parsons coefficient.

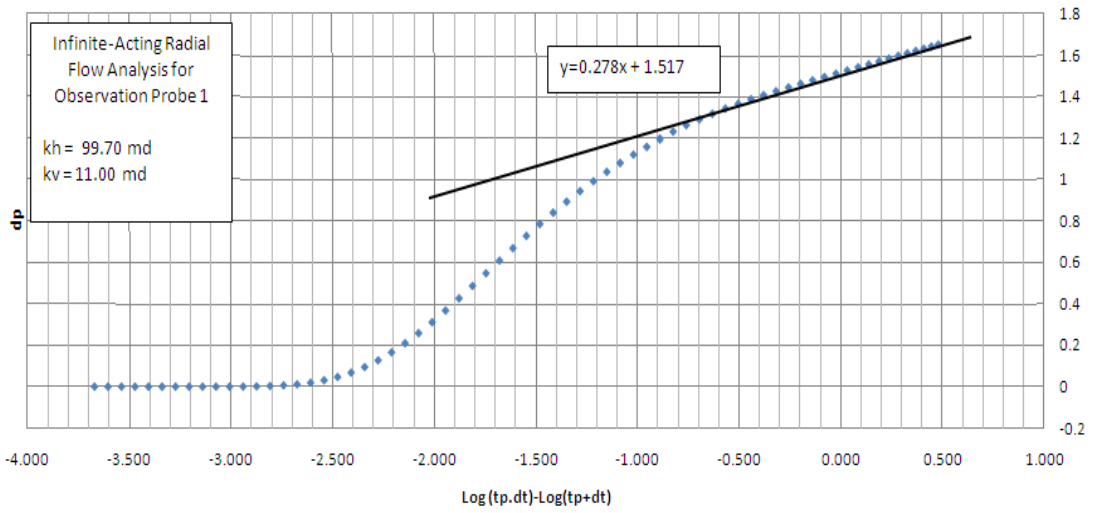

Figure 4-18 : Radial flow (or Horner) plot for observation probe, Case 1 (Probe 1)

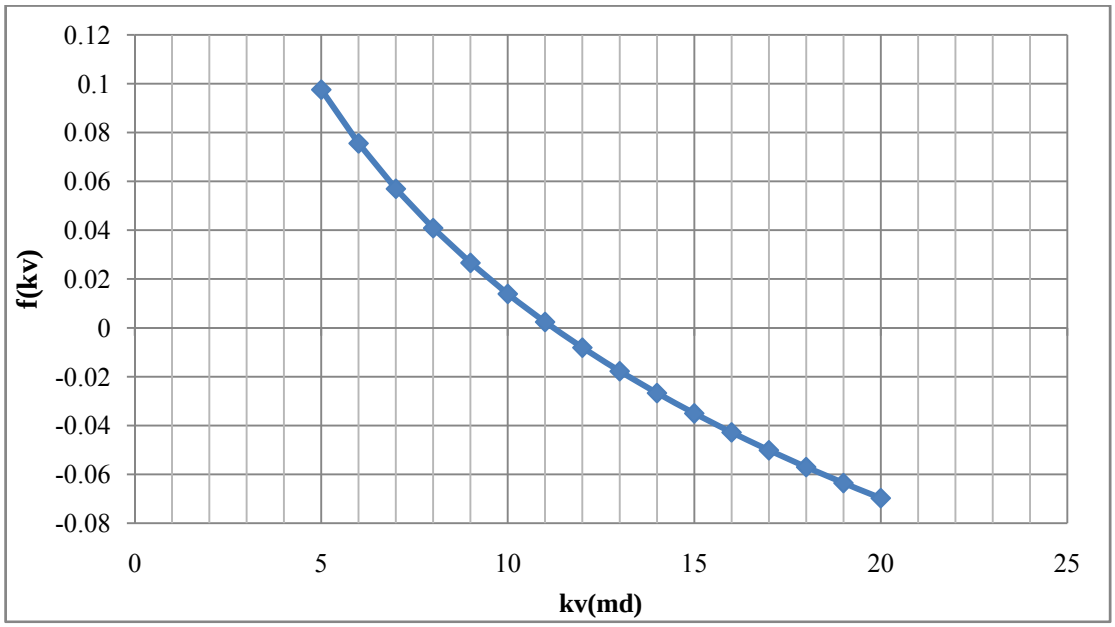

Figure 4-19: $f(k_v)$ vs. k_v , Case 1 (Probe 1)

In real life, the estimated k_h and k_v should be used for pressure response matching against the measured pressure response to validate the feasibility of the obtained estimates to represent the multi-layered reservoir system. **Figure 4-20** to **Figure 4-23** shows the pressure response matching of the obtained estimates permeabilities in a single layer reservoir system representation model against the pressure response of a measured multi-layered reservoir system. In summary, application of the adopted

solutions to the observation-probes buildup data of this IPTT provides values of horizontal and vertical permeability and these values provide good matches of the measured observation-probe pressures.

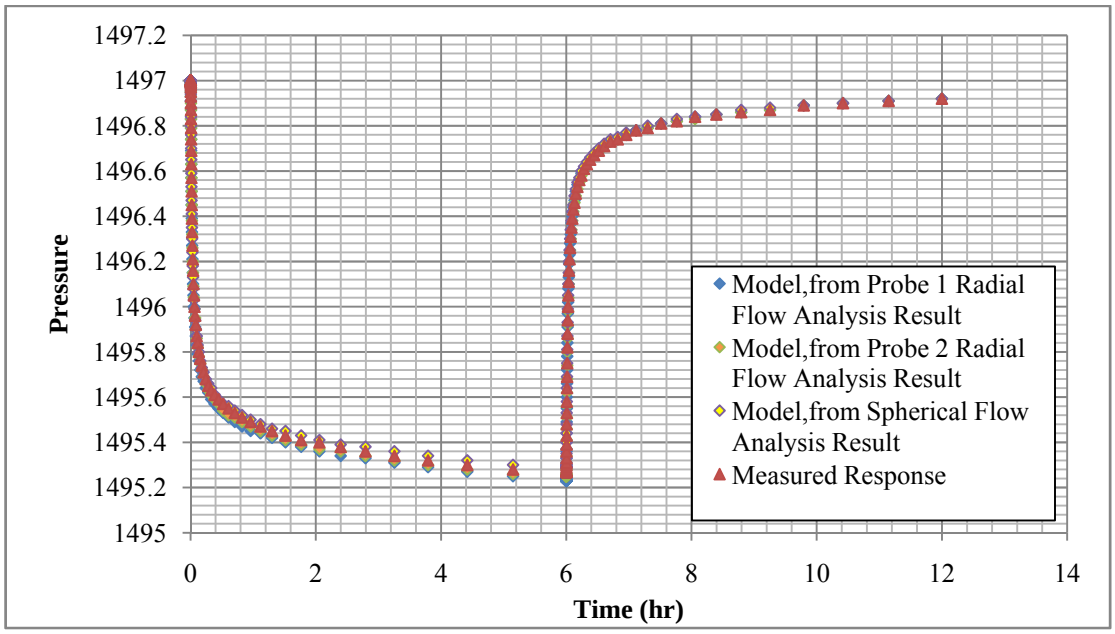

Figure 4-20: Simulated pressure for observation-probe 1 using radial-flow analysis and spherical-flow analysis result, Case 1

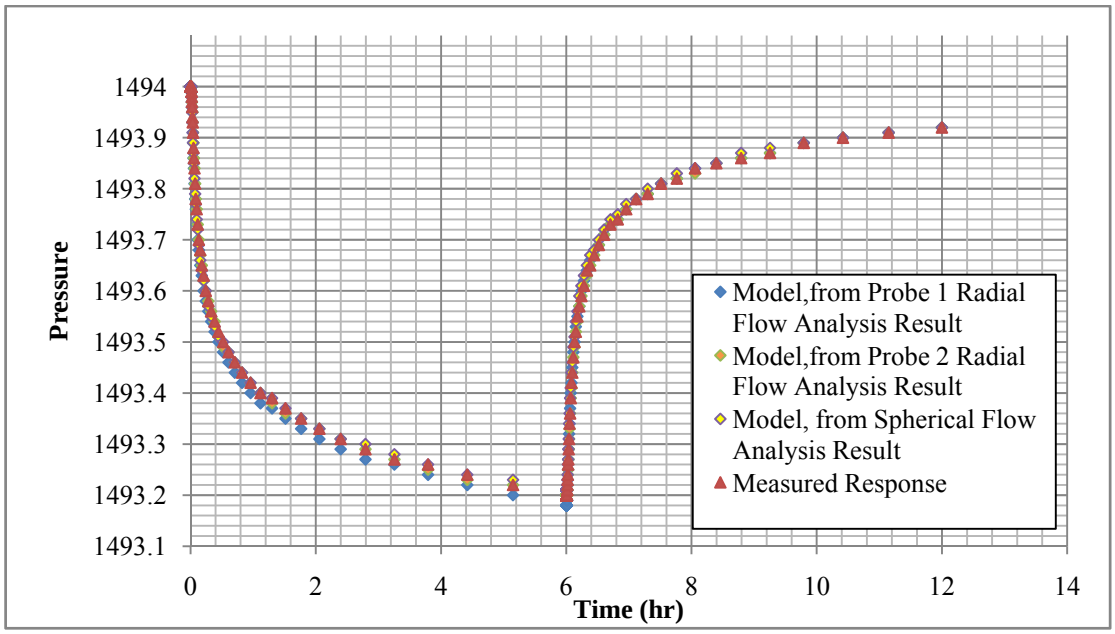

Figure 4-21: Simulated pressure for observation-probe 2 using radial-flow analysis and spherical-flow analysis result, Case 1

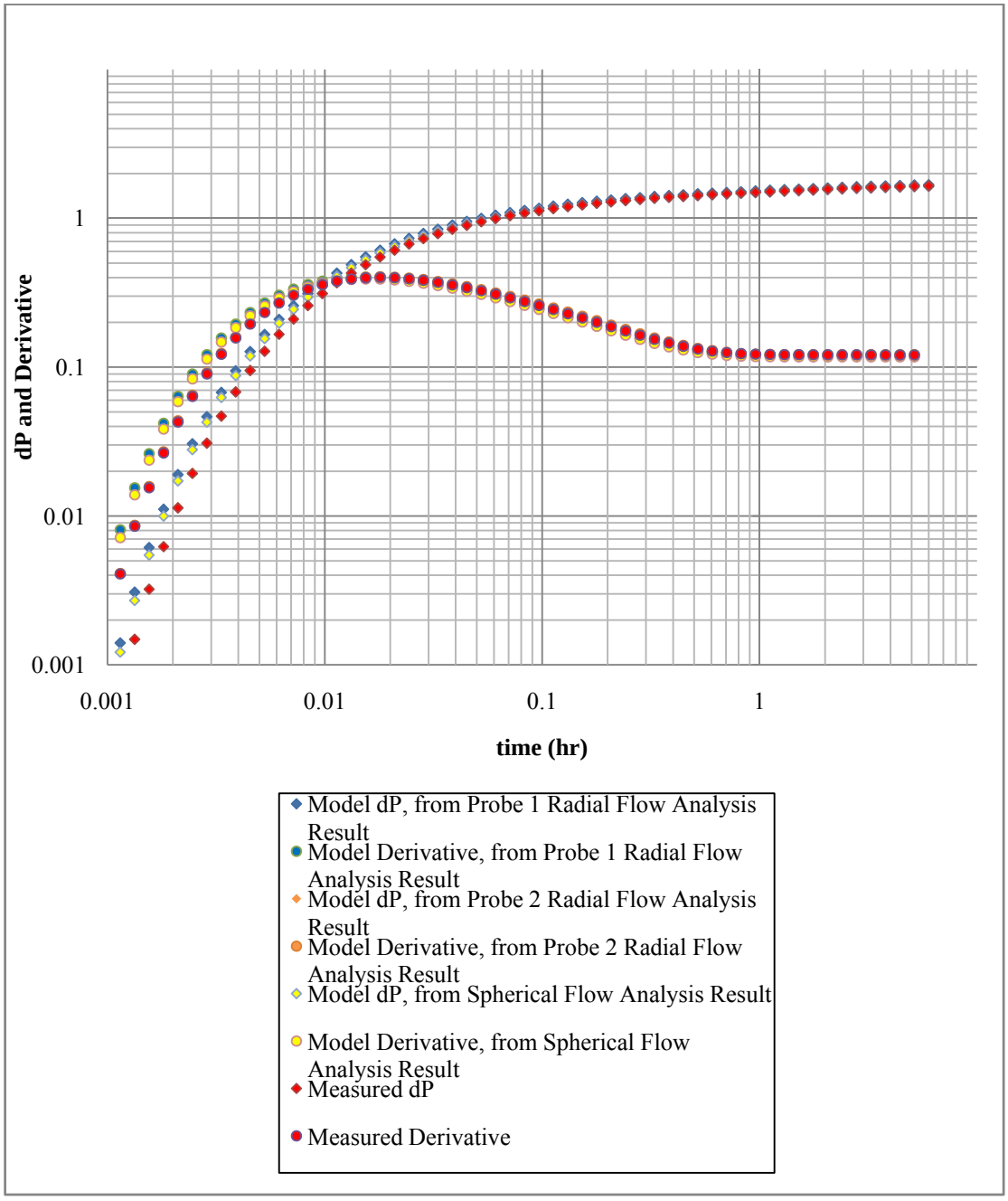

Figure 4-22 : Model pressure change and derivative for observation-probe 1 buildup using the result from radial flow analysis and spherical-flow analysis, Case 1

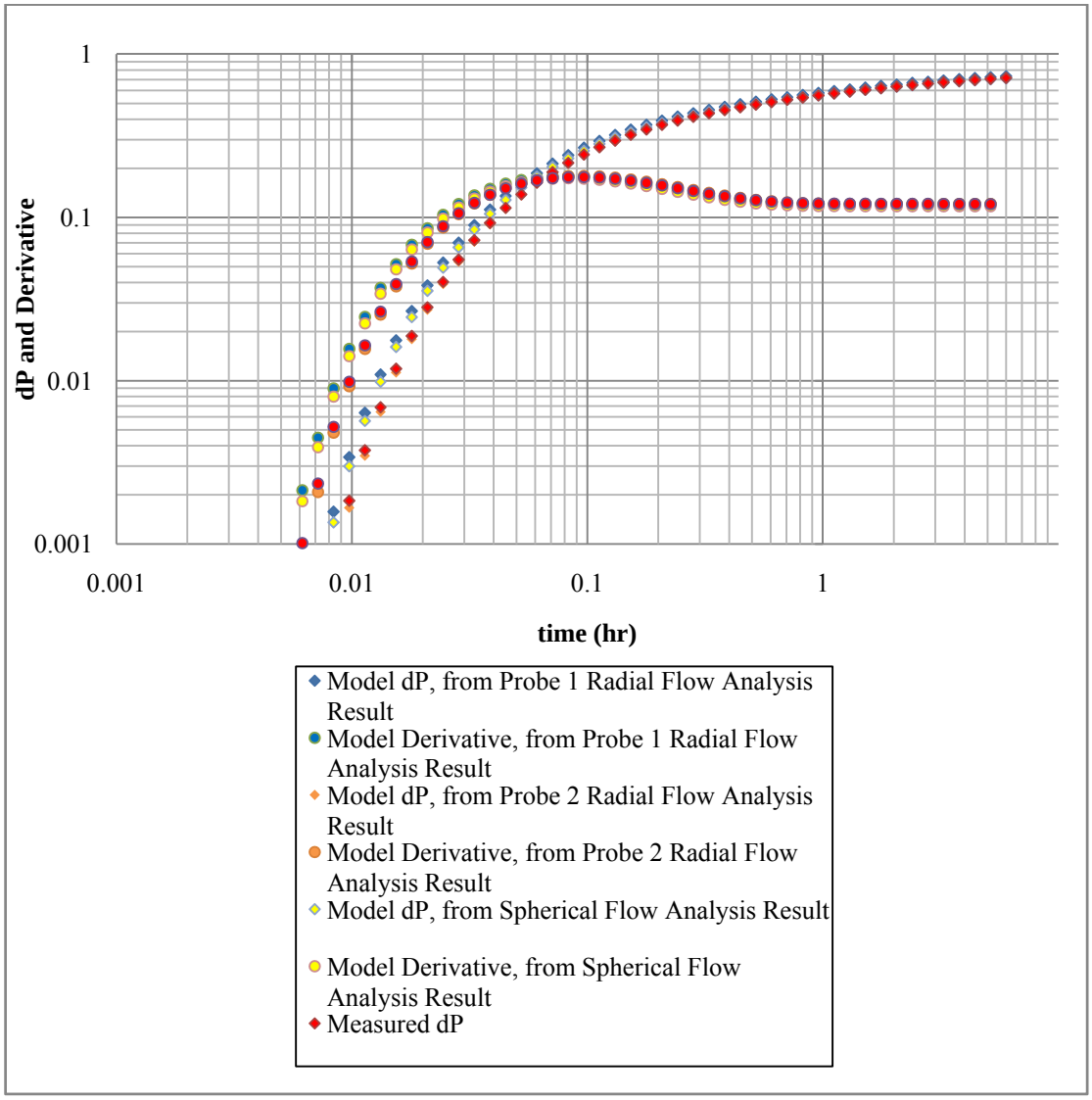

Figure 4-23: Model pressure change and derivative for observation-probe 2 buildup using the result from radial flow analysis and spherical-flow analysis, Case 1

4.2.2 Case 2, Heterogeneity of Dykstra-Parsons Coefficient = 0.06

A numerous synthetic data with increasing heterogeneity from 0.01 by Dykstra-Parsons coefficient has been performed to examine the feasibility of the adopted solutions for increasing heterogeneity of a reservoir. **Figure 4-24** shows the pressure response of observation probe 1 of an increasing heterogeneity reservoir. It is noticeable that beginning with Dykstra-Parsons coefficient of 0.06, the pressure response starts to change.

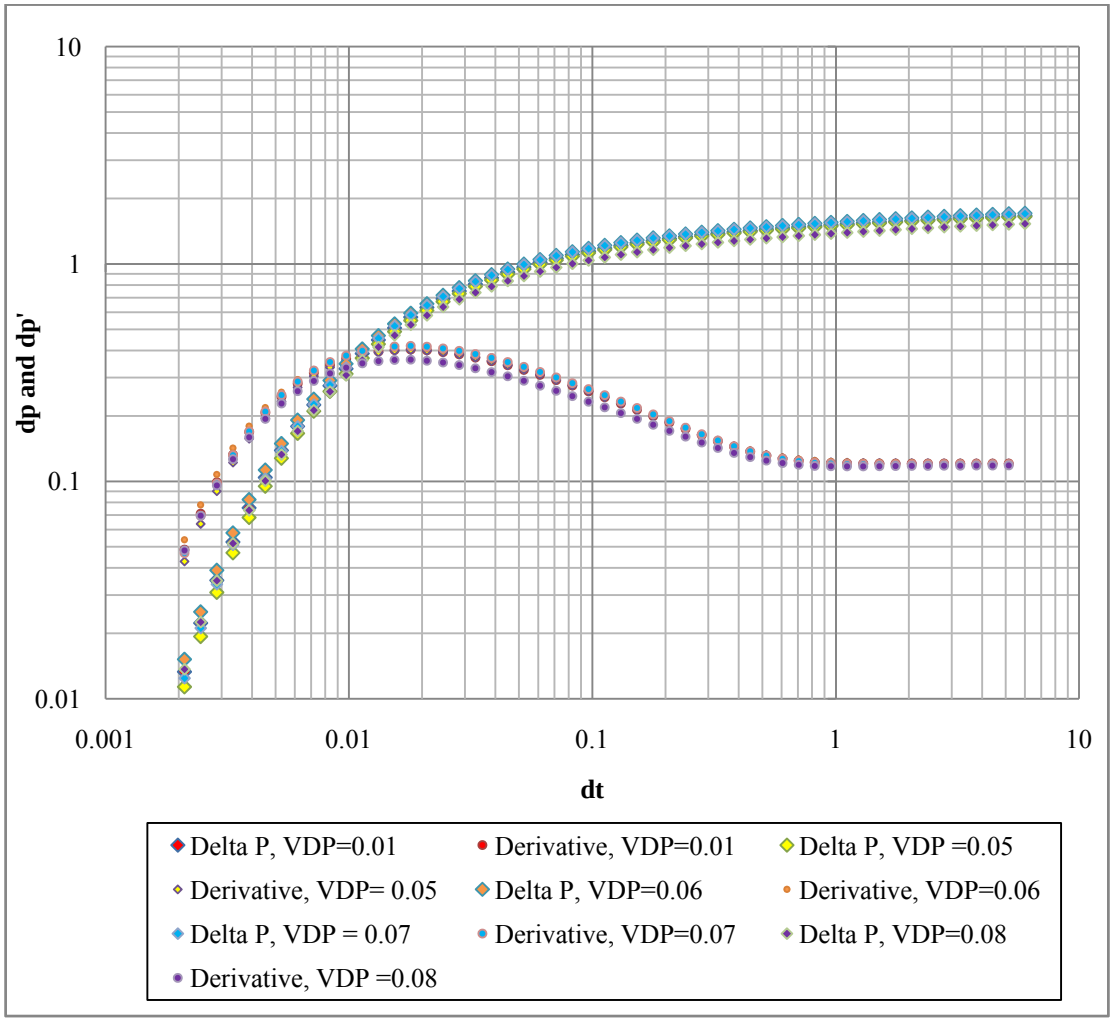

Figure 4-24: Pressure change and derivative at the observation probe 1 during buildup with increasing heterogeneity

Case 2 will demonstrate the applicability of Onur et al. (2011) and Onur et al. (2013) solutions for reservoir with heterogeneity of 0.06 by Dykstra-Parsons coefficient.

Synthetic IPTT Case 2, the input parameters used to simulate the IPTT is using the same input as Case 1 except the permeability with Dykstra-Parsons coefficient of 0.06 :

Table 4-5: Permeability Input for Synthetic IPTT for Case 2

Layers	h (ft)	k_h (md)	k_v (md)
1	8	101.06	10.67
2	8	99.65	10.42
3	8	85.70	11.08
4	8	106.47	10.12
5	8	95.48	10.73
6	8	98.21	9.84
7	8	97.90	9.54
8	8	101.82	9.83
9	8	109.57	9.28
10	8	96.18	9.75
11	8	100.03	10.65
Arithmetic Average		99.28	10.17
Harmonic Average		98.92	10.15
Geometric Average		99.10	10.16

The test consisted of a 6-hours flowing period followed by a 6-hours buildup. The heterogeneity level for this case is measured at 0.06 by Dykstra-Parsons coefficient. **Figure 4-25** shows the test pressure data for observation probe 1. **Figure 4-26** shows the diagnostic log-log plot of buildup pressure change and derivative at the packer interval and observation probes. The packer and probe 1 buildup data exhibit a clear negative half-slope at Δt= 0.15 hours to Δt= 0.24 hours. **Figure 4-27** displays the observation probe 1 buildup pressure on a spherical-flow plot. And slope of $m_{sp} = -0.172$ and the intercept $a_{tbs=0} = 1496.86psi$ are determined. Spherical cubic-analysis resulted with $k_h = 98.27md$ (Error by 1.02%) and $k_v = 10.66md$ (Error by 4.8%). These values are very close to the averages of the input values given in **Table 4-5**. A drawdown spherical-flow analysis has also carried out (due to this is a synthetic data with constant drawdown of 10 B/D for 6 hours), $k_h = 97.55md$ (Error by 1.74%) and $k_v = 10.57\ md$ (Error by 3.93%) are obtained. The good agreement of the input values and computed values has proved the feasibility of the adopted solution for multi-layered reservoir system with heterogeneity of 0.06 by Dykstra-Parsons coefficient.

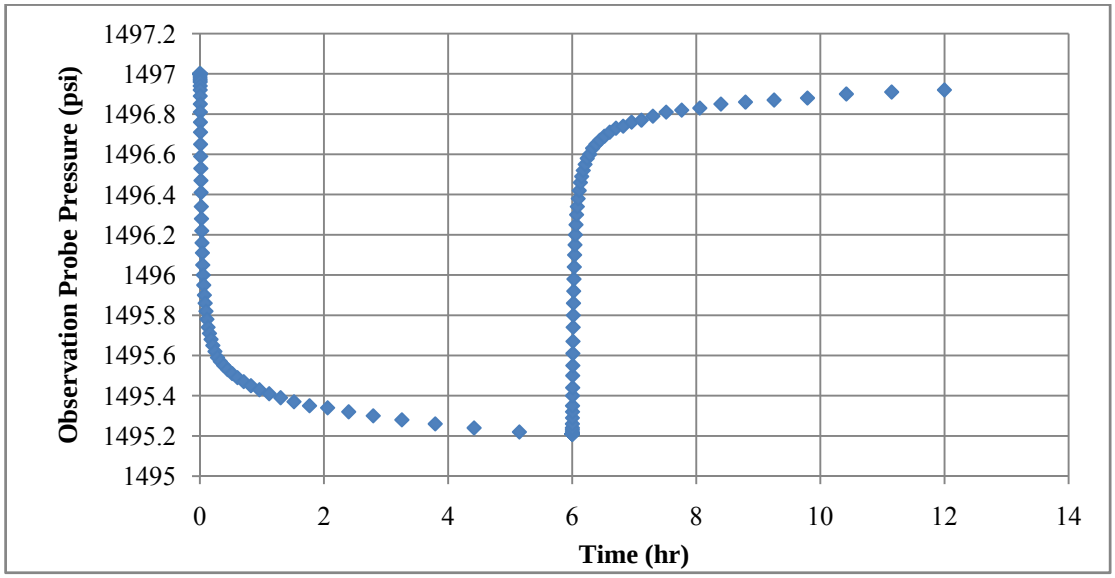

Figure 4-25: Pressure Response for Observation Probe 1, Case 2

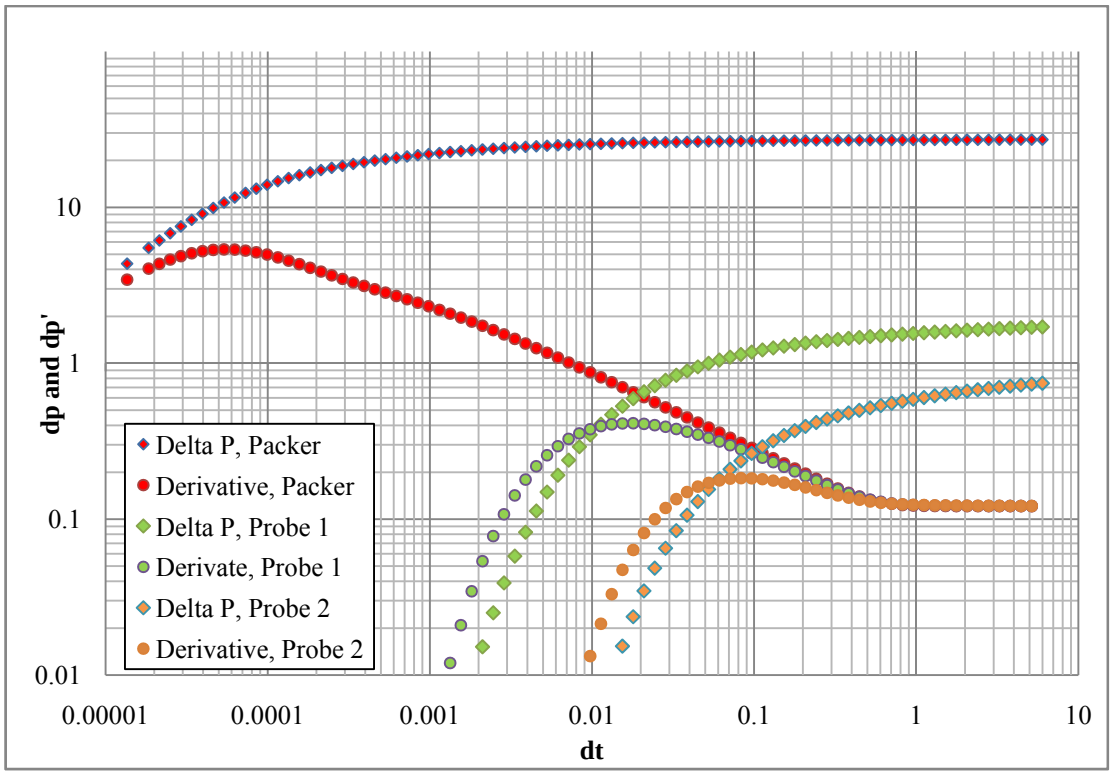

Figure 4-26: Pressure change and derivative at the packer interval and observation probes during buildup, Case 2

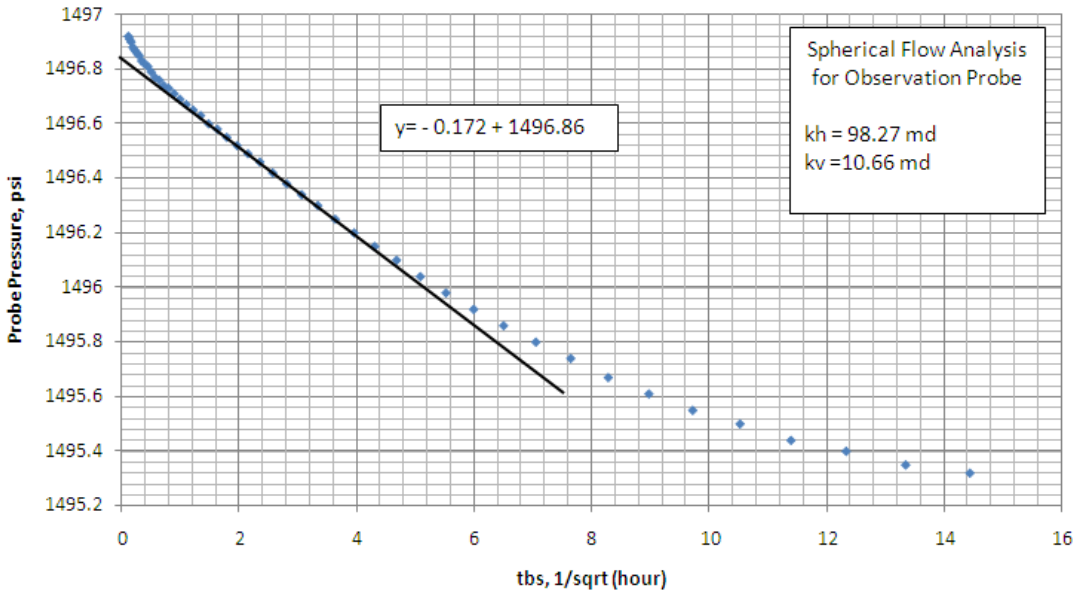

Figure 4-27: Spherical-flow plot for buildup of observation probe , Case 2 (Probe 1)

Radial-flow analysis is used to analyse the observation probes data as well and from **Figure 4-26**, the system reaches radial flow after 1.0 hours of buildup. For this example, $\Delta Z_R = 6.4\ ft$ for probe 1, 14.4 *ft* for probe 2 and $25 r_w \sqrt{k_v/k_h} = 2.80\ ft$, so the requirement of Equation 3.25 is met. **Figure 4-28** presents the radial-flow plot from which the slope *m*=-0.28 and intercept, *b*=1.577 is obtained. Using the steps explained in methodology section, values of $k_h\ and\ k_v$ are computed from obervation probe 1 data where $k_h = 98.99md$ and $k_v = 17.0md$ is obtained through plotting $f(k_v)$ versus k_v as shown in **Figure 4-29**. The k_h value is very close to the averages of the input value given in **Table 4-5** with an error of 0.29%. However, the k_v obtained have 67.16% error. This is due to the methodology used in radial-flow analysis is depending on the intercept of the radial flow plot to compute k_v, the heterogeneity of the reservoir results in varies pressure response which contributed to the intercept of radial-flow plot. A radial-flow analysis is also performed on observation probe 2 with $k_h = 98.99md$ (Error by 0.29%) and $k_v = 12.0md$ (Error by 18%). A drawdown radial-flow analysis has also carried out (due to this is a synthetic data with constant drawdown of 10 B/D for 6 hours), $k_h = 99.34md$ (Error by 0.06%) and $k_v = 17.5\ md$ (Error by 72.00%) are obtained from observation probe 1 data and $k_h = 98.99md$ (Error by 0.29%) and $k_v = 12.0\ md$ (Error by 18%) from observation probe 2 data. The error of the computed k_v with the input values has

proved the adopted radial-flow solution is not applicable to multi-layered reservoir system with heterogeneity of 0.06 by Dykstra-Parsons coefficient. **Figure 4-24** shows further increment of the heterogeneity level result in further deviation of the pressure response from the homogeneous pressure response, hence radial-flow analysis for obtaining value of k_v fails at reservoir with any heterogeneity of more than 0.05 by Dykstra-Parsons coefficient.

Horner plot analysis is also performed to confirm the reliability of the horizontal permeability, k_h obtained through radial flow analysis. Horner plot analysis obtained $k_h = 98.28\, md$.

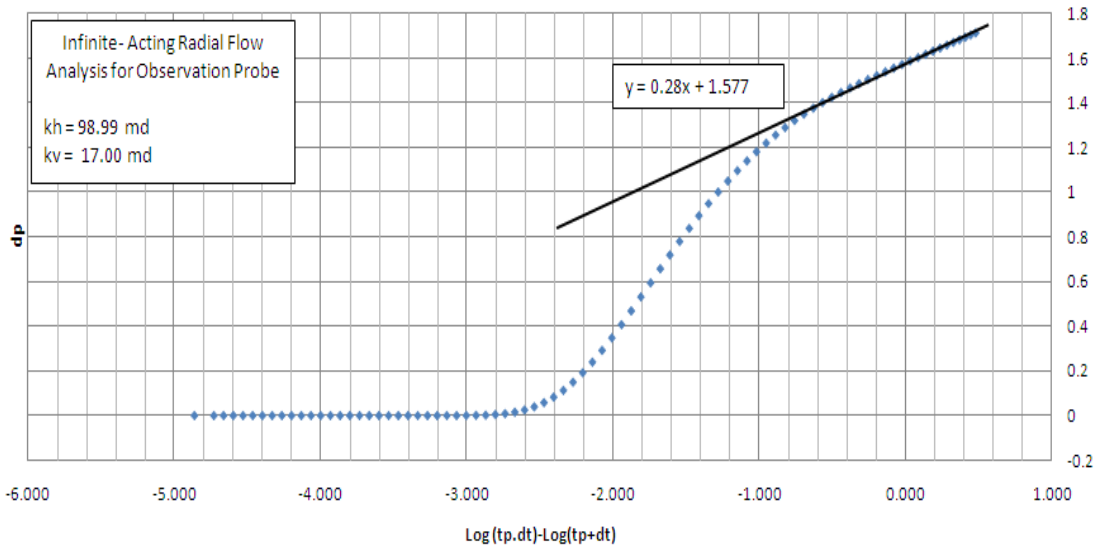

Figure 4-28: Radial-flow (or Horner) plot for observation probe, Case 2 (Probe 1)

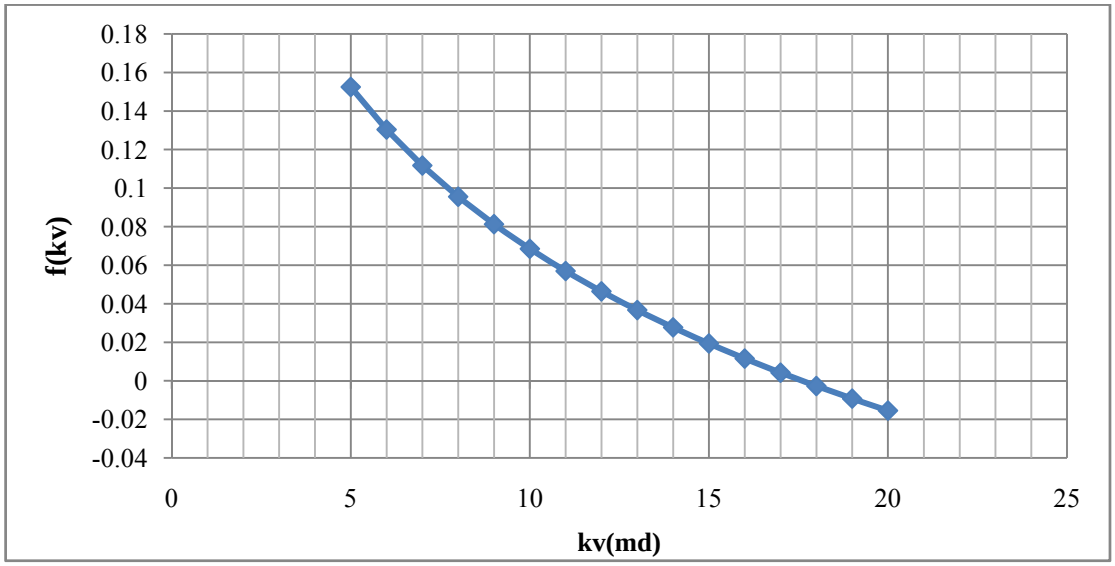

Figure 4-29: $f(k_v)$ vs. k_v , Case 2 (Probe 1)

In real life, the estimated k_h and k_v should be used for pressure response matching against the measured pressure response to validate the feasibility of the obtained estimates to represent the multi-layered reservoir system. **Figure 4-30** to **Figure 4-33** shows the pressure response matching of the obtained estimates permeabilities in a single layer reservoir system representation model against the pressure response of a measured multi-layered reservoir system. In summary, estimated permeability values spherical-flow analysis provide good matches of the measured observation-probes pressures while estimated permeability values from radial-flow analysis did not provide a good matches of the measured observation-probes pressures.

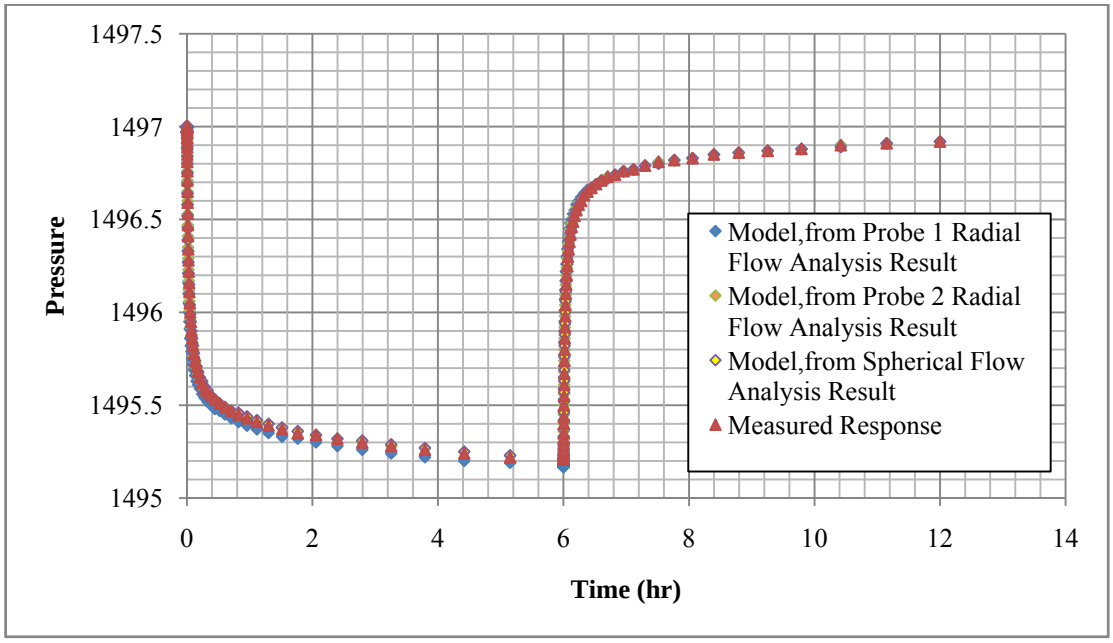

Figure 4-30 : Simulated pressure for observation-probe 1 using radial-flow analysis and spherical-flow analysis result, Case 2

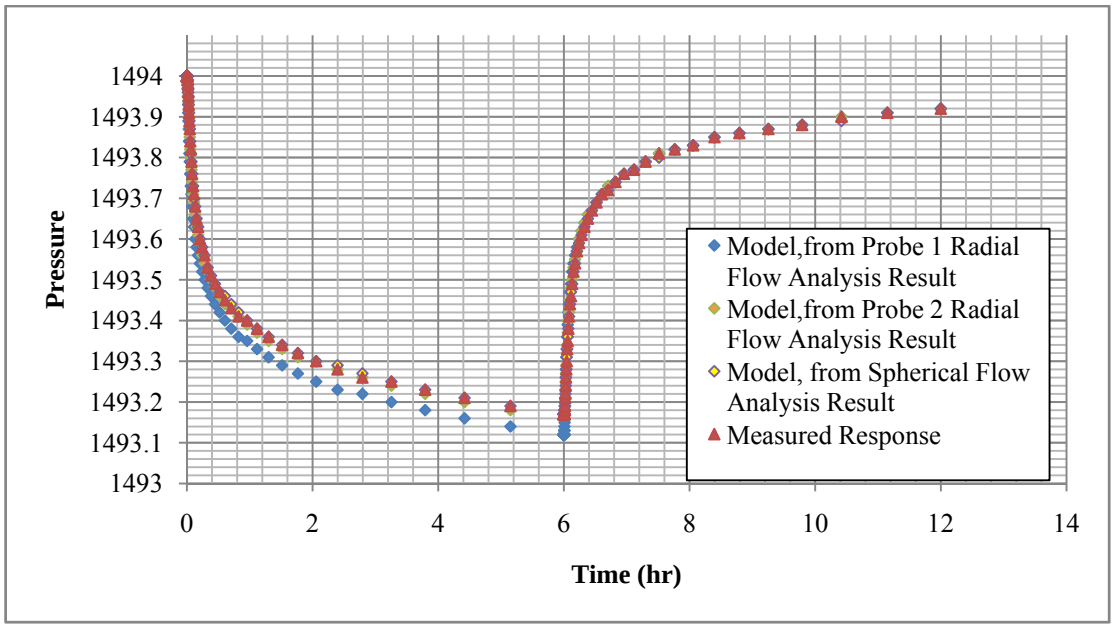

Figure 4-31 : Simulated pressure for observation-probe 2 using radial-flow analysis and spherical-flow analysis result, Case 2

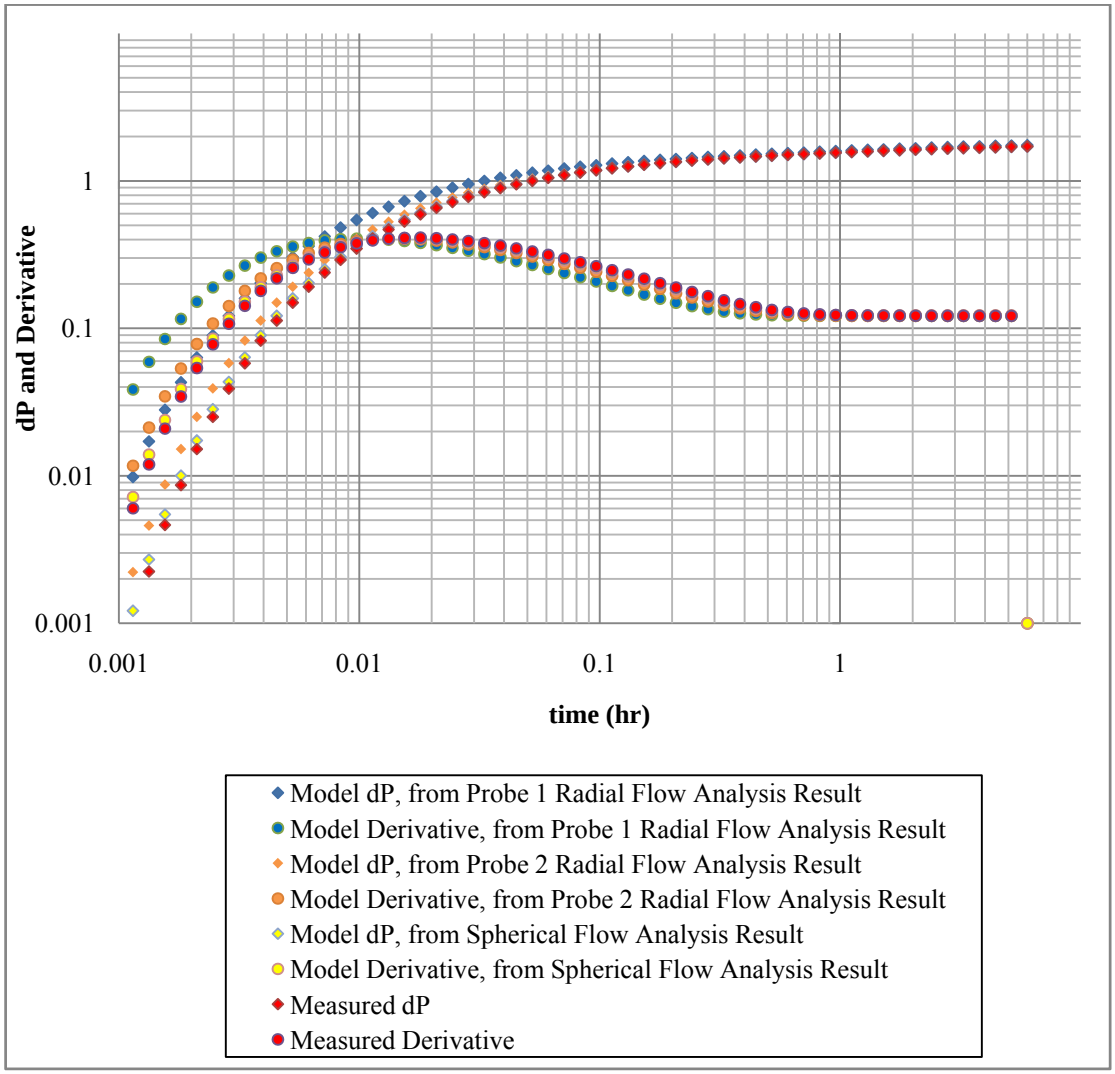

Figure 4-32: Model pressure change and derivative for observation-probe 1 buildup using the result from radial flow analysis and spherical-flow analysis, Case 2

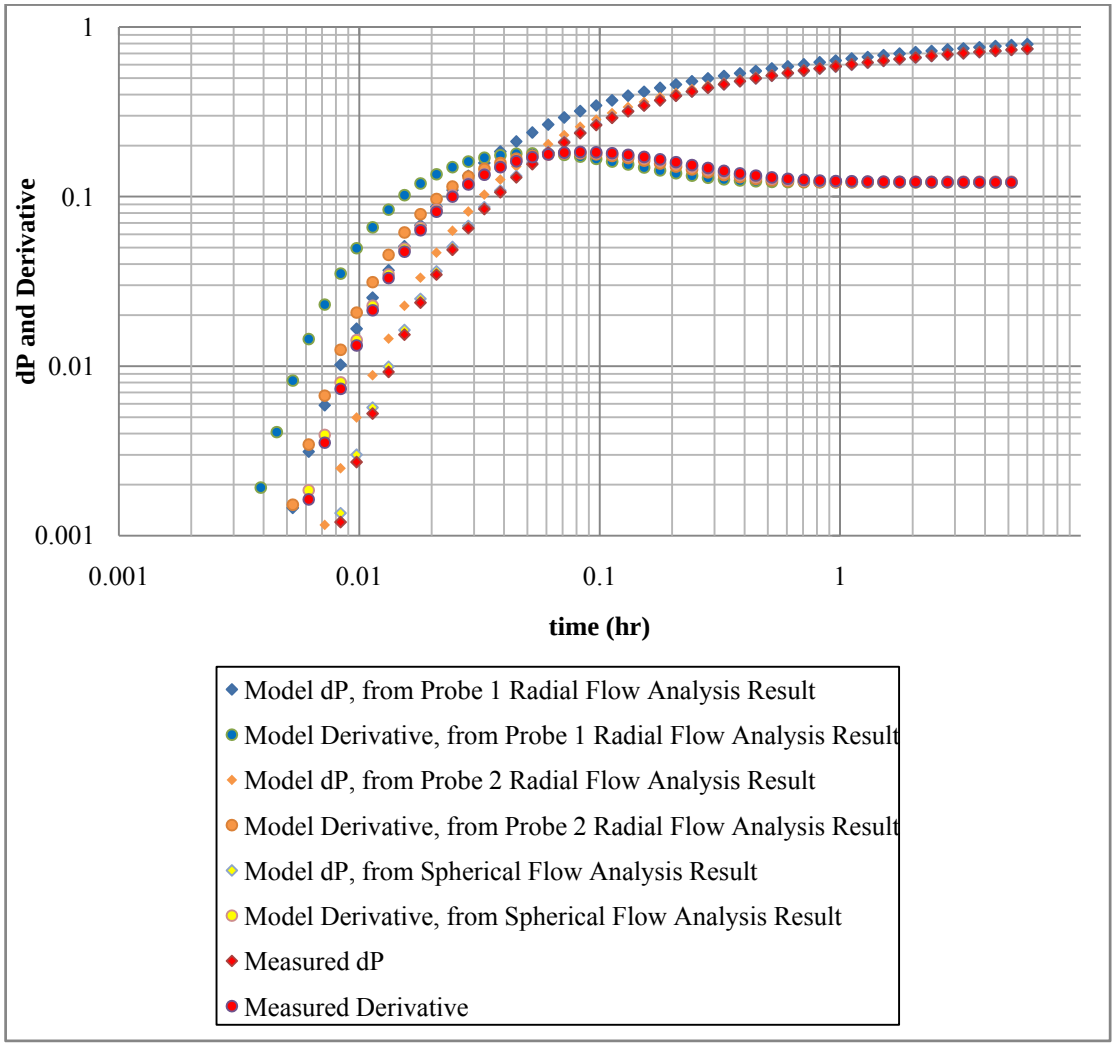

Figure 4-33: Model pressure change and derivative for observation-probe 2 buildup using the result from radial flow analysis and spherical-flow analysis, Case 2

4.2.3 Case 3, Heterogeneity of Dykstra-Parsons Coefficient = 0.30

This case was generated using the same input as Case 1, except the permeabilities were changed to as shown in **Table 4-6** to increase the heterogeneity of the reservoir to Dykstra-Parsons coefficient of 0.30.

Table 4-6 : Permeability Input for Synthetic IPTT for Case 3

Layers	h (ft)	k_h (md)	k_v (md)
1	8	41.17	12.56
2	8	104.81	10.24
3	8	77.55	12.64
4	8	129.21	7.71
5	8	106.50	16.43
6	8	98.52	9.88
7	8	89.32	6.50
8	8	144.70	7.57
9	8	131.24	7.73
10	8	121.51	9.39
11	8	75.92	6.01
Arithmetic Average		101.86	9.70
Harmonic Average		90.81	8.90
Geometric Average		96.93	9.28

The test consisted of a 6-hours flowing period followed by a 6-hours buildup. **Figure 4-34** shows the test pressure data for observation probe 1. **Figure 4-35** shows the diagnostic log-log plot of buildup pressure change and derivative at the packer interval and observation probes. The packer and probe 1 buildup data exhibit a clear negative half-slope at Δt= 0.24 hours to Δt= 0.33 hours. **Figure 4-36** displays the observation probe 1 buildup pressure on a spherical-flow plot. And slope of $m_{sp} = -0.170$ and the intercept $a_{tbs=0} = 1496.86psi$ are determined. Spherical cubic-analysis resulted with $k_h = 97.75md$ (Error by 4.03%) and $k_v = 10.41md$ (Error by 7.32%). These values are very close to the averages of the input values given in **Table 4-6**. A drawdown analysis has also carried out (due to this is a synthetic data with constant drawdown of 10 B/D for 6 hours), $k_h = 97.32md$ (Error by 4.46%) and $k_v = 10.50\ md$ (Error by 8.25%) are obtained. The good agreement of the input values and computed values has proved the feasibility of the adopted spherical-flow solution for multi-layered reservoir system with heterogeneity of 0.30 by Dykstra-Parsons coefficient.

Radial-flow analysis using the adopted solution is not explained for this case because radial-flow analysis is not feasible for multi-layered reservoir system with heterogeneity level above 0.05 by Dykstra-Parsons coefficient as explained in Case 2. However, a summary of the analysis will be presented in section **4.2.5** 58.

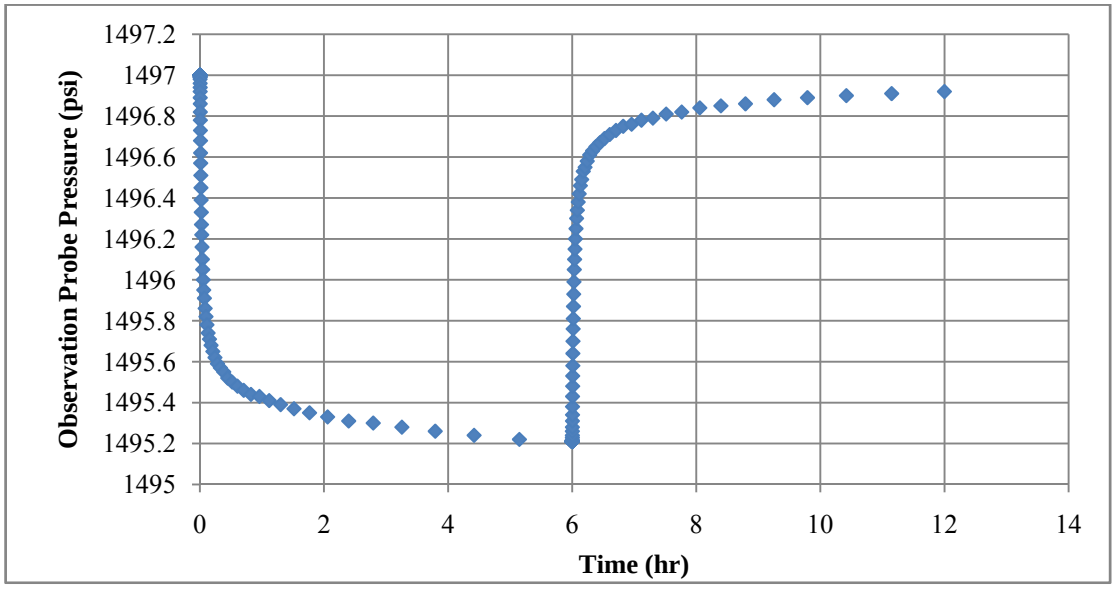

Figure 4-34: Pressure Response for Observation Probe 1, Case 3

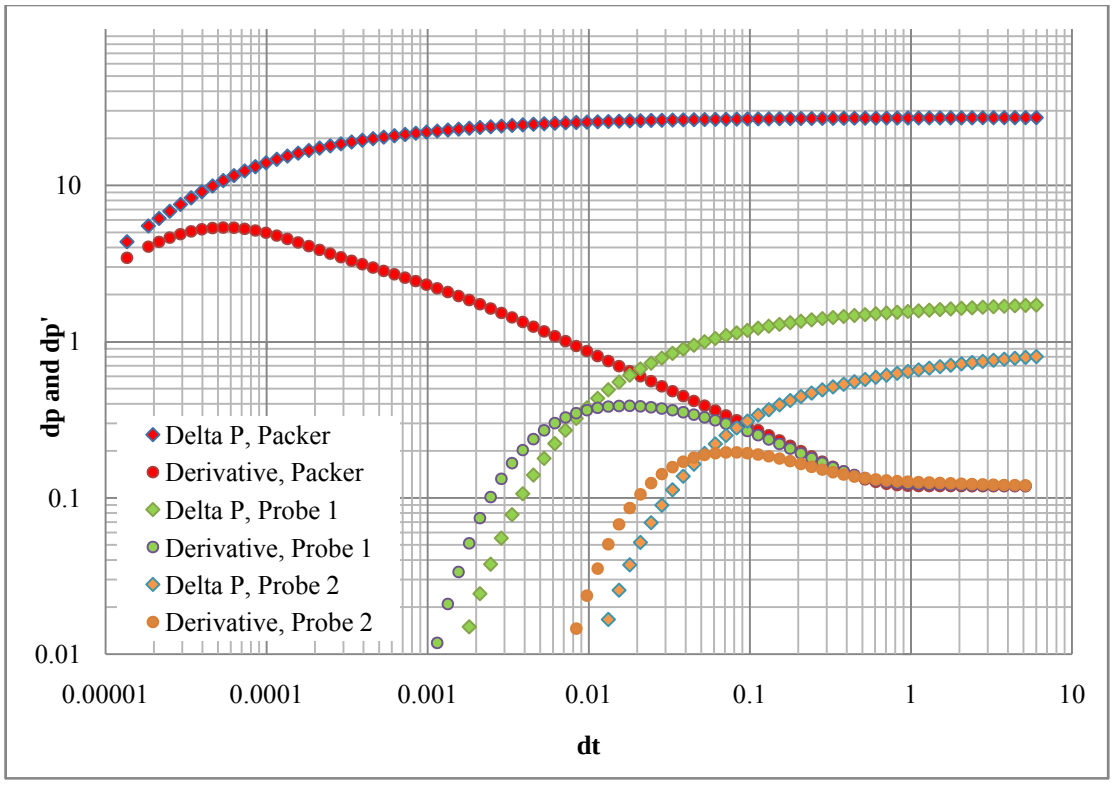

Figure 4-35: Pressure change and derivative at the packer interval and observation probes during buildup, Case 3

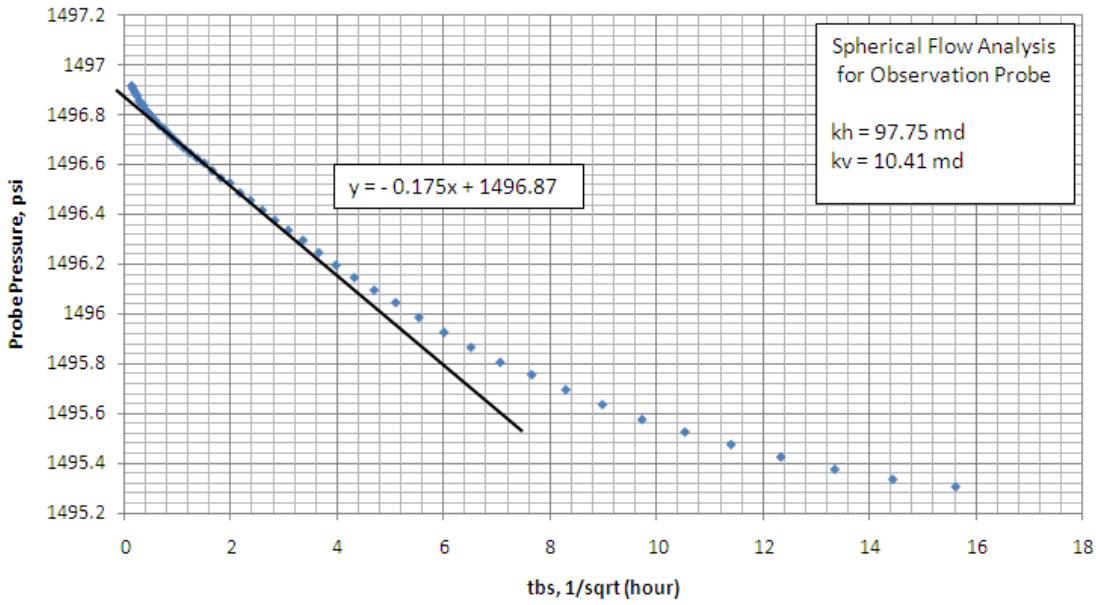

Figure 4-36 : Spherical-flow plot for buildup of observation probe, Case 3 (Probe 1)

The estimated k_h and k_v were used for pressure response matching against the measured pressure response as shown in **Figure 4-37** to **Figure 4-40.** These figures show that the simulated pressure response by using estimated permeabilities from spherical-flow analysis matches the probe 1 measured pressure response. However the simulated pressure response does not matches well with the probe 2 measured pressure response during drawdown. This is due to heterogeneity behaviour of the reservoir. The probe pressure response is found to be dependent on the permeabilities of the immediate layer below it. In this case, vertical permeability of the layer below the probe 2 is 16.43md which differs from the vertical permeability arithmetic average, 9.70md. Hence the simulated pressure response using estimated permeabilities parameters which is close to the arithmetic averages does not matches the measured pressure response of probe 2. Hence, the estimated permeability parameters are not representable to the multi-layered reservoir system.

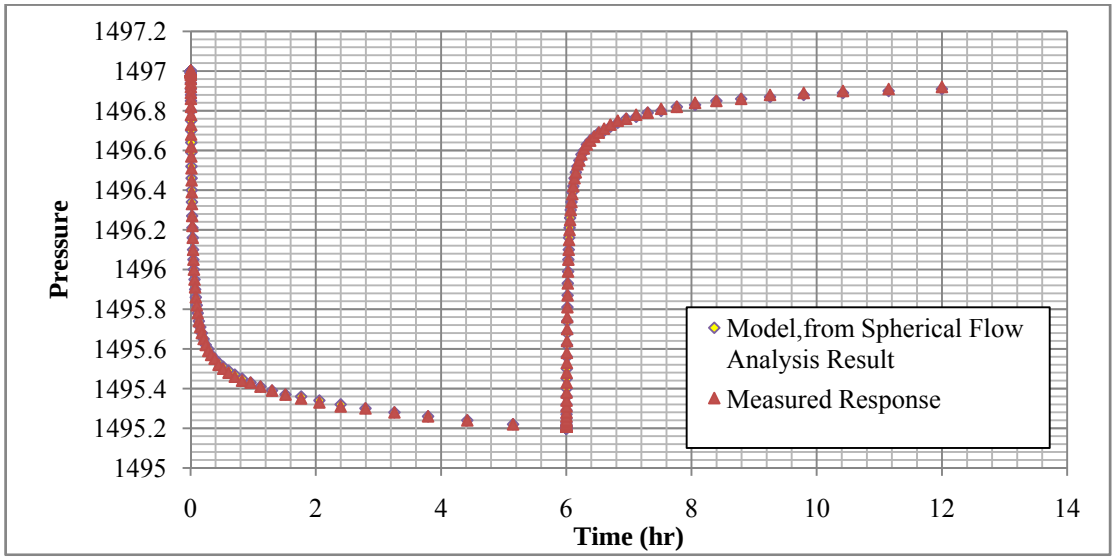

Figure 4-37: Simulated pressure for observation-probe 1 using spherical-flow analysis result, Case 3

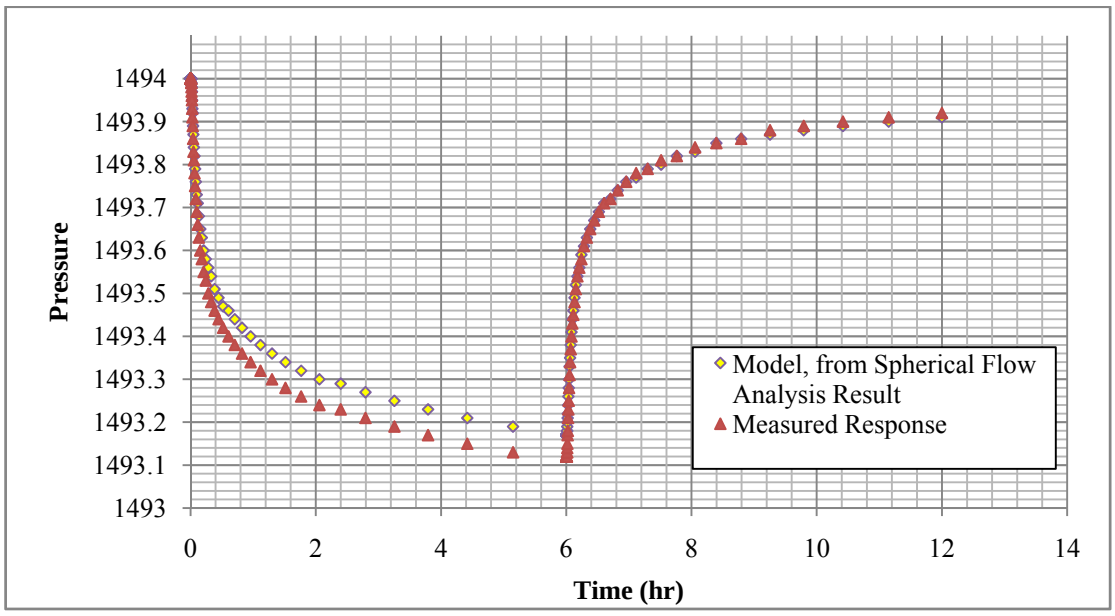

Figure 4-38: Simulated pressure for observation-probe 2 using spherical-flow analysis result, Case 3

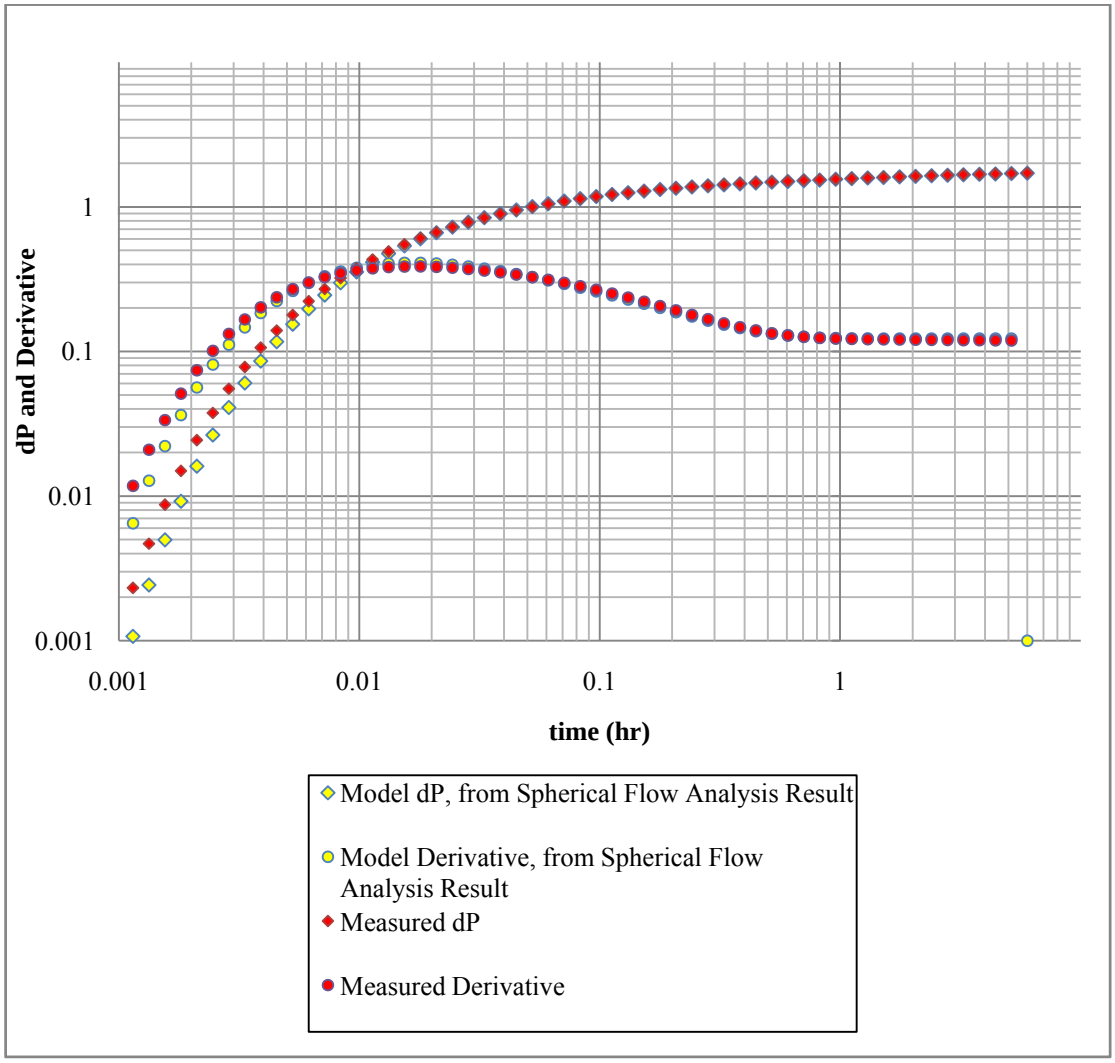

Figure 4-39: Model pressure change and derivative for observation-probe 1 buildup using the result from spherical-flow analysis, Case 3

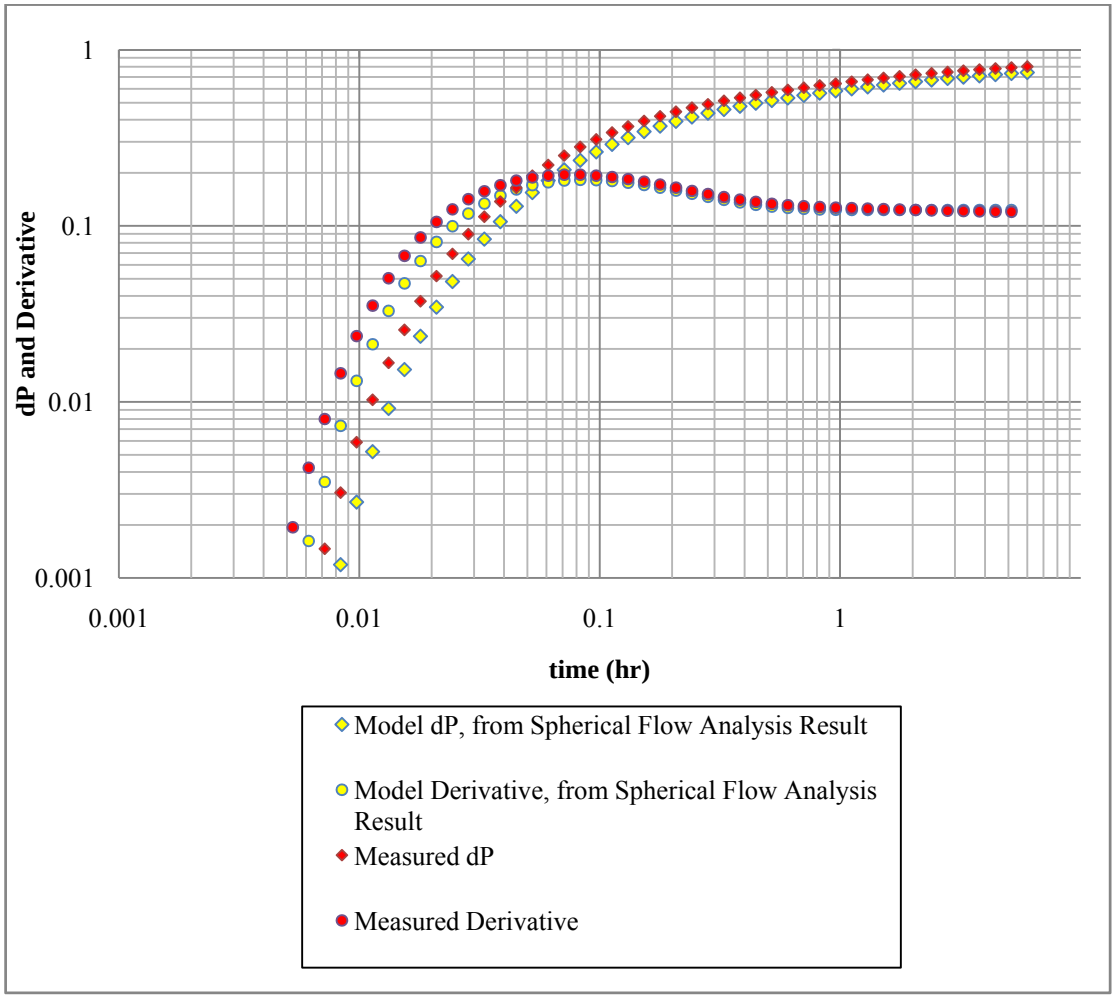

Figure 4-40: Model pressure change and derivative for observation-probe 2 buildup using the result from spherical-flow analysis, Case 3

4.2.4 Case 4, Heterogeneity of Dykstra-Parsons Coefficient = 0.40

This case was also generated using the same input as Case 1, except the permeabilities were changed to as shown in **Table 4-7** to increase the heterogeneity of the reservoir to Dykstra-Parsons coefficient of 0.40.

Table 4-7: Permeability Input for Synthetic IPTT for Case 4

Layers	h (ft)	k_h (md)	k_v (md)
1	8	216.87	5.35
2	8	111.23	11.16
3	8	71.17	17.24
4	8	88.84	8.39
5	8	44.18	5.48
6	8	75.49	10.57
7	8	158.66	8.68
8	8	66.94	6.54
9	8	59.63	20.29
10	8	132.32	8.87
11	8	97.66	5.26
Arithmetic Average		102.53	10.26
Harmonic Average		76.57	7.40
Geometric Average		91.83	9.35

The test is also consisted of a 6-hours flowing period followed by a 6-hours buildup. **Figure 4-41** shows the test pressure data for observation probe 1. **Figure 4-42** shows the diagnostic log-log plot of buildup pressure change and derivative at the packer interval and observation probes. The packer and probe 1 buildup data exhibit a clear negative half-slope at Δt= 0.33 hours to Δt= 0.52 hours. **Figure 4-43** displays the observation probe 1 buildup pressure on a spherical-flow plot. And slope of $m_{sp} = -0.221$ and the intercept $a_{tbs=0} = 1496.90psi$ are determined. Spherical cubic-analysis resulted with $k_h = 67.68md$ and $k_v = 13.62md$. The k_h obtained has an error of 34.00% from the arithmetic average of k_h and the k_v has an error of 32.75% from the arithmetic average of k_v given in **Table 4-7**. A drawdown spherical-flow analysis has also carried out (due to this is a synthetic data with constant drawdown of 10 B/D for 6 hours), $k_h = 67.40md$ (Error by 34.26%) and $k_v = 13.48\ md$ (Error by 31.38%) are obtained. The error of the computed values from the input values has proved the adopted solution of spherical-flow solution is not feasible for multi-layered reservoir system with heterogeneity of 0.40 and more by Dykstra-Parsons coefficient.

Radial-flow analysis using the adopted solution is not explained for this case and a summary of the analysis will be presented in section **4.2.5** 58.

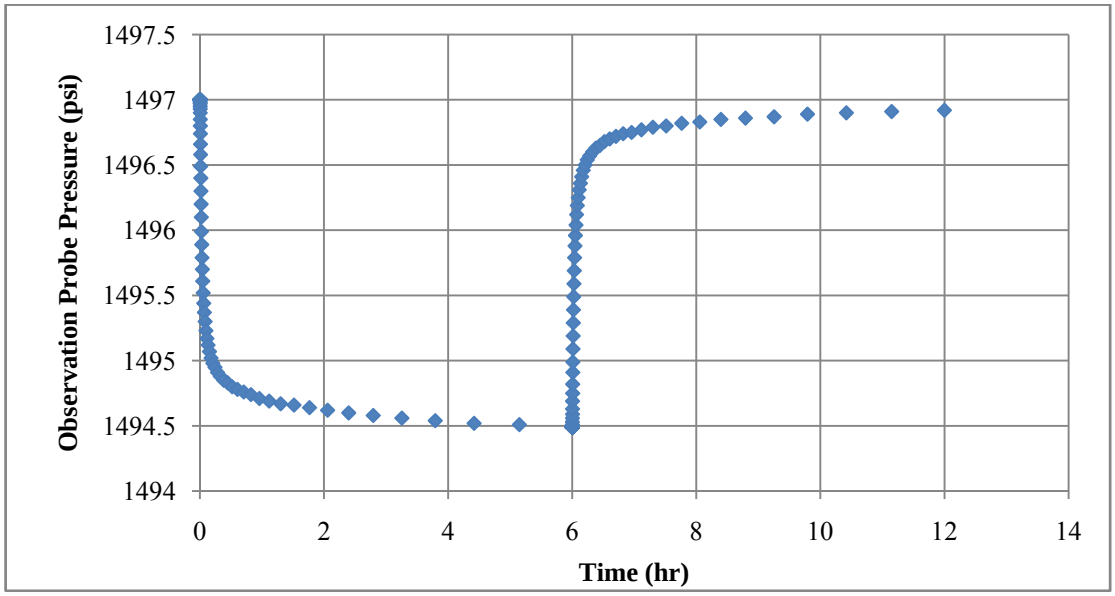

Figure 4-41: Pressure Response for Observation Probe 1, Case 4.

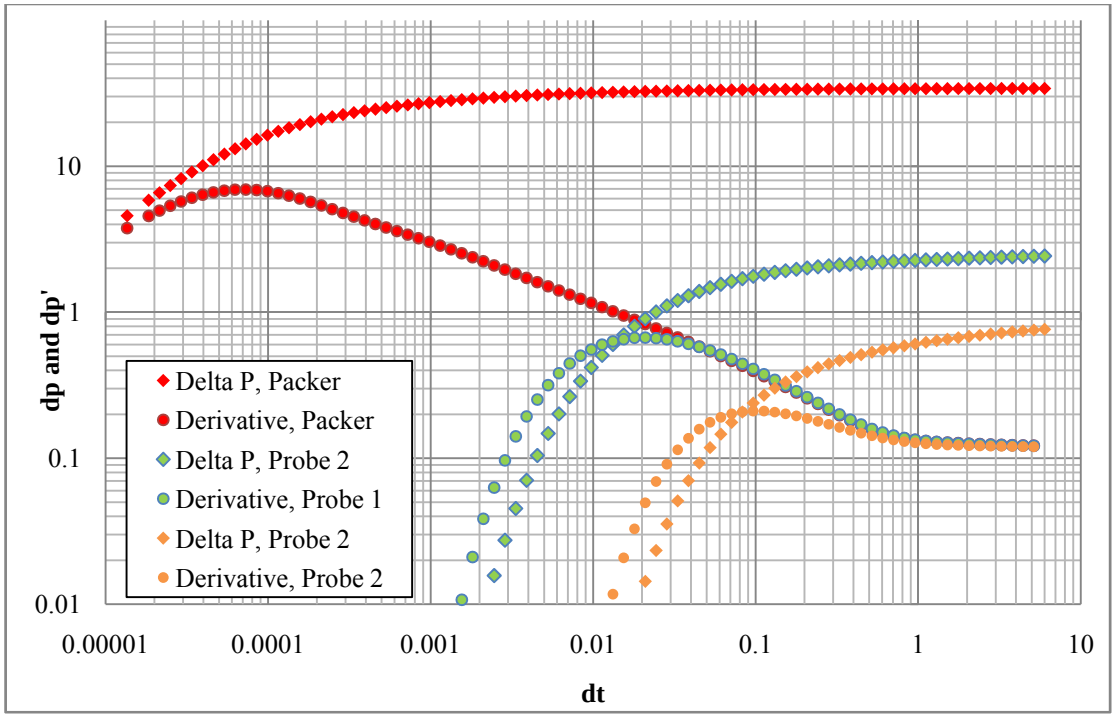

Figure 4-42 : Pressure change and derivative at the packer interval and observation probes during buildup, Case 4.

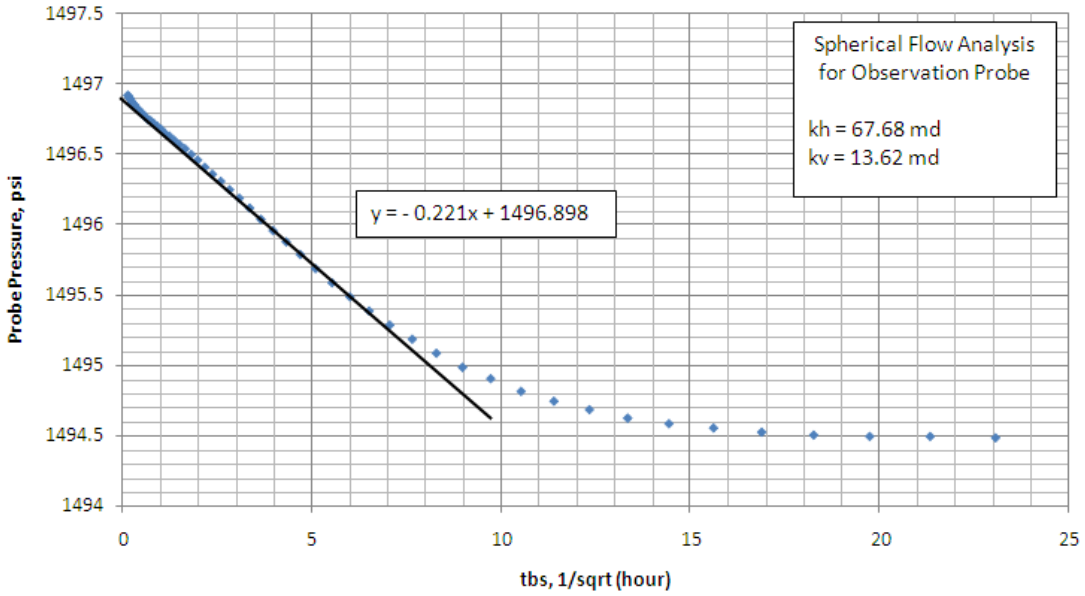

Figure 4-43: Spherical-flow plot for buildup of observation probe, Case 4 (Probe 1).

The estimated k_h and k_v were used for pressure response matching against the measured pressure response as shown in **Figure 4-44** to **Figure 4-47.** These figures show that the simulated pressure response by using estimated permeabilities from spherical-flow analysis does not matches the measured pressure response. Hence, the estimated permeability parameters are not representable to the multi-layered reservoir system.

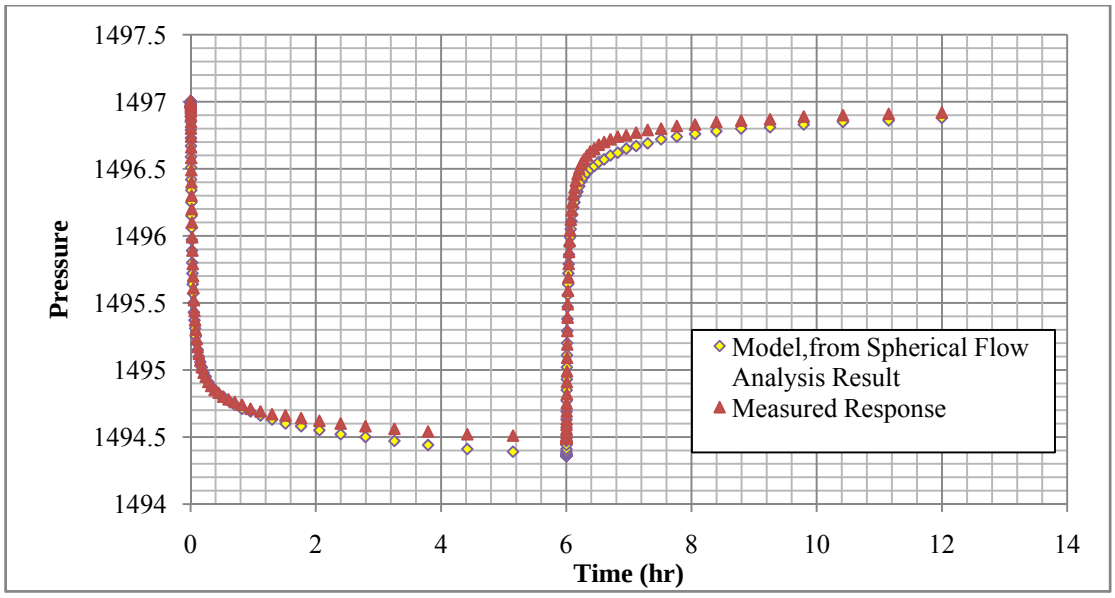

Figure 4-44: Simulated pressure for observation-probe 1 using spherical-flow analysis result, Case 4.

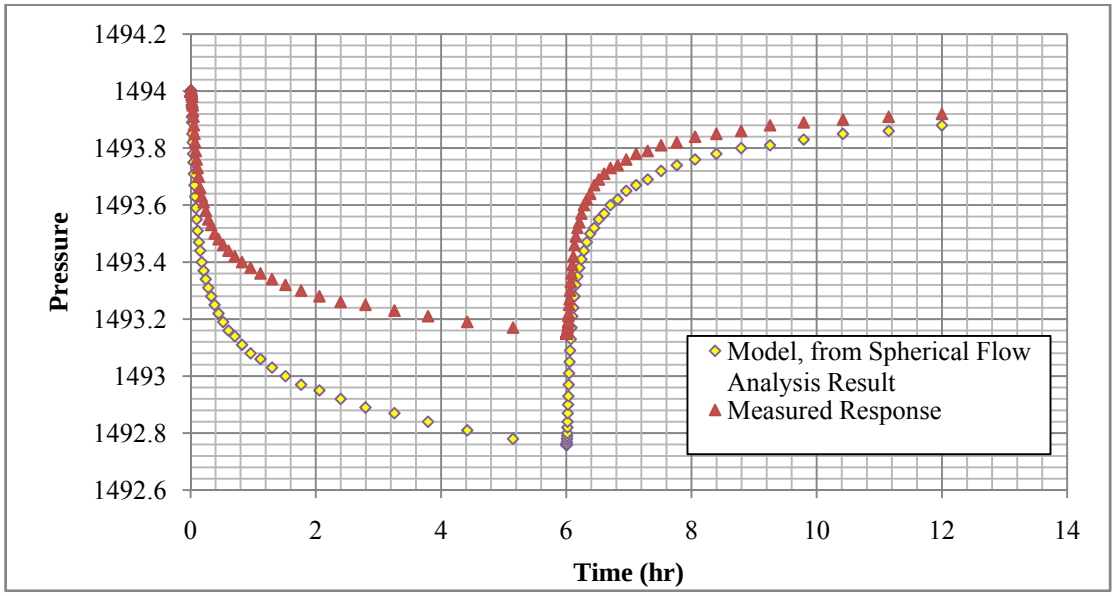

Figure 4-45: Simulated pressure for observation-probe 2 using spherical-flow analysis result, Case 4.

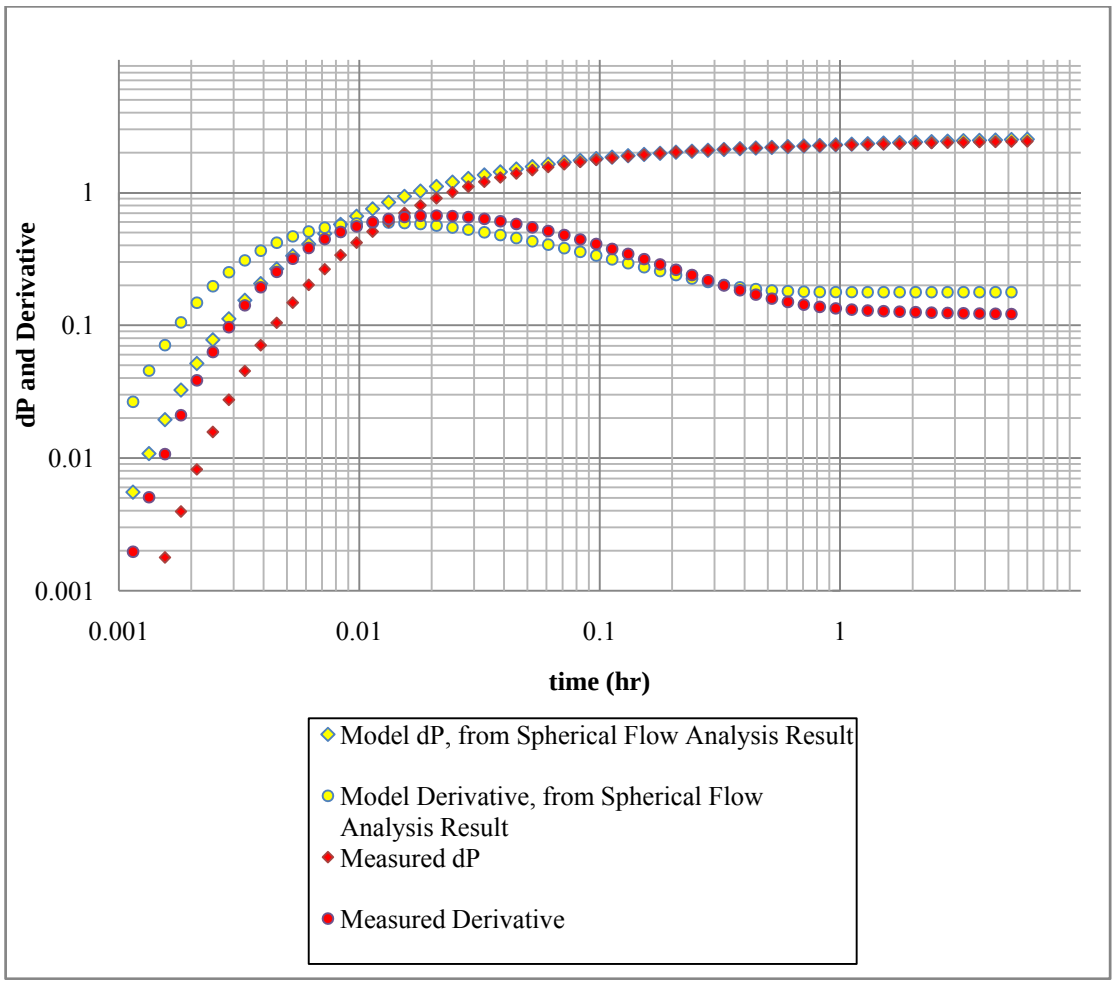

Figure 4-46: Model pressure change and derivative for observation-probe 1 buildup using the result from spherical-flow analysis, Case 4.

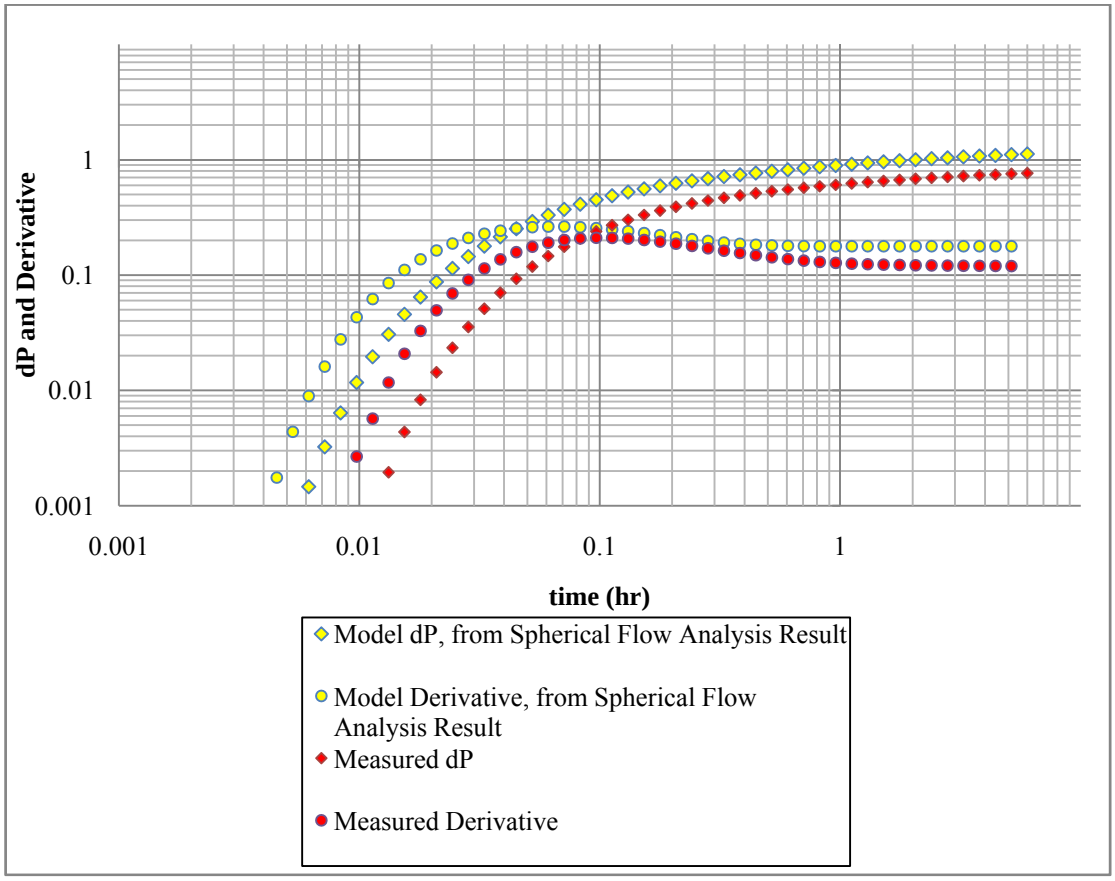

Figure 4-47: Model pressure change and derivative for observation-probe 2 buildup using the result from spherical-flow analysis, Case 4.

4.2.5 Summary of Analysis

Further analysis was conducted with increasing reservoir heterogeneity to examine the feasibility of spherical-flow analysis on increasing heterogeneity reservoir. Input parameters used to simulate the IPTT is using the same input as Case 1 except the permeability values of each layer. Each synthetic IPTT will have different heterogeneity level (increasing Dykstra-Parsons coefficient) and consisted of a 2-hours flowing period with 10bbl/day followed by a 2-hours buildup. Refer to **Appendix-A** for the list of permeability input for each synthetic IPTT. **Table 4-8** shows the summary of the result from the spherical-flow analysis. **Table 4-9** shows the summary of the result from the radial-flow analysis. Only heterogeneity level of up to Dykstra-Parsons coefficient of 0.70 was examined in this report because beyond this heterogeneity level, observation probes do not exhibit spherical-flow and radial-flow regime. Above Dykstra-Parsons coefficient of 0.70, radial-flow regime is found to be require a long buildup time (more than 500 hours of buildup) to be established

in highly heterogeneous reservoir. The estimated permeabilities from both spherical-flow and radial-flow analysis are compared with the arithmetic, harmonic and geometric averages of the input permeabilities value. **Table 4-10** shows the averages of the input permeabilities value. Comparison is made by calculating the percentage error by taking the averages as the true value against the estimated value. This comparison is summarized in **Table 4-11** to **Table 4-13**. **Table 4-11** justified spherical-flow analysis is feasible to up heterogeneity level of Dykstra-Parsons Coefficient of 0.30 where an error of within 10% in the computed permeability parameters and is considered acceptable for practical purposes. In reservoir beyond Dykstra-Parsons coefficient of 0.30, the spherical-flow response could not be measured. Reservoir with Dykstra-Parsons coefficient of 0.70, the observation-probe data do not exhibit a spherical-flow regime. Besides, the computed permeabilites estimates are found to be more representable by arithmetic average of the input permeabilities value compared to the harmonic and geometric averages. Less error is computed from using arithmetic average as true value compare to harmonic and geometric averages. From **Table 4-12** and **Table 4-13**, large error in the computed permeabilities estimates from radial-flow analysis are recorded. The large error justified the conclusion from Case 2, where the adopted radial-flow solution is not applicable to multi-layered reservoir system with Dykstra-Parsons coefficient of 0.06 and above. Furthermore, probe 1 buildup radial-flow analysis with Dykstra-Parsons coefficient of 0.40 and above have either no root or zero in the $f(k_v)$ vs. k_v plot to obtain an estimate for vertical permeability. Therefore, reservoir with Dykstra-Parsons coefficient above 0.05 may require a more complex vertical permeability averaging method to describe the reservoir. However, horizontal permeability is found to be accurately computed from adopted radial-flow analysis solution by using both Probe 1 and 2 buildup data. Computed horizontal permeability has less than 5% error, despite high heterogeneity up to Dykstra-Parsons coefficient of 0.70. **Table 4-12** and **Table 4-13** also proved less error is computed from using arithmetic average as true value compare to harmonic and geometric averages, therefore the computed permeabilites estimates are more represented by arithmetic average of the input permeabilities.

Table 4-8: Summary of Spherical Flow Analysis for Observation Probe 1 using Buildup Data.

Heterogeneity (Dykstra Parson Coefficient)	Probe 1	
	Spherical Flow Analysis, k_h (md)	Spherical Flow Analysis, k_v (md)
0.1	95.70	10.27
0.2	96.91	10.59
0.3	97.75	10.41
0.4	67.68	13.62
0.5	159.73	3.48
0.6	66.18	14.77
0.7	NA	NA

Table 4-9: Summary of Infinite-Acting Radial Flow Analysis for Observation Probes using Buildup Data.

Heterogeneity (Dykstra Parson Coefficient)	Probe 1		Probe 2	
	Radial Flow Analysis, k_h (md)	Radial Flow Analysis, k_v (md)	Radial Flow Analysis, k_h (md)	Radial Flow Analysis, k_v (md)
0.1	98.99	21.00	98.63	12.50
0.2	98.99	201.00	99.34	8.00
0.3	100.79	22.00	100.42	20.00
0.4	98.99	NA	100.06	14.00
0.5	100.79	0.00	101.90	2.00
0.6	103.42	NA	100.42	11.00
0.7	101.90	0.00	100.79	7.50

Table 4-10: Summary of Input Permeabilities Value Average.

Heterogeneity (Dykstra Parson Coefficient)	Arithmetic Average		Harmonic Average		Geometric Average	
	k_h (md)	k_v (md)	k_h (md)	k_v (md)	k_h (md)	k_v (md)
0.1	99.30	9.98	98.43	9.90	98.86	9.94
0.2	100.72	9.81	97.05	9.44	98.91	9.63
0.3	101.86	9.70	90.81	8.90	96.93	9.28
0.4	102.53	10.26	76.57	7.40	91.83	9.35
0.5	100.35	10.57	65.52	6.67	81.50	8.40
0.6	100.90	9.34	54.47	5.38	76.43	7.01
0.7	99.65	9.21	44.51	3.66	72.84	5.94

Table 4-11: Comparison of Probe 1 Buildup Spherical-flow Analysis Estimates with Input Permeabilities Averages.

Heterogeneity (Dykstra Parson Coefficient)	Arithmetic Average		Harmonic Average		Geometric Average	
	% error of k_h	% error of k_v	% error of k_h	% error of k_v	% error of k_h	% error of k_v
0.1	3.63	2.86	2.77	3.69	3.20	3.28
0.2	3.78	7.90	0.14	12.22	2.02	9.94
0.3	4.04	7.35	7.64	16.99	0.84	12.23
0.4	33.99	32.80	11.61	84.01	26.30	45.66
0.5	59.17	67.08	143.80	47.82	95.98	58.55
0.6	34.41	58.17	21.49	174.37	13.41	110.68
0.7	NA	NA	NA	NA	NA	NA

Table 4-12: Comparison of Probe 1 Buildup Radial-flow Analysis Estimates with Input Permeabilities Averages.

Heterogeneity (Dykstra Parson Coefficient)	Arithmetic Average		Harmonic Average		Geometric Average	
	% error of k_h	% error of k_v	% error of k_h	% error of k_v	% error of k_h	% error of k_v
0.1	0.31	110.33	0.57	112.02	0.13	111.19
0.2	1.71	1947.93	2.00	2030.01	0.08	1986.70
0.3	1.05	126.88	10.99	147.24	3.98	137.19
0.4	3.46	NA	29.28	NA	7.80	NA
0.5	0.44	100.00	53.84	100.00	23.67	100.00
0.6	2.49	NA	89.86	NA	35.32	NA
0.7	2.26	100.00	128.96	100.00	39.90	100.00

Table 4-13: Comparison of Probe 2 Buildup Radial-flow Analysis Estimates with Input Permeabilities Averages.

Heterogeneity (Dykstra Parson Coefficient)	Arithmetic Average		Harmonic Average		Geometric Average	
	% error of k_h	% error of k_v	% error of k_h	% error of k_v	% error of k_h	% error of k_v
0.1	0.68	25.20	0.20	26.21	0.23	25.71
0.2	1.37	18.49	2.36	15.22	0.44	16.95
0.3	1.41	106.25	10.58	124.76	3.60	115.63
0.4	2.41	36.50	30.68	89.14	8.97	49.73
0.5	1.54	81.08	55.53	70.01	25.03	76.18
0.6	0.48	17.80	84.35	104.34	31.39	56.90
0.7	1.14	18.57	126.47	104.83	38.37	26.30

4.2.6 Sensitivity of Layers' Thicknesses

Sensitivity of layer height is tested on the adopted solutions for the accuracy of the representation model. Two cases are presented here and both of the cases are synthetic cases by using solution in codes developed by Onur (2013) for dual-packer tool. To access the applicability of the adopted solutions in multi-layered reservoir system with varying layers thickness, Case 5 will be a reservoir system with the last heterogeneity level (Dykstra-Parsons Coefficient=0.05) when radial-flow analysis is still feasible and Case 6 will be a reservoir system with the last heterogeneity level level (Dykstra-Parsons Coefficient=0.30) when spherical-flow analysis is still feasible. The height of each layer is generated randomly from a normal distribution by using μ_h=8ft and σ_h=6.

4.2.6.1 Case 5, Heterogeneity of Dykstra-Parsons Coefficient = 0.05.

Synthetic IPTT Case 5, the input parameters used to simulate the IPTT is using the same input as Case 1 except the flowing probe is placed at z_w = 42.52ft, total thickness, h= 85.03 ft and the following parameters in **Table 4-14**:

Table 4-14: Permeability and Layers Height Input for Synthetic IPTT for Case 5

Layers	h (ft)	k_h (md)	k_v (md)
1	6.10	97.85	9.27
2	1.75	99.53	9.43
3	3.47	93.14	9.77
4	9.74	101.33	10.18
5	10.92	97.69	9.69
6	19.15	100.87	9.28
7	7.44	94.49	10.54
8	17.60	100.86	10.53
9	1.94	98.15	10.02
10	6.21	104.58	10.39
11	0.71	111.72	11.02
Arithmetic Average		99.69	9.94
Harmonic Average		99.61	9.91
Geometric Average		99.65	9.92

The test consisted of a 6-hours flowing period followed by a 6-hours buildup. **Figure 4-48** shows the test pressure data for observation probe 1. **Figure 4-49** shows the diagnostic log-log plot of buildup pressure change and derivative at the packer interval and observation probes. The packer and probe 1 buildup data exhibit a clear negative half-slope at Δt= 0.24 hours to Δt= 0.33 hours. **Figure 4-50** displays the observation probe 1 buildup pressure on a spherical-flow plot. And slope of $m_{sp} = -0.175$ and the intercept $a_{tbs=0} = 1496.86psi$ are determined. Spherical cubic-analysis resulted with $k_h = 101.87md$ (Error by 2.19%) and $k_v = 9.58md$ (Error by 0.04%). These values are very close to the arithmetic average of the input values given in **Table 4-14**. A drawdown spherical-flow analysis has also carried out (due to this is a synthetic data with constant drawdown of 10 B/D for 6 hours), $k_h = 101.96md$ (Error by 2.28%) and $k_v = 10.02\ md$ (Error by 0.80%) are obtained. The good agreement of the input values and computed values has proved the feasibility of the adopted solution for multi-layered reservoir system with random layers height.

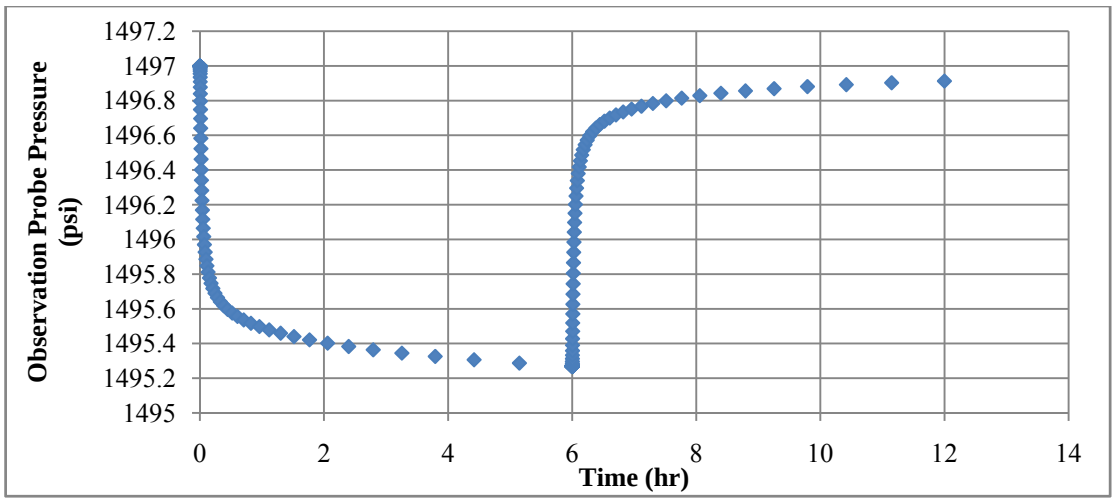

Figure 4-48 : Pressure Response for Observation Probe 1, Case 5

.

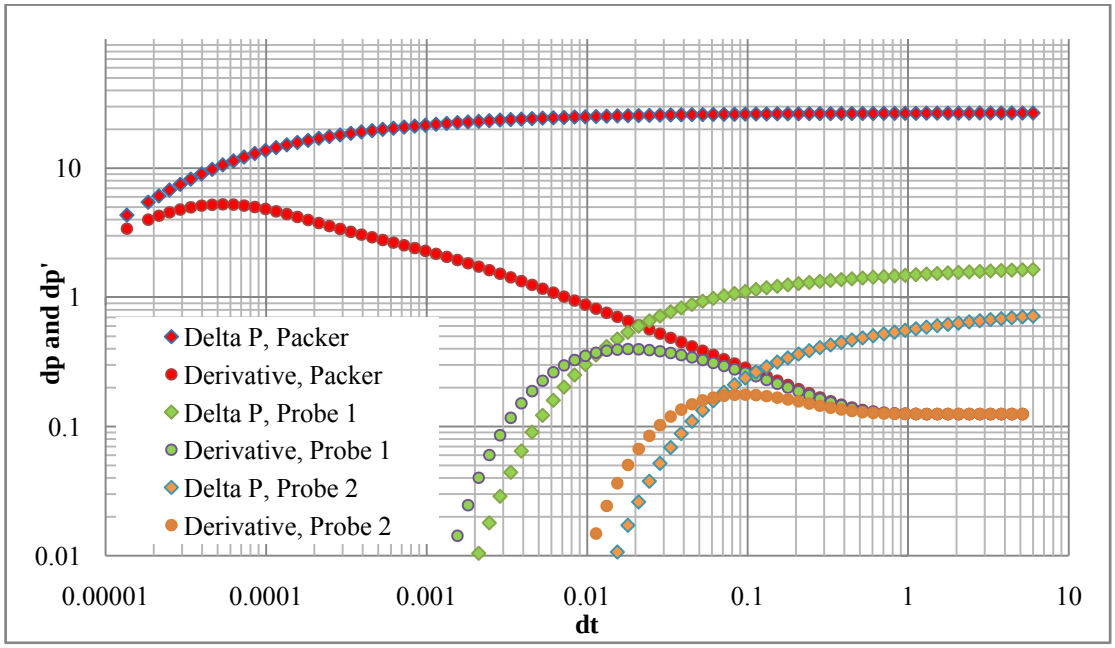

Figure 4-49: Pressure change and derivative at the packer interval and observation probes during buildup, Case 5

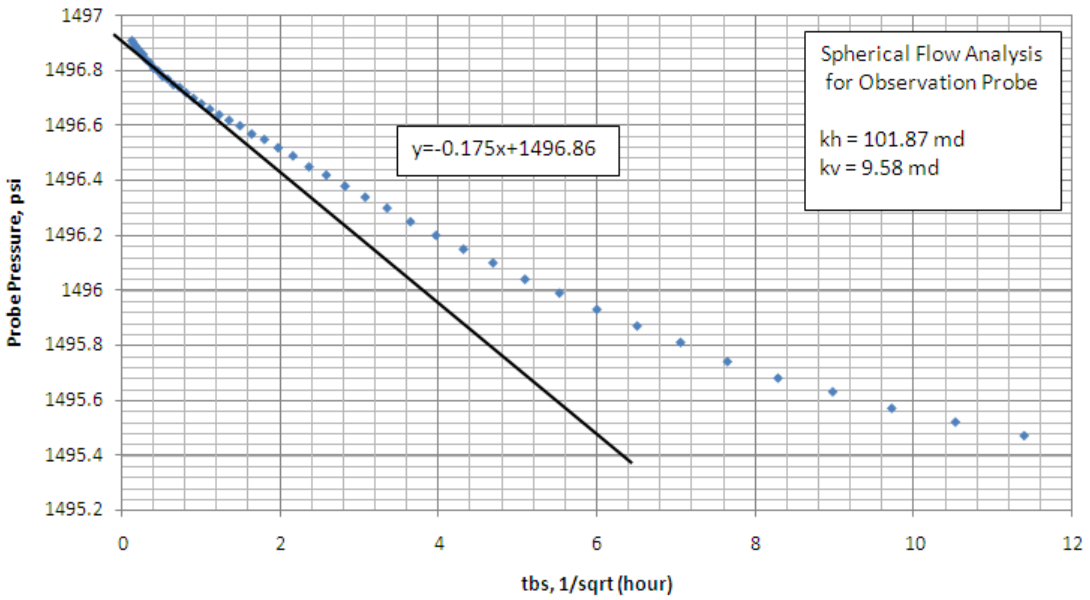

Figure 4-50: Spherical-flow plot for buildup of observation probe, Case 5 (Probe 1)

Radial-flow analysis is used to analyse the observation probes data as well and from **Figure 4-49**, the system reaches radial flow after 1.0 hours of buildup. For this example, $\Delta Z_R = 6.4\ ft$ for probe 1, 14.4 *ft* for probe 2 and $25 r_w \sqrt{k_v/k_h} = 2.80\ ft$,

so the requirement of Equation 3.25 is met. **Figure 4-51** presents the radial-flow plot from which the slope *m*=-0.297 and intercept, *b*=1.507 is obtained. Using the steps explained in methodology section, values of k_h *and* k_v are computed from obervation probe 1 data where $k_h = 99.94md$ (Error by 0.25%) and $k_v = 10.30md$ (Error by 3.62%) is obtained through plotting $f(k_v)$ versus k_v as shown in **Figure 4-52**. These values are very close to the arithmetic average of the input values given in **Table 4-14**. A radial-flow analysis for buildup pressure is also performed on observation probe 2 with $k_h = 99.60md$ (Error by 0.09%) and $k_v = 9.10md$ (Error by 8.45%). A drawdown radial-flow analysis has also carried out (due to this is a synthetic data with constant drawdown of 10 B/D for 6 hours), $k_h = 99.94md$ (Error by 0.25%) and $k_v = 10.30\ md$ (Error by 3.62%) are obtained from observation probe 1 data and $k_h = 99.59md$ (Error by 0.09%) and $k_v = 9.10\ md$ (Error by 8.45%) from observation probe 2 data. In summary, the good agreement of the input values and computed values has proved the feasibility of the adopted radial-flow solution for multi-layered reservoir system with random layers height.

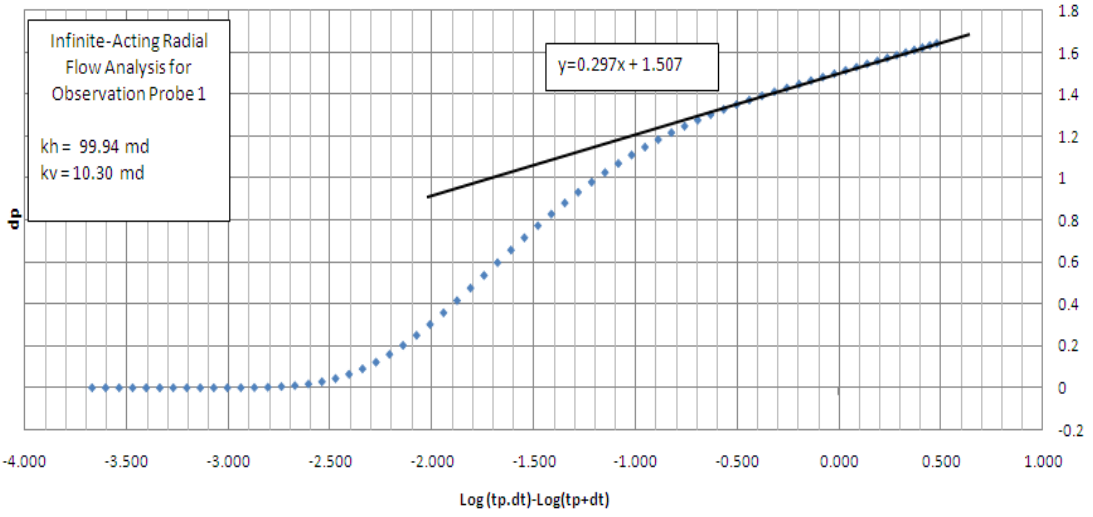

Figure 4-51: Radial-flow (or Horner) plot for observation probe, Case 5 (Probe 1)

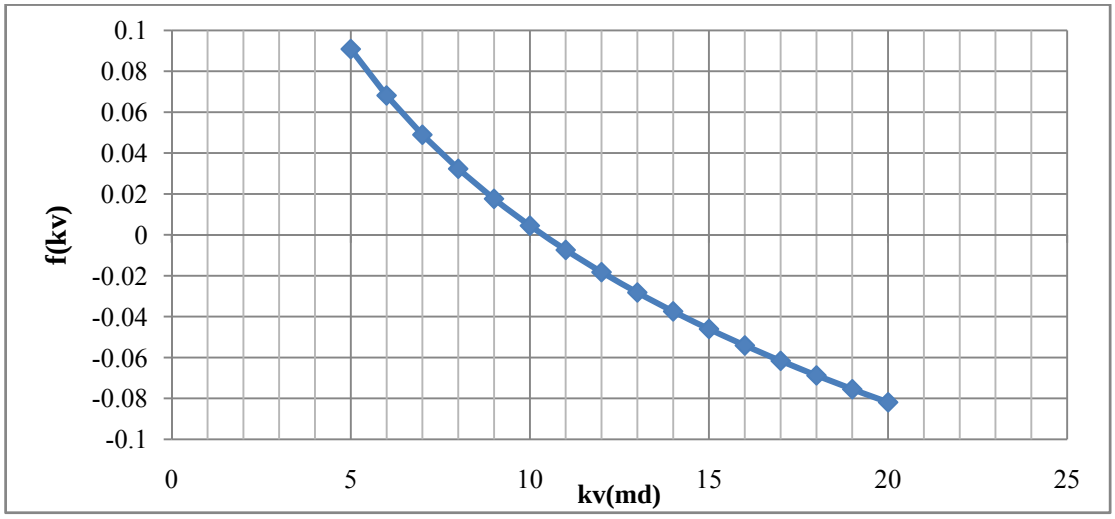

Figure 4-52: $f(k_v)$ vs. k_v , Case 5

4.2.6.2 Case 6, Heterogeneity of Dykstra-Parsons Coefficient = 0.30 .

Synthetic IPTT Case 6, the input parameters used to simulate the IPTT is using the same input as Case 5 except the following parameters in **Table 4-14**:

Table 4-15: Permeability and Layers Height Input for Synthetic IPTT for Case 6

Layers	h (ft)	k_h (md)	k_v (md)
1	6.10	73.44	6.46
2	1.75	130.81	11.44
3	3.47	59.07	5.76
4	9.74	123.80	8.55
5	10.92	61.83	8.69
6	19.15	95.90	13.74
7	7.44	103.83	12.81
8	17.60	91.90	7.53
9	1.94	127.67	11.65
10	6.21	86.70	13.01
11	0.71	148.81	13.52
Arithmetic Average		92.69	10.13
Harmonic Average		88.12	9.34
Geometric Average		90.44	9.73

The test consisted of a 6-hours flowing period followed by a 6-hours buildup. **Figure 4-53** shows the test pressure data for observation probe 1. **Figure 4-54** shows the

diagnostic log-log plot of buildup pressure change and derivative at the packer interval and observation probes. The packer and probe 1 buildup data exhibit a clear negative half-slope at Δt= 0.24 hours to Δt= 0.33 hours. **Figure 4-55** displays the observation probe 1 buildup pressure on a spherical-flow plot. And slope of $m_{sp} = -0.21$ and the intercept $a_{tbs=0} = 1496.87psi$ are determined. Spherical cubic-analysis resulted with $k_h = 86.31md$ (Error by 6.88%) and $k_v = 9.27md$ (Error by 8.49%). These values are very close to the arithmetic average of the input values given in **Table 4-6**. A drawdown analysis has also carried out (due to this is a synthetic data with constant drawdown of 10 B/D for 6 hours), $k_h = 87.68md$ (Error by 5.41%) and $k_v = 10.86\,md$ (Error by 7.20%) are obtained. The good agreement of the input values and computed values has proved the feasiblity of the adopted spherical-flow solution for multi-layered reservoir system with random layers height.

Radial-flow analysis using the adopted solution is not explained for this case because radial-flow analysis is not feasible for multi-layered reservoir system with heterogeneity level above 0.05 by Dykstra-Parsons coefficient as explained in Case 2.

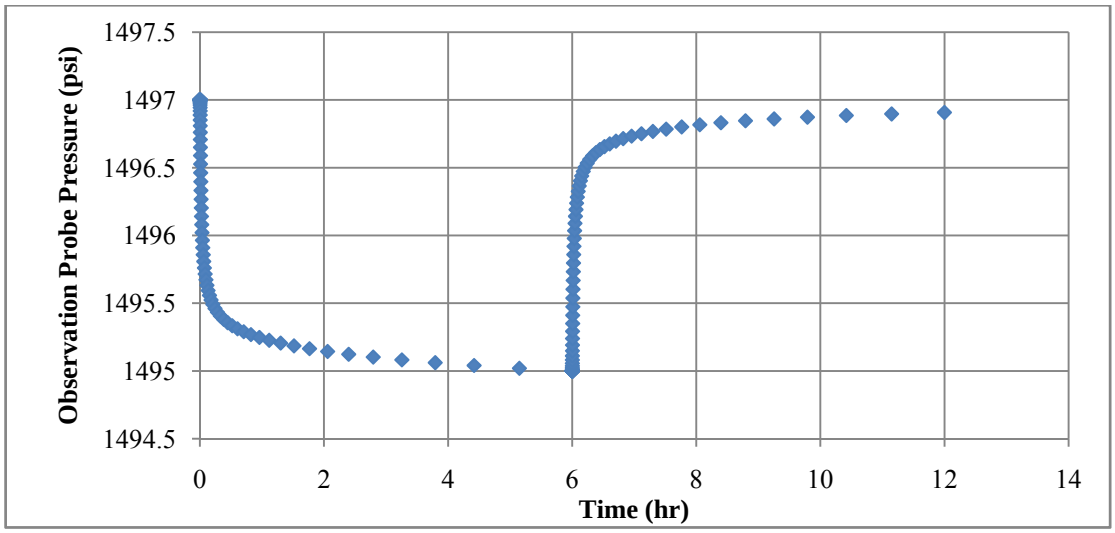

Figure 4-53: Pressure Response for Observation Probe 1, Case 6

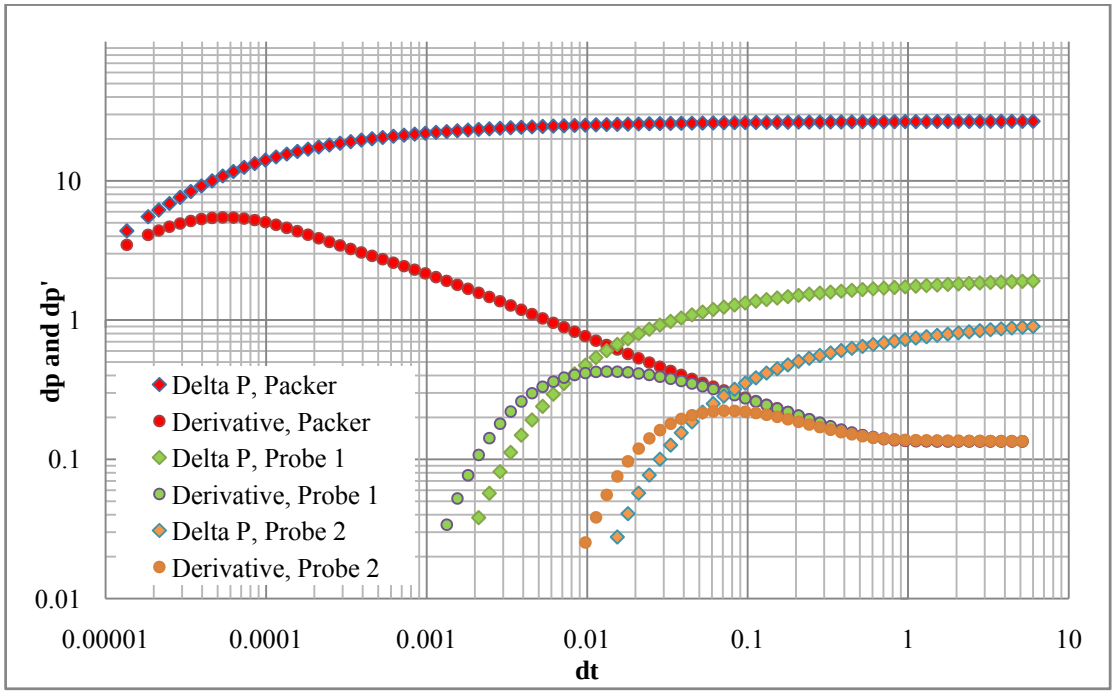

Figure 4-54: Pressure change and derivative at the packer interval and observation probes during buildup, Case 6

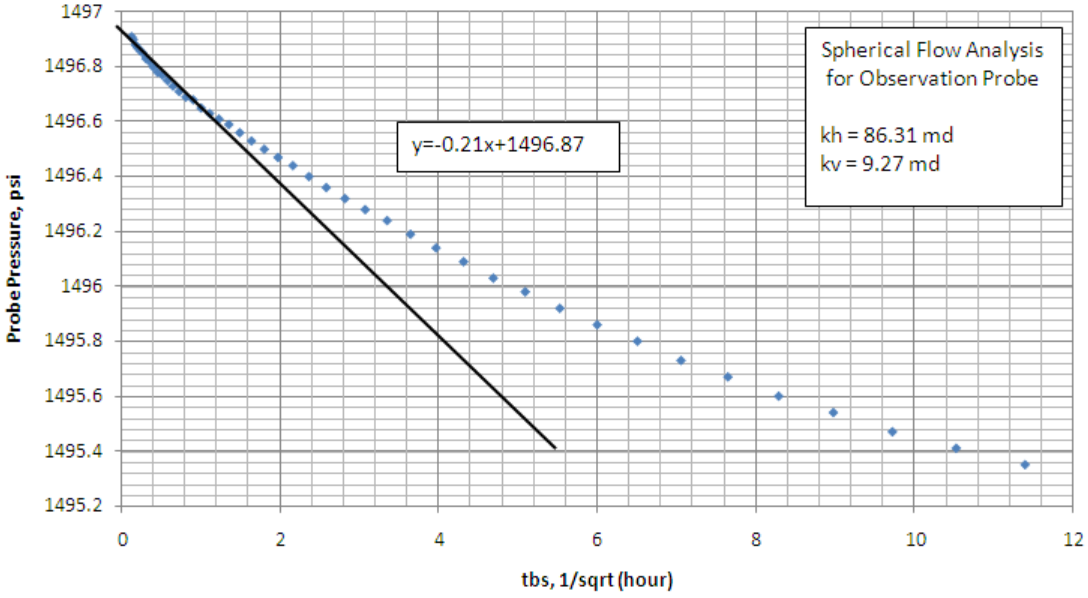

Figure 4-55: Spherical-flow plot for buildup of observation probe, Case 6 (Probe 1)

Chapter 5
CONCLUSIONS AND RECOMMENDATIONS

5.1 Conclusions

Onur et al. (2011) spherical-flow cubic and Onur et al. (2013) radial-flow analyses are able to estimates horizontal and vertical permeability accurately for a pressure response from single-layer reservoir system. In this study, we investigated whether these estimation methods can be extended to multi-layered reservoir systems if the some averages (arithmetic, harmonic, geometric, etc.) of horizontal and vertical permeability of the layered system can represent the corresponding permeability of the equivalent single layer reservoir system to a certain extent. This is because this representation is expected to be a function of multi-layered formation parameters. Initial outcomes have shown Onur et al. (2013) radial-flow analysis has the ability to estimate the horizontal and vertical permeability of the layered system with heterogeneity of less than Dykstra-Parsons coefficient of 0.06. These estimated permeability values are very close to the arithmetic averages of the corresponding layered system permeability. On the other hand, Onur et al. (2011) spherical-flow cubic analysis has the ability to estimate the horizontal and vertical permeability of the layered system with heterogeneity of less than Dykstra-Parsons coefficient of 0.40. These estimated permeability values are also very close to the arithmetic averages of the corresponding layered system permeability. The multi-layered system may be represented by an equivalent single-layer reservoir system from the estimated permeability by using both of the adopted solutions if the permeability heterogeneity is not too high, e.g., the Dysktra-Parson coefficient not exceeding 0.4. Further numerical experiments are conducted to study the sensitivity of layers height for the accurate representation of the model and the results have shown Onur et al. (2013) radial-flow analysis and Onur et al. (2011) spherical-flow cubic analysis has the ability to estimate the horizontal and vertical permeability of the layered system with varying layers thicknesses.

5.2 Recommendation for Future Work

Further future work such as study of the effect other formation parameters such as porosity, rock compressibility, viscosity and etc. on the accuracy of the representation of the model can be considered. Furthermore, other work considers research such as research on a more accurate averaging model to describe the multi-layered reservoir will also be a valuable research. This study can also be extended to test the feasibility of the adopted solutions on estimation of three-dimensional permeabilities.

REFERENCES

Ahmed, T., & McKinney, P. D. (2005). *Advanced Reservoir Engineering.* MA. USA: Elsevier Inc.

Atlas Wireline Services. (1987). *Formation Multi-tester (FMT) Principles, Theory and Interpretation.* Western Atlas International, Atlas Wireline Services.

Bourdet, D., Ayoub, J., & Pirard, Y. (1989). Use of Pressure Derivative in Well-Test Interpretation. *SPE Formation Evaluation 4(2)* , 293-302.

Bourdet, D. (2002). *Well Test Analysis : The Use of Advanced Interpretation Models.* Amsterdam: Elsevier Science.

Dykstra, H., & Parsons, R. (1950). The Prediction of Oil Recovery by Waterflood. *Secondary Recovery of Oil in United States* , 160-74.

Ireland, T., Joseph, J., Richardson, S., & Colley, N. (1992). The MDT Tool : A Wireline Testing Breakthrough. *Oilfield Review 4(2)* , 46-57.

Kasap, E., Huang, K., Shwe, T., & Georgi, D. (1996). *Robust and Simple Graphical Solution for Wireline Formation Tests : Combined Drawdown and Buildup Analyses.* Paper SPE 36525 presented at SPE Annual Technical Conference and Exhibition, Denver, Colorado, USA, 6-9 October 1996.

Kuchuk, F. (1994). Pressure Behaviour of the MDT Packer Module and DST in Crossflow-Multilayer Reservoir. *Journal of Petroleum Science and Engineering 11(2)* , 123-135.

Kuchuk, F., & Onur, M. (2002). Estimating Permeability Distribution from 3D Interval Pressure Transient Test. *Journal of Petroleum Science and Engineering 39(2)* , 5-27.

Larsen, L. (2006). *Modeling and Analyzing Source and Interference Data from Packer-Probe and Multi-Probe Tests.* Paper SPE 102698 presented at 2006 SPE Annual Technical Conference and Exhibition,San Antonio,Texas, 24-27 September 2006.

Onur, M., & Kuchuk, F. (2000). *Nonlinear Regression Analysis of Well-Test Pressure Data with Uncertain Variance.* Paper SPE 62918 presented at 2000 SPE Annual Technical Conference,Dallas,Texas, 1-4 October 2000.

Onur, M., Hegeman, P., & Kuchuk, F. (2004). *Pressure-Transient Analysis of Dual Packer-Probe Wireline Formation Testers in Slanted Wells.* Paper SPE 90250 presented at SPE Annual Technical Conference and Exhibition,Houston,Texas,26-29 September 2004.

Onur, M., Hegeman, P., & Kuchuk, F. (2011). *A Novel Analysis Procedure for Estimating Thinkness-Independent Horizontal and Vertical Permeabilities From Pressure Data at an Observation Probe Acquired by Packer-Probe Wireline Formation Testers.* Paper SPE 148403 presented at International Petroleum Technology Conference,Doha,7-9 December 2009.

Onur, M., Hegeman, P., & Gok, I. (2013). *A Novel Infinite-Acting Radial-Flow Analysis Procedure for Estimating Horizontal and Vertical Permeability from an Observation-Probe Pressure Response.* Paper SPE 164797 to be presented at the EAGE Annual Conference & Exhibition incorporating SPE Europe,London, United Kingdom, 10-13 June 2013

Onur, M. (2013). MdtPackerProbe (Version 1.03) (Codes).

Pop, J., Badrv, R., Morris, C., Wilkinson, D., Tottrup, P., & Jonas, J. (1993). *Vertical Interference Testing with a Wireline Conveyed Straddle Packer Tool* . Paper SPE 26841 presented at the SPE Annual Technical Conference & Exhibition,Houston Texas, 3-6 October 1993.

Prats, M. (1970). A Method for Determining the Net Vertical Permeability Near a Well From In-Situ Measurement. *J. Pet Tech 22 (5)* , 637-643.

Schlumberger. (2006). *Fundamentals of Formation Testing.* Texas: Schlumberger Marketing Communications.

Zimmerman, T., Mc.Innis, J., Hoppe, J., Pop, J., & Long, T. (1990). *Application of Emerging Wireline Formation Technologies* . Paper OSEA 90105 presented at the Offshore South East Asia Conference,Singapore, 4-7 December.

Appendix-A

Table A- 1: Permeability Input for Synthetic IPTT for Reservoir with Dykstra-Parsons Coefficient of 0.10.

Layers	h (ft)	k_h (md)	k_v (md)
1	8	88.08	9.58
2	8	107.67	9.41
3	8	88.95	8.67
4	8	97.80	9.19
5	8	104.59	10.86
6	8	97.26	11.99
7	8	94.49	9.71
8	8	95.91	10.17
9	8	111.80	9.71
10	8	88.13	11.06
11	8	117.63	9.44
Arithmetic Average		99.30	9.98
Harmonic Average		98.43	9.90
Geometric Average		98.86	9.94

Table A- 2: Permeability Input for Synthetic IPTT for Reservoir with Dykstra-Parsons Coefficient of 0.20.

Layers	h (ft)	k_h (md)	k_v (md)
1	8	119.49	9.03
2	8	126.53	8.21
3	8	75.64	10.43
4	8	94.06	10.07
5	8	80.48	6.10
6	8	70.76	9.55
7	8	115.75	10.28
8	8	96.38	10.54
9	8	108.72	12.48
10	8	123.44	12.89
11	8	96.63	8.37
Arithmetic Average		100.72	9.81
Harmonic Average		97.05	9.44
Geometric Average		98.91	9.63

Table A- 3: Permeability Input for Synthetic IPTT for Reservoir with Dykstra-Parsons Coefficient of 0.30.

Layers	h (ft)	k_h (md)	k_v (md)
1	8	41.17	12.56
2	8	104.81	10.24
3	8	77.55	12.64
4	8	129.21	7.71
5	8	106.50	16.43
6	8	98.52	9.88
7	8	89.32	6.50
8	8	144.70	7.57
9	8	131.24	7.73
10	8	121.51	9.39
11	8	75.92	6.01
Arithmetic Average		101.86	9.70
Harmonic Average		90.81	8.90
Geometric Average		96.93	9.28

Table A- 4: Permeability Input for Synthetic IPTT for Reservoir with Dykstra-Parsons Coefficient of 0.40.

Layers	h (ft)	k_h (md)	k_v (md)
1	8	216.87	5.35
2	8	111.23	11.16
3	8	71.17	17.24
4	8	88.84	8.39
5	8	44.18	5.48
6	8	75.49	10.57
7	8	158.66	8.68
8	8	66.94	6.54
9	8	59.63	20.29
10	8	132.32	8.87
11	8	97.66	5.26
Arithmetic Average		102.53	10.26
Harmonic Average		76.57	7.40
Geometric Average		91.83	9.35

Table A- 5: Permeability Input for Synthetic IPTT for Reservoir with Dykstra-Parsons Coefficient of 0.50.

Layers	h (ft)	k_h (md)	k_v (md)
1	8	88.05	4.87
2	8	35.98	10.76
3	8	253.60	5.34
4	8	140.00	8.19
5	8	78.76	9.02
6	8	164.58	2.25
7	8	25.21	27.80
8	8	61.78	15.85
9	8	42.67	5.89
10	8	128.75	5.93
11	8	84.48	20.38
Arithmetic Average		100.35	10.57
Harmonic Average		65.52	6.67
Geometric Average		81.50	8.40

Table A- 6: Permeability Input for Synthetic IPTT for Reservoir with Dykstra-Parsons Coefficient of 0.60.

Layers	h (ft)	k_h (md)	k_v (md)
1	8	70.38	4.17
2	8	94.44	18.43
3	8	16.52	27.27
4	8	190.97	3.21
5	8	29.85	6.36
6	8	94.06	8.63
7	8	267.84	3.02
8	8	125.79	8.78
9	8	84.39	13.71
10	8	106.58	2.14
11	8	29.13	6.99
Arithmetic Average		100.90	9.34
Harmonic Average		54.47	5.38
Geometric Average		76.43	7.01

Table A- 7: Permeability Input for Synthetic IPTT for Reservoir with Dykstra-Parsons Coefficient of 0.70.

Layers	h (ft)	k_h (md)	k_v (md)
1	8	131.33	11.69
2	8	9.54	1.60
3	8	23.91	19.57
4	8	46.46	3.15
5	8	167.87	14.07
6	8	190.06	5.67
7	8	206.02	6.67
8	8	84.18	1.10
9	8	121.79	27.74
10	8	63.82	7.84
11	8	51.16	2.21
Arithmetic Average		99.65	9.21
Harmonic Average		44.51	3.66
Geometric Average		72.84	5.94